LEARNING HAND/EYE COORDINATION
BY AN ACTIVE OBSERVER
PART I: ORGANIZING CENTERS

Jean-Yves Hervé
Computer Vision Laboratory
Center for Automation Research
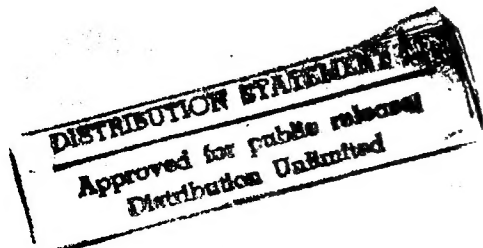University of Maryland
College Park, MD 20742

COMPUTER VISION LABORATORY

DTIC
SELECTED
JAN 0 6 1995
B

CENTER FOR AUTOMATION RESEARCH

UNIVERSITY OF MARYLAND
COLLEGE PARK, MARYLAND
20742-3275

DTIC QUALITY INSPECTED 3

LEARNING HAND/EYE COORDINATION
BY AN ACTIVE OBSERVER
PART I: ORGANIZING CENTERS

Jean-Yves Hervé

Computer Vision Laboratory
Center for Automation Research
University of Maryland
College Park, MD 20742

Abstract

This report, the first of a three-part series, presents preliminary results in a study on the role of the active observer in the hand/eye coordination problem.

It was shown in [11] that the hand/eye coordination problem can be represented, for a given pose of the observer, by the singularities of a surface, the PCS. Small changes in the pose of the observer generally produce smooth deformations of the PCS. There are configurations, however, from which arbitrarily small modifications of the point of view result in profound changes in the topological nature of the PCS. This paper studies these bifurcation configurations and, furthermore, investigates the possibility of determining *a priori* displacements of the observer that can achieve a desired effect on the PCS such as simplifying its topology or reducing the number of singularities separating the current configuration from a goal to be reached.

The result of this analysis takes the form of the "family portrait" of all possible aspects of the PCS, indexed by the geometry of the manipulator and the pose of the observer relative to it. A hand/eye system is then completely coordinated—has "learned its PCS"—when a "portrait" has been matched with the experimental data gathered by the low-level controller [3].

19950104 043

1. Introduction

1.1 Active vision

This report, which presents preliminary investigations of the effects and uses of observer displacements in the hand/eye coordination problem, is part of a broader study of active vision and of the role of the active observer engaged in a particular task. What are "good" activities for the observer, what are desirable effects of these activities, and how can they be achieved, both purely in terms of the perceptual process and in the context of the task at hand? How is active vision related to the learning problem? These are some of the problems that I would like to address. But maybe I should begin by making a small point of denominational orthodoxy and, backed up by early writ on the topic, discuss what is and is not active vision, and where the present work—hopefully—fits into the whole scheme.

We can observe that "when humans see and understand, they actively look, their eyes converge or diverge, they adjust to the level of illumination and they move their head" [2]. We can establish lists of possible actions (eye and head movements, vergence, focusing, changing the position, orientation, or nature of light sources, etc.). We can even study—independently or in conjunction—the effects of such actions on the measurements or results of various perceptual modules. But psychologists have not waited for computer vision researchers to point out the beneficial effects of head and eye movements, for example on reaching tasks [20]. Even in computer vision, most studies stressing the importance of the observer's position and orientation relative to the scene and to the light sources were in fact undertaken long before the introduction of active vision as a research topic ['Gibso50,Horn77,Marr82']. It was also well established by then that information about the scene could be extracted from the optical flow resulting from the observer's displacements [6]. So is active vision just a new, catchy name for old ideas?

The answer is naturally negative: active vision is not the subfield of computer vision that deals with the case of a mobile observer that can zoom, focus, or control its vergence. Computing the optical flow is not an active vision task. Neither is visual tracking for its own sake.[1] On the other hand, choosing the observer's motion parameters so as to reduce the ambiguity of the optical flow (and hence make its interpretation easier), or tracking an object specifically in order to facilitate its recognition, are (would be?) active vision problems. Active vision is concerned with "[manipulating] the constraints underlying the observed phenomena in order to improve the quality of the perceptual results" [1].

To this day, one can essentially distinguish four main types of "active vision":

- The first kind, which I will call hardware-based, for lack of a better nomenclature, is best represented by the work of E. Krotkov on vergence and focusing [16]. In this case, there is a direct relation between a physical parameter, or set of parameters, of the visual apparatus and measurements made about the scene. The problem of the active observer is then to adjust these parameters or their variations so as to get, say, the best overall focus on some part of the image.

---

[1] Neither problem being any less worthy for this simple reason, needless to say.

Availability Codes

Dist | Avail and/or Special

A-1

- Another type of active vision is concerned with the choice of displacements for the observer that make the (quantitative) visual reconstruction modules perform better. We know from earlier work that some motions of the observer can make an ill-posed problem become well posed [1]. But it is also possible to determine *a priori* what motion would optimize the stability of reconstruction computations [10].

- It is also possible to choose a displacement of the observer so as to facilitate the understanding of the scene. For example, the displacement can be chosen so that new faces and vertices become visible in the case of a polyhedral world [21] or so as to facilitate the reconstruction of simple smooth shapes [17].

- Finally, the last type of active vision, of which the present work is to our knowledge the first representative, addresses the problem of choosing activities of the observer that facilitate the performance of the perceptual process in the execution of a particular navigation task: obstacle avoidance, prey catching, or—in the case of this paper—hand/eye coordination.

1.2 Hand/eye coordination: background

1.2.1 Position-based *vs.* image-based methods

We are interested here in the hand/eye coordination problem, that is, in the visual control of a robot manipulator in hand positioning tasks, a problem that, when referring to humans, is also sometimes called "reaching" in the psychology literature. In particular, we will not be addressing here the problem of fine motion of the fingers, not because this is not an interesting issue, but because it is highly unlikely that it can be performed based solely on visual information: At least during the learning stage, some tactile information must be used. Our goal here is therefore, using only visual information, to be able to position the manipulator's end-effector in the immediate vicinity of any visible and accessible object in the environment.

In the computer vision community, hand/eye coordination has generally been treated as a particular case of the calibration or pose estimation problem: once the pose of the camera, the manipulator, and the target object relative to each other have been determined, a classical, sensorless trajectory could then be planned that performs the positioning task.[2]

That pose estimation process, however, is not necessary, as [30] demonstrated in the case of a 3-dof eye-in-hand system (Figure 1(a)). This work showed in particular that, for a variety of visual feedbacks and after proper calibration of the system, hand positioning tasks can be performed by applying to the manipulator's joints an image-based visual servoing (IBVS) control, which does not require the computation of any 3D information. This work was later refined in [29] and extended to higher degree of mobility manipulators by [5], which further confirmed the strength of image-based methods.

---

[2] It is clear by now that this statement of the problem is unduly optimistic, as it makes the pose estimation problem seem almost trivial. Even the most sophisticated calibration techniques available today do not provide precise enough estimates for a path to be generated *once and for all*. Several iterations of the pose estimation/path planning/motion process (or static, position-based look-and-move control, to follow the nomenclature of [25]) are necessary, as the authors themselves point out [27].
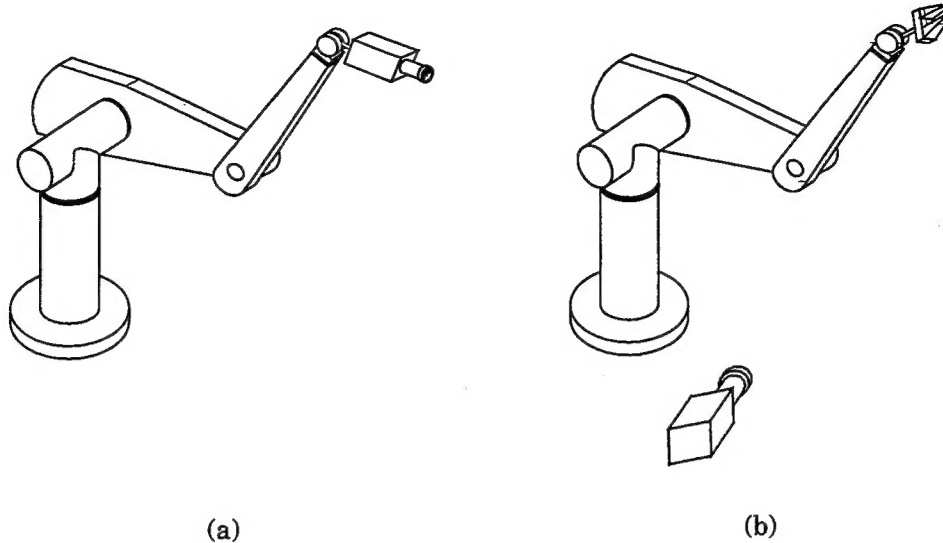
<div align="center">(a)   (b)</div>

Figure 1 — Hand/eye configurations: (a) Eye in hand (b) Eye looking at hand.

In this new approach, the object of study of the perceptual module is no longer an n-tuple of coordinates in Cartesian space, but the Perceptual Kinematic Map (or PKM), κ, which directly maps the Joint Space $\mathcal{J}$ to the *Camera Space* [26], or space of measured image features, $\mathcal{C}$. There remains the problem of initial calibration, which, although not as crucial as with the look-and-move type of control, is computed through a long and complicated process and—so far—practically requires an eye-in-hand configuration for the hand/eye system. Both for obvious anthropomorphic reasons and because it would allow more interesting tasks to be performed, it would seem preferable to have a mobile camera looking at the hand (Figure 1(b)) and to be able to *learn* the PKM while performing simple arm and head motions.

1.2.2 Three approaches to the learning problem

One way of addressing this learning problem is to feed the (applied) joint displacements and the resulting (measured) image space displacements to a neural network or an associative memory. This approach is probably best represented by [24] and [23], which present a real-time implementation in the case of an eye-in-hand industrial system, i.e. one restricted to a conveyor-belt environment. One must also mention the paradoxical case of [22], which, while deliberately non-practical (being restricted to the case of planar pendulums), nevertheless led to an implementation and is so far alone in having addressed the problem of obstacle avoidance (in the pendulum's plane).

However, as is generally the case with problems that we know how to model mathematically, robotics problems in particular, it is not really clear what advantage connectionist approaches[3] offer over more classical adaptive control (or, more generally, parameter recovery) techniques that explicitly exploit the model of the problem. For example, [26] studies, for some cases of the camera looking at the hand, the analytic form of the PKM, in which only the coefficients are unknown, since they depend on the pose of the camera.

---

[3] As learning techniques, and not as implementation techniques.

The hand/eye coordination problem is then reduced to a parameter recovery problem and it can be solved by observing movements of the hand and a simple best-fit minimization procedure.

In many ways, the approach we proposed in [11] can be seen as a geometrical, qualitative counterpart to the analytical, quantitative method of [26]. In this earlier paper, we showed that, for a given pose of the camera, the PKM can be represented by a hypersurface called the Perceptual Control Surface, or PCS, whose shape is defined qualitatively by the location and type of its singularities, as shown in Figure 2. The singularities of the PCS are detected and identified during the execution of simple hand positioning tasks that can be performed before the shape of the surface is known, for example by applying the kind of low-level image-based control described in [12].
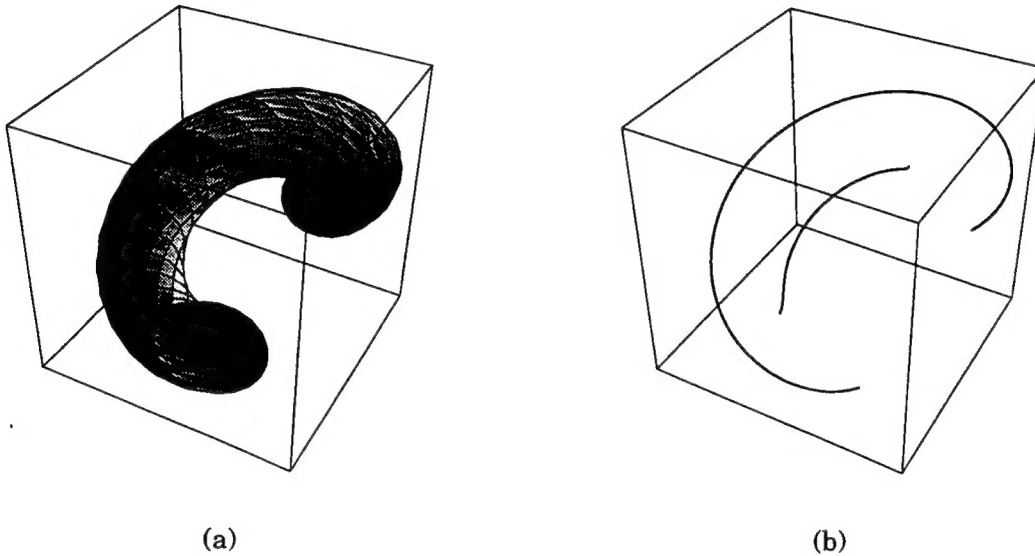

(a)   (b)

Figure 2 — (a) A Perceptual Control Surface (PCS); (b) Its singularities.

1.3 The reduced, "arm" PCS

We proposed in [11] to study the PCS of the complete 6-dof PKM, which we planned to learn based on information gathered, in the course of simple point-to-point displacement tasks, by the basic controller sketched out in [12]. In fact, all versions of our controller, from this early version to the full-fledged simulation and implementation presented in [3] have so far performed hand positioning tasks by simultaneously activating all the joints of the manipulator. We did so, primarily, because we were deliberately trying to keep the controller simple. At the time, it seemed more important to understand the basic properties and drawbacks of this type of control than try to optimize it. In particular, for proper functioning of the Kalman filter that we use, no joint should stay inactive for more than a few steps.

Although, as our system demonstrated, it is possible to control all joints together during the entire course of the trajectory, there are several reasons to prefer separating the control of the "arm" and "wrist" joints. The simple (approximative) geometrical jus-

4

tification "arm=position, wrist=orientation" is not as compelling in the case of a visually guided manipulator as it is in classical, "sensorless" robotics: the difference between position and orientation that is so clear in the Cartesian space appears somewhat blurred in the image space. Of more direct application to the PCS-based approach that we have chosen here, it is obvious that the PCS of the 3-dof arm is much simpler to study and model than that of the whole 6-dof manipulator.

The last, and probably most compelling reason is that the results gathered by psychologists and physiologists clearly show that humans (who are as good a model for flexible, vision-guided systems as we are likely to encounter) effectively separate arm movements from wrist movements. Vince [28] showed that the response curve for fast hand movements is a symmetrical sigmoid curve (Figure 3(a)). Movements precisely aimed at a target still produce a sigmoidal response curve, but the curve is no longer symmetrical; it instead displays a prolonged deceleration, an *extended homing-in* phase (Figure 3(b)).
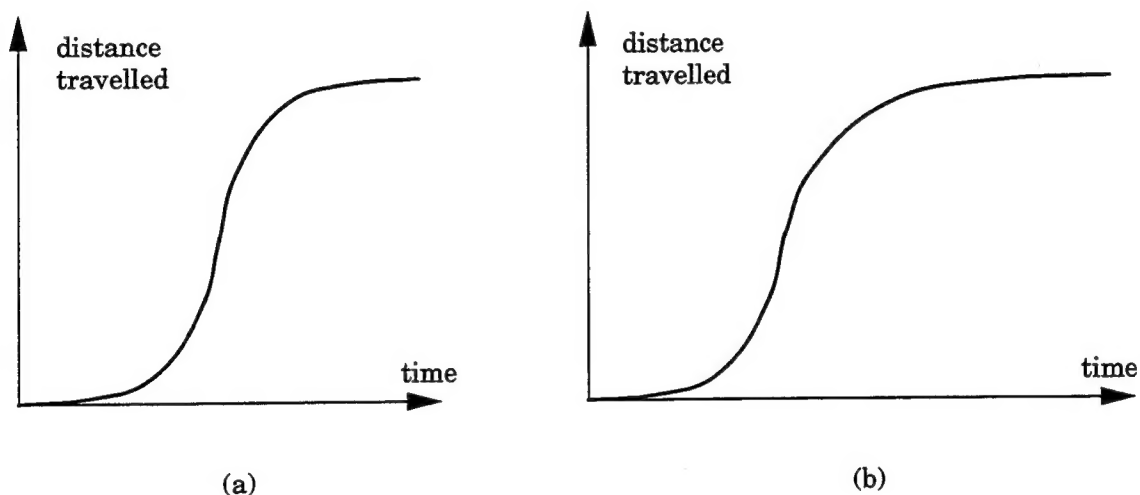

Figure 3 — Trajectories of aimed movements: (a) fast movement, (b) precise movement.

If the speed of the movement is increased, then the curve finally merges with the one measured for fast trajectories performed with the eyes closed, probably because visual processes are too slow to provide useful information. Welford [31] argued that fast movements were *ballistic*, that is, programmed in advance and run without correction (this requires the existence of an internal representation of the movement or *motor program*). Similarly, he suggested that the initial phase of precise hand movement is ballistic, while the slower homing-in phase is performed under visual control. These observations are further refined by the work of Jeannerod on prehension. [15] distinguishes between arm transport and manipulation components. "The important point is that in mature reaching there appears to be temporal coordination between the transportation and manipulation components. That is, finger closure is temporally coordinated with the deceleration breakpoint of arm transport" [18].

We can interpret these results in terms of our PCS-based approach as follows: We can distinguish between arm movements that can eventually—after the corresponding PCS

has been learned—be performed ballistically, and fine wrist movements that are only applied only once the hand is close to its target. The object of our study, of which this report is only a first step, is the learning of the "arm" PCS.

We will deal here with the case of the 2D pendulum and of the 2-degree-of-mobility manipulator shown in Figures 4(a) and 4(b) respectively. First, because 2-dof robot arms can already perform interesting tasks that we may want to control visually, such as pointing a light or laser beam (or paint gun) in a particular direction. Also, because if we are one day to control manipulation tasks in obstacle-cluttered workcells, then the trajectory of each individual link, and not only of the end-effector, must be monitored and controlled as well. The PKM of a 3-dof manipulator will be the object of another report.
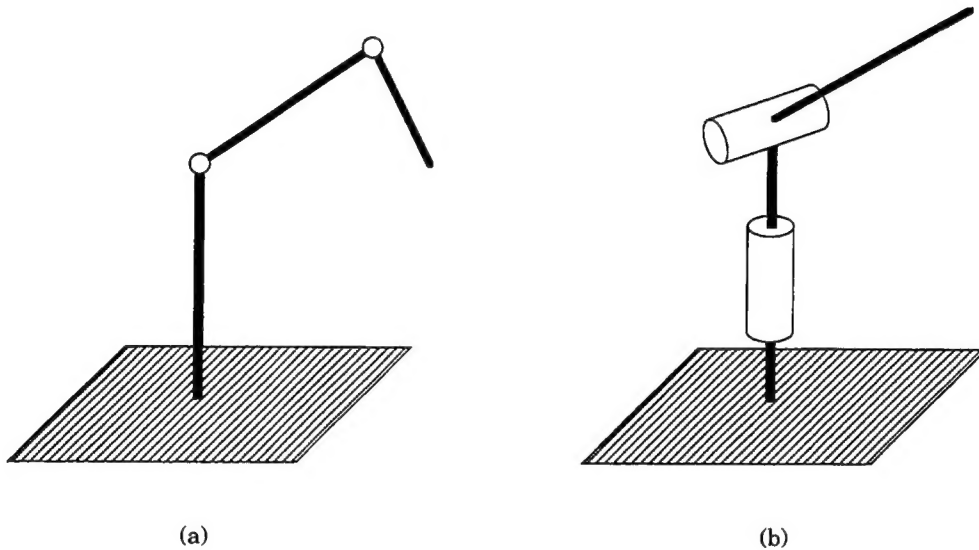

(a)   (b)

Figure 4 — (a) Double pendulum. (b) 2-degree-of-mobility manipulator.

1.4 Presentation of the Problem

We suggested in [11] that, since displacements of the camera can change the topology of the PCS, the pose of the camera could (and therefore should) be chosen so as to result in "good" changes in the topology of the PCS. For example, the total number of singularities could be reduced or, more simply, the number of singularities between the current position and the goal.

As an example, let us consider the hand/eye configuration represented in Figure 5(a) and the corresponding singularities, drawn in the joint space (Figure 5(b)). We notice that it is impossible to plan a path between joint configurations q_i and q_f that does not cross a singularity.[4] It is, however, *sometimes* possible, simply by changing the pose of the observer, as shown in Figure 5(c), to modify the topology of the PCS so that it is now

---

[4] We should emphasize the fact that, with our PKM-based approach, the path is actually planned in the image space. We just show here how the problem appears in the joint space.

6

possible to plan a path between q_i and q_f that does not cross a singularity.[5] In this case, we see that an active observer can improve the performance of the low-level controller.
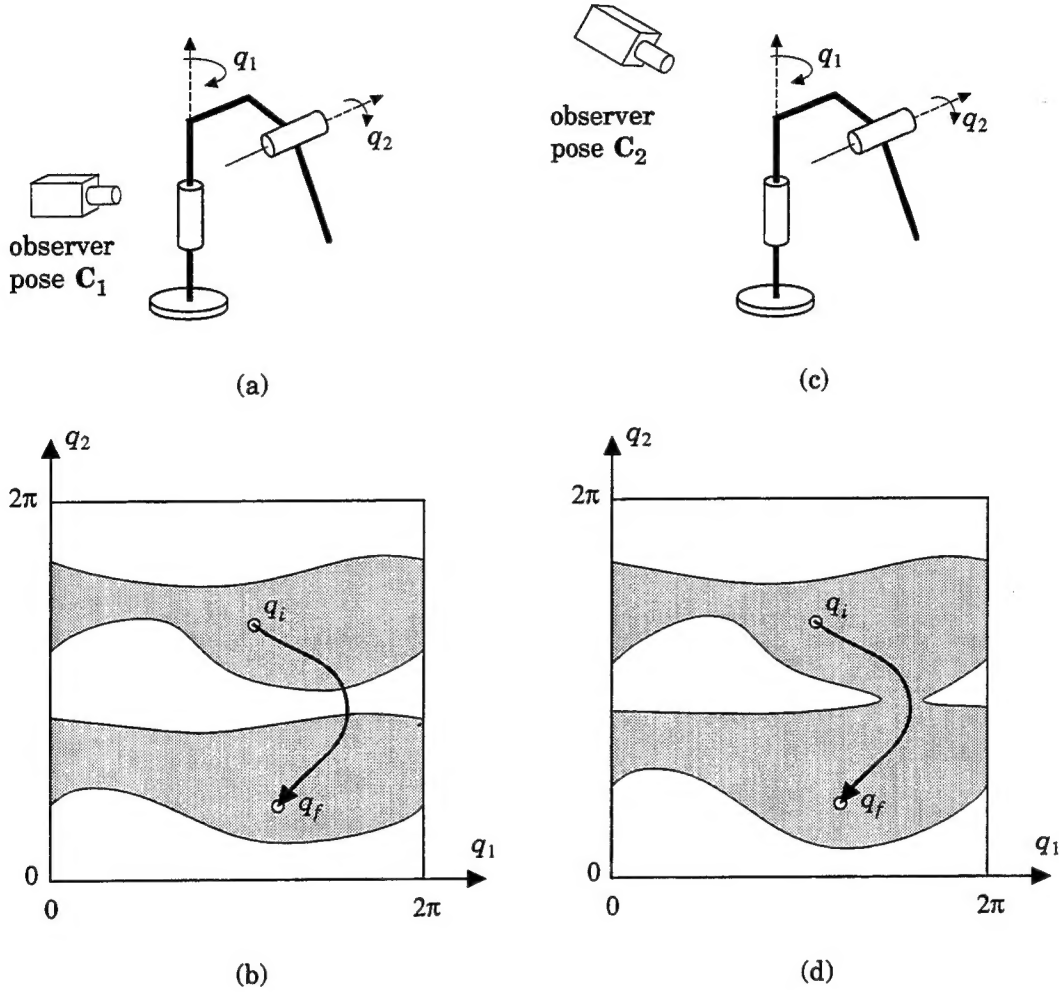
Figure 5 — Effect of a displacement of the observer on the geometry of singularities of the PKM

What is more interesting is that movements of the observer will help in learning the shape of the PCS. We will see in this report that we can obtain a "family portrait" of the possible configurations of the singularities, that is, a finite set of 2D curves, indexed by the position of the camera relative to the manipulator. The learning of the PCS can therefore be guided by the prior recognition of a particular configuration of the family portrait, using measurements made by the low-level controller.

---

[5] Obviously, only "perceptual" singularities (see Sections 3 and 4) can be so modified: displacements of the observer have no effect on kinematic singularities.

2. Model and Notation

2.1 Kinematic map

We follow here the classical formalism for the derivation of an n-degree-of-freedom manipulator's kinematic map [4], which associates a coordinate system with each link of the kinematic chain. The links being numbered S_0 to S_n (here $n = 2$), from the base to the end effector, $n + 1$ corresponding reference frames $\mathcal{R}_i = (O_i, \vec{x}_i, \vec{y}_i, \vec{z}_i)_{i=0,n}$ are defined, so that the state of joint J_i connecting S_i to S_{i-1} is represented by its four Denavit-Hartenberg parameters: two angles, α_i and θ_i, and two distances, a_i and b_i (see Figure 6). The manipulator is calibrated when these parameters have been precisely determined.[6]
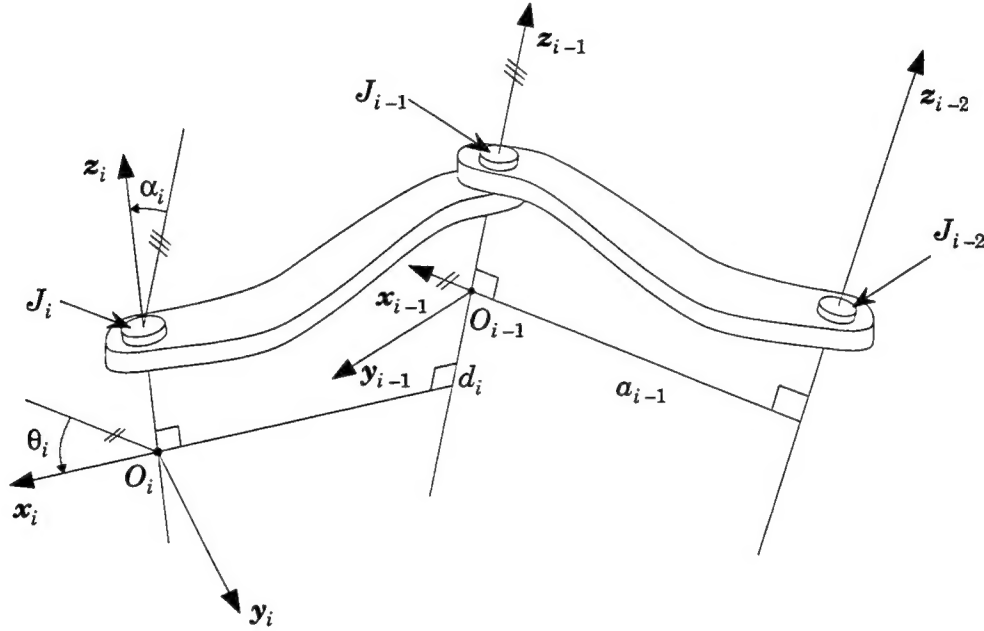

Figure 6 — Definition of the D-H parameters for joint J_i

One of the D-H parameters is the joint variable, $\mathbf{q}_i$: d_i in the case of a prismatic joint, θ_i in the case of a revolute joint, which is the one that we are concerned with here. Throughout this paper, I will use the notation $C_i = \cos q_i$, $S_i = \sin q_i$, $C_{ij} = \cos(q_i + q_j)$, and $S_{ij} = \sin(q_i + q_j)$. The homogeneous transformation matrix between $\mathcal{R}_{i-1}$ and $\mathcal{R}_i$ can then be expressed as follows:

$$\mathbf{A}_{i+1}^i = \begin{bmatrix} C_i & -\cos\alpha_i\, S_i & \sin\alpha_i\, S_i & a_i\, C_i \\ S_i & \cos\alpha_i\, C_i & -\sin\alpha_i\, C_i & a_i\, S_i \\ 0 & \sin\alpha_i & \cos\alpha_i & d_i \\ 0 & 0 & 0 & 1 \end{bmatrix}. \tag{1}$$

Since we are only treating here the case of 2-dof manipulators, it is sufficient to track a point M that is attached to the terminal link of the arm. The kinematic map κ then

---

[6] Although the nominal values of the D-H parameters are given by the manufacturer, [13] reports that end-effector positioning errors can be reduced from several centimeters to a few millimeters by a refined determination of the parameters.

8

simply maps the joint vector $\mathbf{q} = (q_1, q_2)'$ to the Cartesian coordinates of M relative to $\mathcal{R}_0$, $\mathbf{M}_0$:

$$\kappa : \mathcal{J} \longrightarrow \mathcal{K}$$
$$\mathbf{q} \longmapsto \mathbf{M}_0$$

If we assume without loss of generality that M is identified with $O_2{}^7$ (the origin of the terminal link's coordinate system $\mathcal{R}_2$), then $\mathbf{M}_0$ is given by the fourth column of the global transition matrix $\mathbf{A}_2^0 = \mathbf{A}_1^0 \cdot \mathbf{A}_2^1$. Since we are only interested in the position of M and not in the orientation of S_2, the kinematic Jacobian matrix $\mathbf{K}$ is then simply the 3×2 matrix obtained by differentiating $\mathbf{M}_0$:

$$\mathbf{K} = \frac{\partial \mathbf{M}_0}{\partial \mathbf{q}}. \tag{2}$$

2.2 Perceptual Kinematic Map

The PKM is a mapping between the joint space and the camera space that maps the joint coordinates to a vector of image features. In the case we are considering here, this vector will be the image coordinates of m, the projection of M onto the image plane.

$$\pi : \mathcal{J} \longrightarrow \mathcal{C}$$
$$\mathbf{q} \longmapsto \mathbf{m} = (x, y)'.$$

Let $\mathcal{R} = (O, \vec{x}, \vec{y}, \vec{z})$ be the coordinate system associated with the camera. The coordinate vector of M relative to $\mathcal{R}$ is $\mathbf{M} = (X, Y, Z)'$:

$$\mathbf{M} = \begin{pmatrix} X \\ Y \\ Z \end{pmatrix} = \mathbf{E}_{\psi,\theta,\phi} \cdot \mathbf{M}_0 + \mathbf{T}_0 \tag{3}$$

$$= \mathbf{E}_{\psi,\theta,\phi} \cdot \mathbf{M}_0 - \mathbf{E}_{\psi,\theta,\phi} \cdot \mathbf{C}, \tag{4}$$

where $\mathbf{E}_{\psi,\theta,\phi}$ is the 3×3 Euler rotation matrix of angles ψ, θ, and ϕ, $\mathbf{T}_0$ is the coordinate vector of O_0 relative to $\mathcal{R}$, and $\mathbf{C} = -\mathbf{E} \cdot \mathbf{T}_0 = (X_c, Y_c, Z_c)'$ is the coordinate vector of the camera's optical center relative to $\mathcal{R}_0$.

If we adopt for the camera the classical model of a pinhole of focal length f, then m is obtained from M by a perspective projection: $\mathbf{m} = f/Z \cdot \mathbf{M}$ and, by differentiating $\mathbf{m}$ with respect to the joint variables, we obtain

$$\frac{\partial \mathbf{m}}{\partial \mathbf{q}} = \frac{\partial \mathbf{m}}{\partial \mathbf{M}} \cdot \frac{\partial \mathbf{M}}{\partial \mathbf{q}}$$

$$= \frac{1}{Z} \cdot \mathbf{D} \cdot \mathbf{E}_{\psi,\theta,\phi} \cdot \frac{\partial \mathbf{M}_0}{\partial \mathbf{q}}$$

$$= \frac{1}{Z} \cdot \mathbf{D} \cdot \mathbf{E}_{\psi,\theta,\phi} \cdot \mathbf{K} \cdot \dot{\mathbf{q}}, \qquad \text{where } \mathbf{D} = \begin{pmatrix} f & 0 & -x \\ 0 & f & -y \end{pmatrix}.$$

---

[7] The Denavit-Hartenberg representation leaves the choice of the origin O_n of the end-effector's coordinate system to the discretion of the user. The location of O_n is generally chosen so that as many D-H parameters as possible are set to zero in the case of the sensorless problem. We are more interested here in simplifying the expression of the PKM.

The Jacobian matrix of the PKM is therefore the product of the "perceptual" and of the kinematic Jacobian matrices:

$$\mathbf{J} = \frac{1}{Z} \cdot \mathbf{D} \cdot \mathbf{E}_{\psi,\theta,\phi} \cdot \mathbf{K} = \mathbf{P} \cdot \mathbf{K}. \tag{5}$$

2.3 Bifurcations

We will be studying in this paper the *bifurcations* of singularities of the PKM under the effect of observer movements. At singularities, the Jacobian matrix $\mathbf{J}$ does not have full rank, which results in its determinant being zero. We see from Equation (5) that $J = \det \mathbf{J}$ is a function of the joint configuration, parameterized by the pose of the manipulator relative to the camera, given by the translation vector $\mathbf{T}_0$ and by the Euler angles ψ, θ, and ϕ. We regroup these pose parameters into a single vector $\mathbf{p}$ so that the equation of our bifurcation problem is

$$J(\mathbf{q}; \mathbf{T}_0, \psi, \theta, \phi) = J(\mathbf{q}; \mathbf{p}) = 0. \tag{6}$$

The object of our study will therefore be the qualitative changes that the locus of solutions of (6) undergoes as $\mathbf{p}$ varies over $\mathbb{R}^6$.

Throughout this paper, I will use the notation, classification, and methodology of [7], to which the reader is invited to refer when the minimalist overview given in Appendix A does not suffice. In particular, I will restrict the problem to the case of one state variable and one bifurcation parameter and treat all other parameters as perturbation parameters. Generally, I will be treating the second joint angle, q_2, as the state variable, the first joint variable, q_1, as a bifurcation parameter, and the components of the pose vector $\mathbf{p}$ as perturbation parameters. The analysis proceeds as follows:

- Localization of the singularities and of the bifurcation points. In particular, we want to differentiate between perceptual singularities, which are susceptible of bifurcations under observer displacements, and kinematic singularities, which are not.

- In the neighborhood of a given bifurcation point, and for different values of the perturbation parameters, generation of the bifurcation diagram in order to determine likely candidates among the "family portrait" of elementary bifurcations given by [7].[8]

- Proof that one of these likely candidates is the correct bifurcation problem. Once this is done, the complete persistent bifurcation diagrams can be given.

- Finally, we must establish the correspondence between the physical, pose parameters of the initial bifurcation problem and the perturbation parameters of the corresponding universal unfolding. Only then will we know which topological transformations are actually possible, and how the active observer can achieve them.

---

[8] This step, although crucial, is not discussed here since it is little more than a way to facilitate the identification of the correct normal form. Once this has been done, and the equivalence has been proved, the partial, experimental results collected during this "exploration" step are superseded by those provided by the next step.

As we shall see in the next section, the PCS of a 2D pendulum is a rather tame topological creature, studied here only for the sake of completeness. In essence, the role of the observer with such a manipulator could be summarized as: "Stay out of the way." On the other hand, the PCS of a 2-dof manipulator exhibits a surprisingly complex topological behavior, depending on the point of view of the observer. This behavior will be the subject of Sections 4 and 5.

(a)   (b)
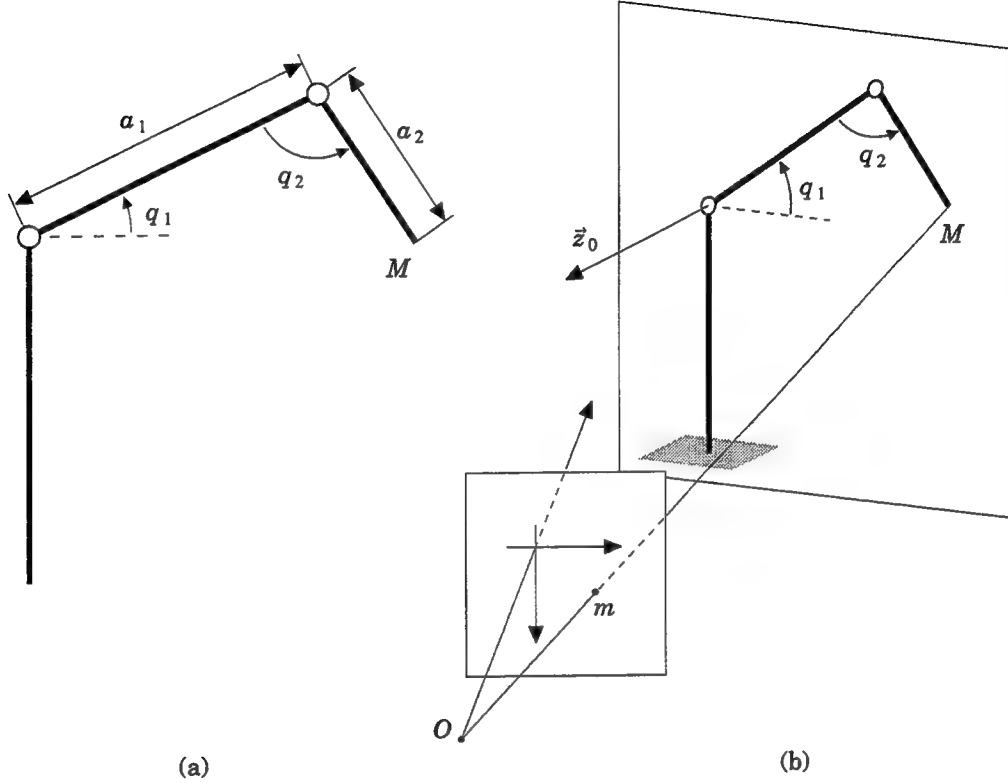
Figure 7 — Hand/eye coordination with a 2D pendulum

3. Case of the 2D Pendulum

3.1 The PKM and its Jacobian matrix

Pendulums are planar manipulators whose joints are all parallel to each other. In practice, a 2D pendulum configuration can be constituted by links S_1, S_2, and S_3 (and joints J_2 and J_3) of a classical manipulator such as a PUMA 560, i.e. by keeping the waist joint fixed. Comparing Figures 7 and 6, we see that $d_1 = d_2 = 0$ and $\alpha_1 = \alpha_2 = 0$. The kinematic map of our 2D pendulum is therefore

$$\kappa: \quad \mathcal{J} \longrightarrow \mathcal{K}$$

$$\mathbf{q} \longmapsto \mathbf{M}_0 = \begin{pmatrix} a_1\,C_1 + a_2\,C_{12} \\ a_1\,S_1 + a_2\,S_{12} \\ 0 \end{pmatrix}.$$

11

3.2 Singularities

Both the kinematic Jacobian matrix and the perceptual Jacobian matrices are 2×2 square matrices. It ensues that $\det \mathbf{J} = \det(\mathbf{P} \cdot \mathbf{K}) = \det \mathbf{P} \cdot \det \mathbf{K}$. We can therefore study independently the singularities of $\mathbf{K}$ and $\mathbf{P}$.

Singularities of $\mathbf{K}$:

$$\mathbf{K} = \begin{pmatrix} -a_1 S_1 - a_2 S_{12} & -a_2 S_{12} \\ a_1 C1 + a_2 C_{12} & a_2 C_{12} \end{pmatrix},$$

After trivial simplifications, we get $\det \mathbf{K} = a_1 a_2 S_2$. Kinematic singularities are therefore solely encountered for $q_2 = 0$ or $q_2 = \pi$ (modulo 2π), which corresponds to configurations where the arm is completely folded or completely extended.

Singularities of $\mathbf{P}$:

It follows from (5) that

$$\mathbf{P} = \frac{1}{Z} \cdot \mathbf{D} \cdot \mathbf{E}_{\psi,\theta,\phi} \quad \Rightarrow \quad \det \mathbf{P} = \frac{1}{Z^2} \cdot \det \left(\mathbf{D} \cdot \mathbf{E}_{\psi,\theta,\phi} \right).$$

Although the factor $1/Z^2$ depends on all the variables and parameters along the kinematic and perceptual chains, it does not affect the study of singularities so we will treat it as a constant from now on.

$$\mathbf{D} \cdot \mathbf{E}_{\psi,\theta,\phi} = \begin{pmatrix} f & 0 & -x \\ 0 & f & -y \end{pmatrix} \cdot \begin{pmatrix} C_\phi C_\psi - S_\phi C_\theta S_\psi & -C_\phi S_\psi - S_\phi C_\theta C_\psi & 0 \\ S_\phi C_\psi + C_\phi C_\theta S_\psi & -S_\phi S_\psi + C_\phi C_\theta C_\psi & 0 \\ S_\theta S_\psi & S_\theta C_\psi & 0 \end{pmatrix}$$

$$= \begin{pmatrix} f \cdot (C_\phi C_\psi - S_\phi C_\theta S_\psi) - x S_\theta S_\psi & f \cdot (-C_\phi S_\psi - S_\phi C_\theta C_\psi) - x S_\theta C_\psi \\ f \cdot (S_\phi C_\psi + C_\phi C_\theta S_\psi) - y S_\theta S_\psi & f \cdot (-S_\phi S_\psi + C_\phi C_\theta C_\psi) - y S_\theta C_\psi \end{pmatrix}.$$

Most terms in the developed form of $\det \mathbf{P}$ cancel out and we obtain the following simple form:

$$\det \mathbf{P} = \frac{f}{Z^2} \cdot (x,y,f) \cdot \begin{pmatrix} S_\phi S_\theta \\ -C_\phi S_\theta \\ C_\theta \end{pmatrix}. \tag{7}$$

The rightmost term in (7) happens to be the normal to the plane of the manipulator. We can therefore draw the following conclusions:

- ψ has no effect on perceptual singularities. This result should not be surprising since the axis of this rotation is perpendicular to the plane of the manipulator.

- A joint configuration $\mathbf{q}$ is a *perceptual* singularity of the PKM if and only if line Om lies in the plane of the manipulator. In other words, $\mathbf{q}$ is a singular joint configuration if and only if the camera's optical center lies in the plane of the manipulator.

- Further analysis reveals that the rank of $\mathbf{P}$ cannot be zero.

12

We can plot the PCS and its singularities using the same graphic trick as in [11], that is, we give depth to the surface by plotting (x, q_1, y) as a function of q_1 and q_2 (see [9] for details and justifications). Figure 8 shows a PCS (the same as in Figure 2, but seen from a different point of view) and its singularities: the two singular curves corresponding to $q_2 = 0$ and $q_2 = \pi$ and that constitute the "skeleton" of the PCS.
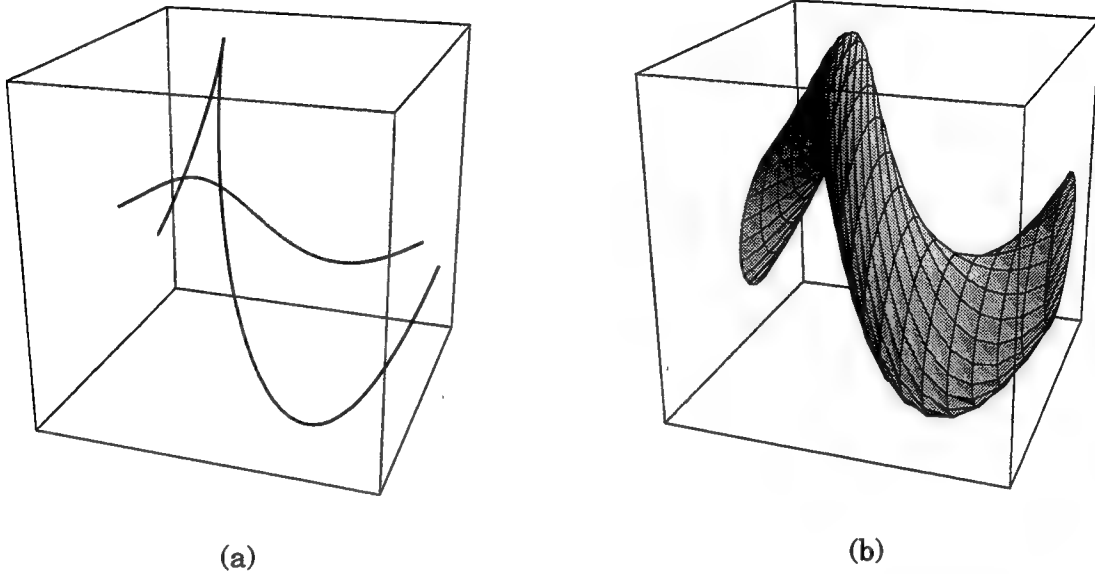

<div align="center">(a)   (b)</div>

Figure 8 — (a) The singularities of the PCS, which define the "skeleton of the surface."
(b) The corresponding PCS itself.

3.3 Bifurcations

The 2D pendulum does not offer much to the observer in terms of possibilities of topologically interesting actions. On the one hand, there are two kinematic singularities on which camera displacements have no significant topological effects. On the other hand, there is one particular degenerate plane, that of the pendulum itself, in which the camera's optical center simply must not lie.

The observer can therefore obtain a topological modification of sorts by passing through the plane of the pendulum. As we see in Figure 9, the PCS is flattened and the displacements of m occur in the image along the dark straight line shown in Figure 9(d).

Any displacement of the observer whose projection's endpoint lies on this line simply keeps the observer in a degenerate configuration. Solely in terms of the topology of the PCS, i.e. degenerate vs. non-degenerate,[9] a good displacement of the observer is therefore any displacement that contains a component normal to the pendulum's plane.

---

[9] As is generally the case with methods based on a topological analysis, we can only talk of "good" and "bad" displacements, without intermediate graduations. For example, the results presented here do not allow us to satisfactorily answer the question: Which of the the two "good" displacements shown in Figure 9(d) is better?

(a)

(b)

(c)

(d)
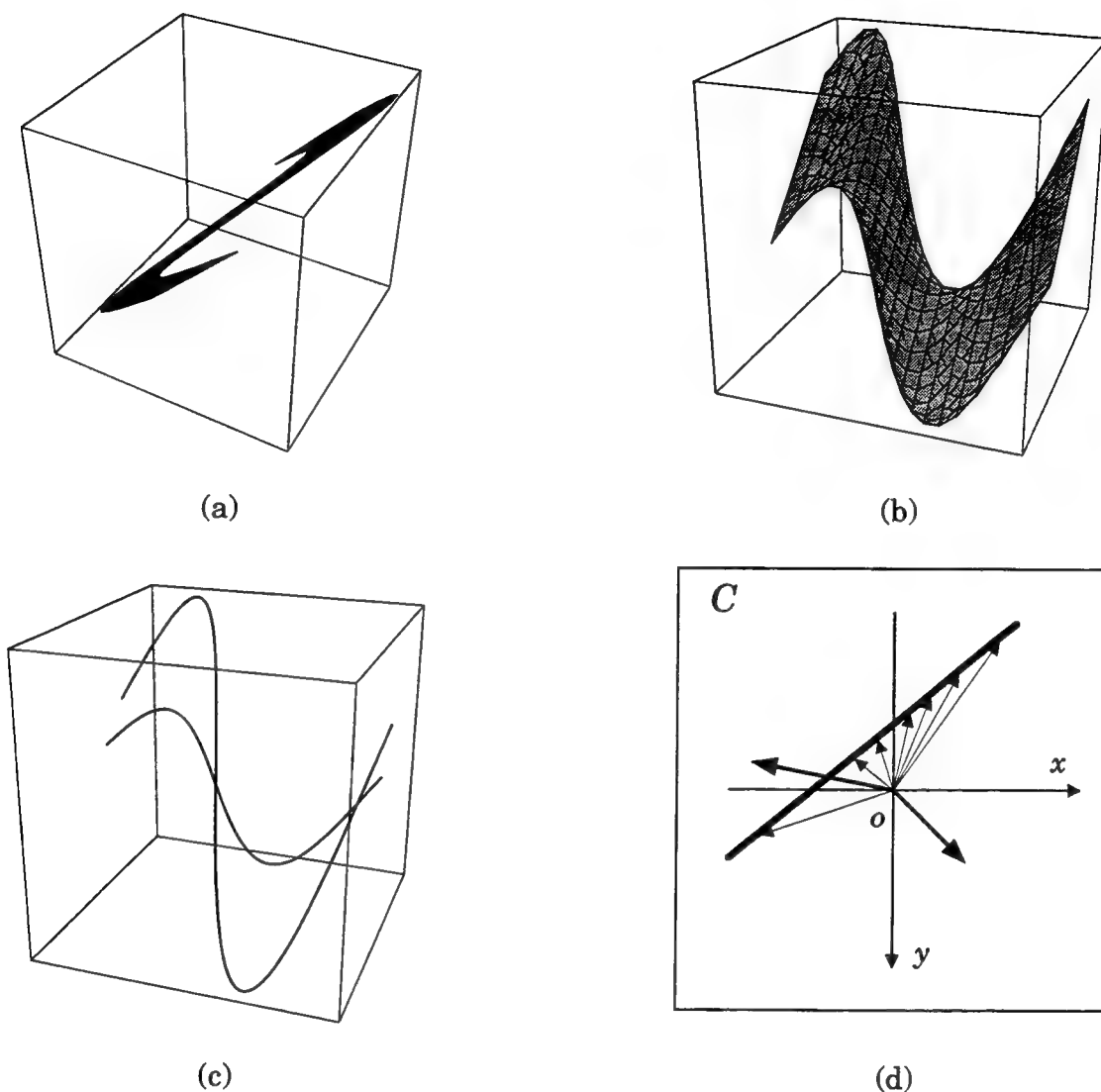
Figure 9 — (a) and (b) Different views of a degenerate PCS. (c) Its singularities. (d) The scene in the camera space.

Figure 10 shows the transformation of the PCS as the optical center crosses the pendulum's plane. In Figure 10(a), we can see the trajectory followed by the observer, parallel to the Z axis of the pendulum. The PCS corresponding to $Z_c > 0$ is shown in Figure 10(b). For $Z_c = 0$, the observer lies in the plane of the pendulum and we get the flat, degenerate PCS (Figure 10(c)), but as soon as that plane has been crossed, the non-degenerate PCS is observed again (Figure 10(d)). Not surprisingly, however, since the pendulum is seen from the other side of its plane of motion, the sign of the torsion of the PCS around its main axis has changed.

(a)

(b)

$Z_c > 0$ $Z_c = 0$ $Z_c < 0$

(c)   (d)   (e)

Figure 10 — Changes in the topology of the PCS as the observer crosses the pendulum's plane

15

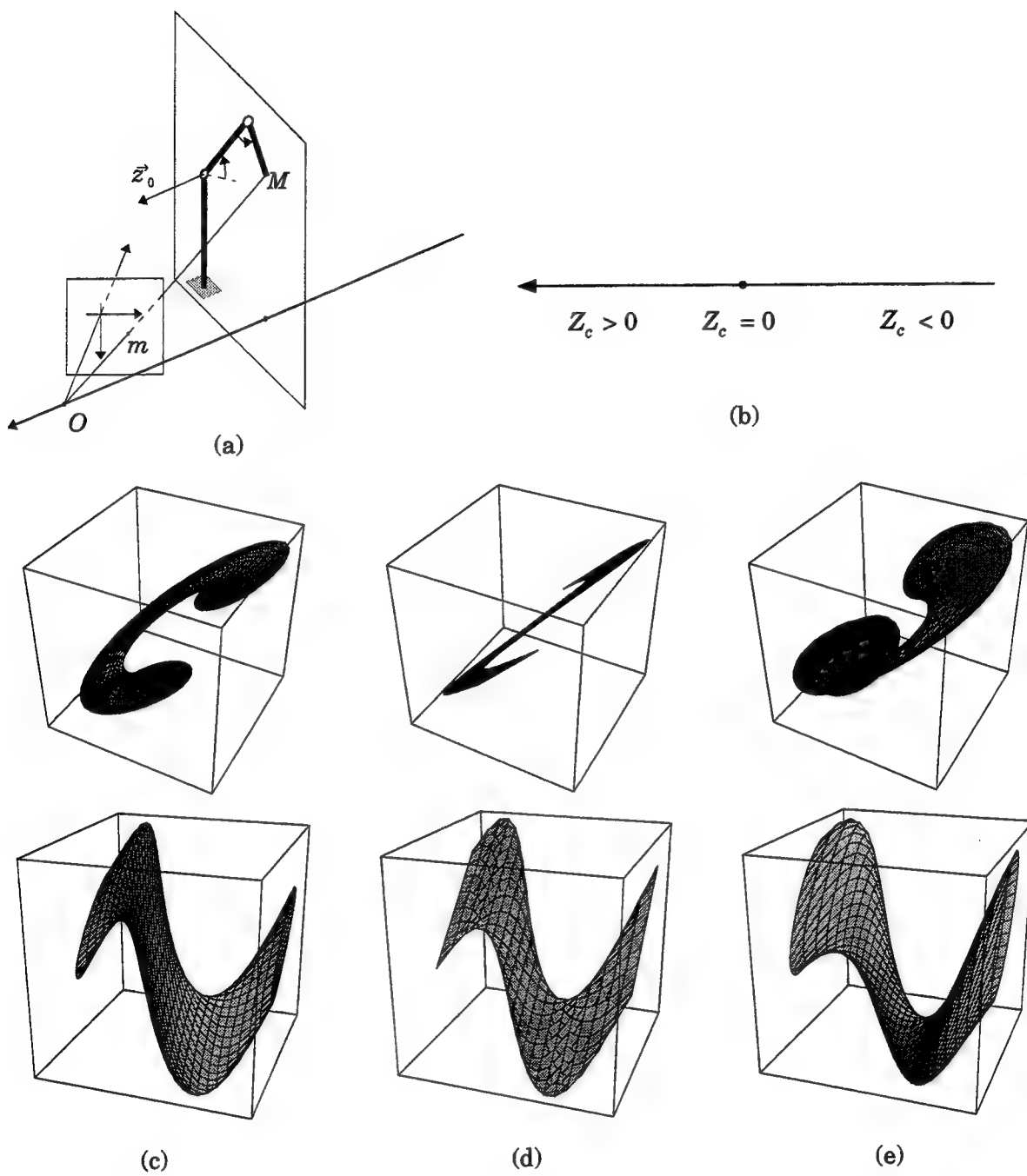# 4. Singularities of the 2-dof (2R) Manipulator

4.1 Kinematic Singularities

4.1.1 The D-H parameters

The type of manipulator we are considering here has its rotation axes perpendicular to each other, which corresponds to the configuration presented by the first two joints, J_0 and J_1 of most manipulators. This amounts to setting the D-H parameters α_0, α_1, and α_2 to $0, \pm\pi/2$, and 0 respectively, as shown in Figure 11. By far the most common type of industrial manipulator is the one with $a_1 = 0$ and $d_2 \neq 0$. Configurations with $a_1 = d_2 = 0$ are generally reserved for small manipulators such as the Mitsubishi Movemaster II arm on which we happen to have performed our experiments, while the case $d_2 = 0, a_1 \neq 0$ is rarely encountered. Finally, a_2 cannot be zero for this type of manipulator and generally $|a_2| \geq |a_1|$, $|a_2| \geq |d_2|$. Since $a_2 \neq 0$, we could therefore use it as a unit and normalize all the parameters but we will simply[10] assume from now on that it is strictly positive.

4.1.2 The kinematic map

In the case of the 2R 2-dof manipulator, the kinematic map κ maps two joint coordinates to the three Cartesian coordinates of the endpoint, M, relative to $\mathcal{R}_0$:

$$\kappa : \mathbb{R}^2 \longrightarrow \mathbb{R}^3$$

$$\begin{pmatrix} q_1 \\ q_2 \end{pmatrix} \longmapsto \mathbf{M}_0 = \begin{pmatrix} X_0 \\ Y_0 \\ Z_0 \end{pmatrix}.$$

The homogeneous transition matrices $\mathbf{A}_{ij}$ take the following form:

$$\mathbf{A}_{01} = \begin{pmatrix} C_1 & 0 & -S_1 & a_1 C_1 \\ S_1 & 0 & C_1 & a_1 S_1 \\ 0 & -1 & 1 & 0 \\ 0 & 0 & 0 & 1 \end{pmatrix} \qquad \mathbf{A}_{12} = \begin{pmatrix} C_2 & -S_2 & 0 & a_2 C_2 \\ S_2 & C_2 & 0 & a_2 S_2 \\ 0 & 0 & 1 & d_2 \\ 0 & 0 & 0 & 1 \end{pmatrix}.$$

The global transition matrix is then

$$\mathbf{A}_{02} = \begin{pmatrix} C_1 C_2 & -C_1 S_2 0 & -S_1 & a_1 C_1 + a_2 C_1 C_2 - d_2 S_1 \\ S_1 C_2 & -S_1 S_2 & C_1 & a_1 S_1 + a_2 S_1 C_2 + d_2 C_1 \\ -S_2 & -C_2 & 0 & -a_2 S_2 \\ 0 & 0 & 0 & 1 \end{pmatrix}.$$

We compute the kinematic map's Jacobian matrix, following (2):

$$\mathbf{K} = \begin{pmatrix} -a_1 S_1 - a_2 S_1 C_2 - d_2 C_1 & -a_2 C_1 S_2 \\ a_1 C_1 + a_2 C_1 C_2 - d_2 S_1 & -a_2 S_1 S_2 \\ 0 & -a_2 C_2 \end{pmatrix}. \tag{8}$$

---

[10] I would rather not give up the ability to check the homogeneity of my equations by posing $a_2 = 1$.
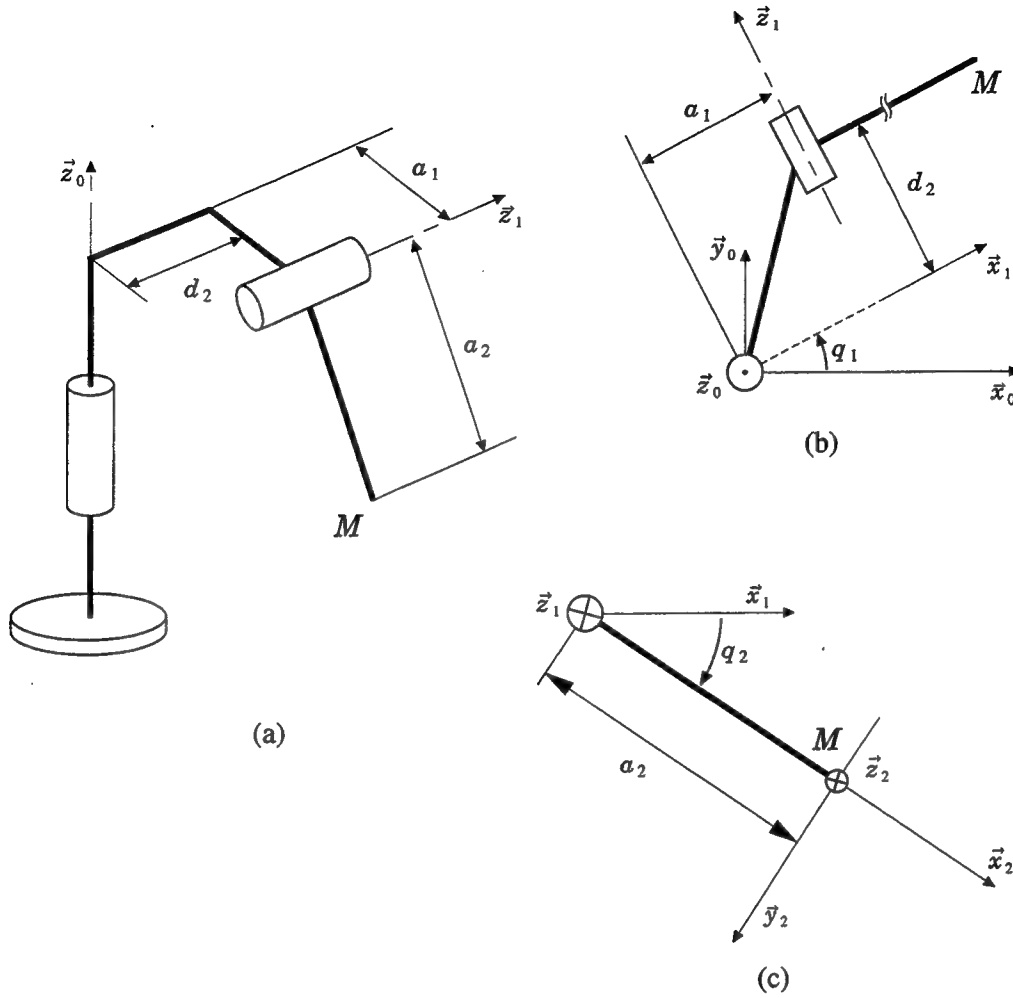
Figure 11 — Denavit-Hartenberg parameters for a 2-dof manipulator

4.1.3 Kinematic singularities

Kinematic singularities are configurations (q_1, q_2), for which $\mathbf{K}$ does not have full rank, that is, $\det \mathbf{K} = 0$. From the lower right element of $\mathbf{K}$ we can distinguish (since, as we mentioned earlier, $a_2 \neq 0$) two cases.

- Case 1: $C_2 = 0$. Then the joint configuration is singular if and only if

$$\begin{vmatrix} -a_1 S_1 - d_2 C_1 & C_1 \\ a_1 C_1 - d_2 S_1 & S_1 \end{vmatrix} = a_1 = 0,$$

   which, as we mentioned, is true for most manipulators.

- Case 2: $C_2 \neq 0$. Then in order for the joint configuration to be singular, the elements on the left column of $\mathbf{K}$ must be zero:

$$\begin{cases} -a_1 S_1 - a_2 S_1 C_2 - d_2 C_1 = 0 \\ a_1 C_1 + a_2 C_1 C_2 - d_2 S_1 = 0, \end{cases} \tag{9}$$

17

Combining both equations, we obtain $d_2 = 0$, which, as we mentioned earlier, is false for most industrial manipulators, but true for our Mitsubishi Movemaster II. After substituting in (9), we get

$$S_1 \cdot (a_1 + a_2 C_2) = C_1 \cdot (a_1 + a_2 C_2) = 0$$

Since S_1 and C_1 cannot be simultaneously equal to zero, we must therefore have $C_2 = \cos q_2 = -a_1/a_2$.

In conclusion:

If $a_1 = 0$ (whether d_2 is null or not), a singularity is observed for $q_2 = \pm\pi/2$ and any value of q_1. In this configuration, the Cartesian motion produced by the two joints are locally collinear and can therefore be chosen to cancel each other out.

If $d_2 = 0$, a singularity is observed for $q_2 = \pm \arccos(-a_1/a_2)$ and any value of the first joint angle, q_1. In this configuration, the endpoint lies along the axis of the first joint, making it therefore—locally—reducing the manipulator to one degree of freedom.

4.2 Singularities of the PKM

Since, as in the case of the 2D pendulum, we are only tracking one hand point, the perceptual Jacobian matrix is simply

$$\mathbf{P} = \frac{1}{Z} \cdot \mathbf{D} \cdot \mathbf{E}_{\psi,\theta,\phi}.$$

The rank of $\mathbf{J} = \mathbf{P} \cdot \mathbf{K}$ is less than 2 if and only if there exists a vector $\mathbf{u} \in \mathbb{R}^3$, $\mathbf{u} \neq \mathbf{0}$ such that $\mathbf{J} \cdot \mathbf{u} = \mathbf{P} \cdot \mathbf{K} \cdot \mathbf{u} = \mathbf{0}$. In other words, the configuration is singular if and only if $\operatorname{Im}\mathbf{K} \cap \operatorname{Ker}\mathbf{P} \neq \{\mathbf{0}\}$.

Identification of Ker$\mathbf{P}$:

$$\operatorname{Ker}\mathbf{P} = \left\{ \mathbf{v} \in \mathbb{R}^3 : \mathbf{D} \cdot \mathbf{E} \cdot \mathbf{v} = \mathbf{0} \right\}.$$

Since $\mathbf{E}$ is an orthogonal matrix, we can define $\mathbf{w}$ such that $\mathbf{v} = \mathbf{E}' \cdot \mathbf{w} = \mathbf{E}^{-1} \cdot \mathbf{w}$. Then, $\mathbf{D} \cdot \mathbf{E} \cdot \mathbf{v} = 0 \iff \mathbf{D} \cdot \mathbf{w} = 0 \iff \exists \nu \in \mathbb{R} : \mathbf{w} = \nu \cdot \mathbf{m}$ or, since $\mathbf{m}$ and $\mathbf{M}$ are collinear,

$$\operatorname{Ker}\mathbf{P} = \left\{ \mu \cdot \mathbf{E}' \cdot \mathbf{M} : \mu \in \mathbb{R} \right\}. \tag{10}$$

Identification of Im$\mathbf{K}$: From (8), we see that

$$\operatorname{Im}\mathbf{K} = \left\{ \alpha\, \mathbf{e}_1 + \beta\, \mathbf{e}_2 : (\alpha, \beta) \in \mathbb{R}^2 \right\}, \tag{11}$$

where $\quad \mathbf{e}_1 = \begin{pmatrix} -a_1 S_1 - a_2 S_1 S_2 - d_2 C_1 \\ a_1 C_1 + a_2 C_1 C_2 - d_2 S_1 \\ 0 \end{pmatrix}$ and, since $a_2 \neq 0$, $\mathbf{e}_2 = \begin{pmatrix} C_1 S_2 \\ S_1 S_2 \\ C_2 \end{pmatrix}$.

Singularities of π:

We can see from (10) and (11) that a necessary and sufficient condition for joint configuration $\mathbf{q} = (q_1, q_2)'$ to be singular is that $\det(\mathbf{e}_1, \mathbf{e}_2, \mathbf{E}' \cdot \mathbf{M}) = 0$.

It turns out that the equations are simpler if the six camera pose parameters are regrouped into the three coordinates of the optical center relative to the robot's base coordinate system $\mathcal{R}_0$. We will therefore develop $\mathbf{M}$ in our equations using (4) rather than (3), so that

$$\mathbf{E}'_{\psi,\theta,\phi} \cdot \mathbf{M} = \mathbf{M}_0 - \mathbf{C} = \begin{pmatrix} a_1 C_1 + a_2 C_1 C_2 - d_2 S_1 - X_c \\ a_1 S_1 + a_2 S_1 C_2 + d_2 C_1 - Y_c \\ -a_2 S_2 - Z_c \end{pmatrix}.$$

The condition for the existence of a singularity then becomes

$$\begin{vmatrix} -a_1 S_1 - a_2 S_1 S_2 - d_2 C_1 & C_1 S_2 & a_1 C_1 + a_2 C_1 C_2 - d_2 S_1 - X_c \\ a_1 C_1 + a_2 C_1 C_2 - d_2 S_1 & S_1 S_2 & a_1 S_1 + a_2 S_1 C_2 + d_2 C_1 - Y_c \\ 0 & C_2 & -a_2 S_2 - Z_c \end{vmatrix} = 0, \qquad (12)$$

which, after a few simplification steps, can be expressed as an equation in terms of the first joint variable, q_1:

$$\begin{aligned} &\left[a_1 a_2 + \left(a_1^2 + a_2^2 + d_2^2 \right) C_2 + a_1 Z_c S_2 + a_1 a_2 C_2^2 + a_2 Z_c C_2 S_2 \right] + \\ &\left[(-a_1 X_c - d_2 Y_c) C_2 - a_2 X_c C_2^2 \right] \cdot C_1 + \\ &\left[(-a_1 Y_c + d_2 X_c) C_2 - a_2 Y_c C_2^2 \right] \cdot S_1 = 0, \end{aligned} \qquad (13)$$

or

$$\beta_0 + \beta_1 \cdot C_1 + \beta_2 \cdot S_1 = 0, \qquad (14)$$

where the β_i are functions of the second joint variable q_2 and of the pose vector $\mathbf{C}$:

$$\begin{aligned} \beta_0(q_2) &= a_1 a_2 + \left(a_1^2 + a_2^2 + d_2^2 \right) C_2 + a_1 Z_c S_2 + a_1 a_2 C_2^2 + a_2 Z_c C_2 S_2, \\ \beta_1(q_2) &= (-a_1 X_c - d_2 Y_c) C_2 - a_2 X_c C_2^2, \\ \beta_2(q_2) &= (-a_1 Y_c + d_2 X_c) C_2 - a_2 Y_c C_2^2. \end{aligned}$$

4.2.1 Case 1: if $\beta_1 \neq 0$ or $\beta_2 \neq 0$

We are trying to find a solution for q_1 as a function of q_2 parameterized by $\mathbf{p}$. For this purpose, we define

$$\beta = \sqrt{\beta_1^2 + \beta_2^2} \quad \text{and} \quad \gamma_0 = -\beta_0/\beta.$$

There are now two cases:

- If $|\gamma_0| > 1$, there is no solution to (14), and therefore no singularity.

- If $|\gamma_0| \leq 1$, we can define $\theta \in [0, 2\pi[$ such that $\cos\theta = \beta_1/\beta$ and $\sin\theta = \beta_2/\beta$.

Then, $(C_1, S_1) \cdot \begin{pmatrix} \cos\theta \\ \sin\theta \end{pmatrix} = \gamma_0$ and the solution to (14) is given by Figure 12:

$$q_1 = \pm \arccos\gamma_0 - \theta \pm 2k\pi, \quad k \in \mathbb{N}.$$

We can already observe that if γ_0 can vary on a neighborhood of 1 (or -1), then a bifurcation will be observed at this point since $n(1^-) = 2$, $n(1) = 1$, and $n(1^+) = 0$. We will study in Appendix B whether this bifurcation is in fact defined and if others exist.
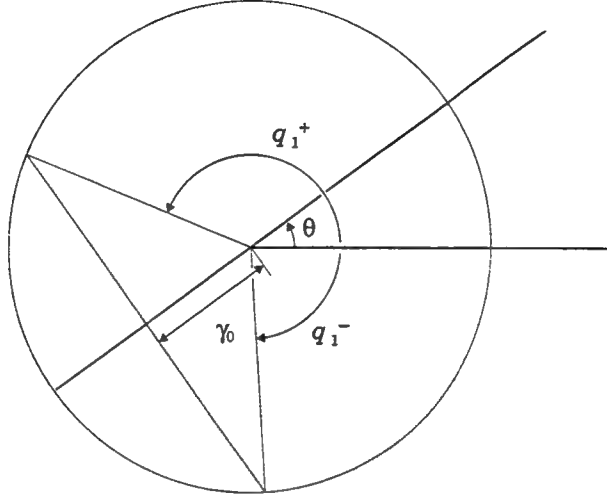

Figure 12 — Solution for $\beta_1^2 + \beta_2^2 \neq 0$

4.2.2 Case 2: $\beta_0 = \beta_1 = \beta_2 = 0$

If $\beta_1 = \beta_2 = 0$, then by factoring out C_2 we get

$$\begin{cases} C_2 (a_1 X_c + d_2 Y_c + a_2 X_c C_2) = 0 \\ C_2 (a_1 Y_c - d_2 X_c + a_2 Y_c C_2) = 0, \end{cases}$$

so that there are again two cases:

- If $C_2 = 0$, then using $\beta_0 = 0$, we obtain $a_1 a_2 + a_1 Z_c S_2 = 0$. So, if $a_1 = 0$, we find again the kinematic singularity we studied in the last subsection. On the other hand, if $a_1 \neq 0$, then there is a perceptual singularity for $Z_c = -a_2 S_2$, i.e. $Z_c = -a_2$ if $q_2 = \pi/2$ and $Z_c = a_2$ if $q_2 = 3\pi/2$.

- If $C_2 \neq 0$, then

$$\begin{cases} a_1 X_c + d_2 Y_c + a_2 X_c C_2 & = 0 \\ a_1 Y_c - d_2 X_c + a_2 Y_c C_2 & = 0. \end{cases}$$

We have a system of linear equations in unknowns X_c and Y_c. The discriminant of the system is

$$D = (a_1 + a_2 C_2)^2 + d_2^2. \tag{15}$$

- If $D = 0$, then $d_2 = 0$ and $C_2 = -a_1/a_2$, which is a kinematic singularity (rarely encountered since generally $d_2 \neq 0$) that we have already studied and on which camera displacements have no effect.

20

- If $D \neq 0$, then a necessary condition for the existence of a singularity is therefore that $X_c = Y_c = 0$ (i.e. the observer is standing along the first joint's rotation axis). In this case, since $\beta_0 = 0$, we must have:

$$a_1 a_2 + \left(a_1^2 + a_2^2 + d_2^2 \right) C_2 + a_1 a_2 C_2^2 = -S_2 \left(a_1 + a_2 C_2 \right) Z_c.$$

* If $S_2 = 0$, then $C_2 = \pm 1 \Rightarrow 2 a_1 a_2 = \pm \left(a_1^2 + a_2^2 + d_2^2 \right)$. This is a viewer-independent condition involving only the D-H parameters, and that is false for all manipulators which we have checked.

* If $S_2 \neq 0$ and $C_2 = -a_1/a_2$, the condition for the existence of a singularity ($\beta_0 = 0$) cannot be satisfied since it requires $d_2 = 0$, in which case we would have $D = 0$, which contradicts the initial hypothesis.

* If $S_2 \neq 0$ and $C_2 \neq -a_1/a_2$, then a perceptual singularity is observed for

$$Z_c = - \frac{a_1 a_2 + \left(a_1^2 + a_2^2 + d_2^2 \right) C_2 + a_1 a_2 C_2^2}{S_2 \left(a_1 + a_2 C_2 \right)}.$$

5. Bifurcations for the 2-dof (2R) Manipulator

5.1 Presentation of the problem

5.1.1 Choice of a state variable

We are interested in the effects that displacements of the observer may have on the topology of the PCS. In other words, we are trying to determine the effect that changes of values for X_c, Y_c, and Z_c may have on the locus of solutions (q_1, q_2) to Equation (13) that we studied in the last subsection.

We therefore have a family of equations with two variables and three perturbation parameters:

$$
\begin{aligned}
G(q_1, q_2; X_c, Y_c, Z_c) = & \left[a_1 a_2 + \left(a_1^2 + a_2^2 + d_2^2 \right) C_2 + a_1 Z_c S_2 + a_1 a_2 C_2^2 + a_2 Z_c C_2 S_2 \right] + \\
& \left[\left(-a_1 X_c - d_2 Y_c \right) C_2 - a_2 X_c C_2^2 \right] \cdot C_1 + \\
& \left[\left(-a_1 Y_c + d_2 X_c \right) C_2 - a_2 Y_c C_2^2 \right] \cdot S_1 \\
= & \ 0.
\end{aligned}
$$

21

Throughout this paper, we will use a capital letter to refer to the family of equations parameterized by the pose of the observer, $G(q_1, q_2; \mathbf{p})$ (resp., $H(q_2, q_1; \mathbf{p})$), while the corresponding small letter name, $g(q_1, q_2)$ (resp. $h(q_2, q_1)$), will be used to refer to a particular element of this family, whenever the context is clear.

The mathematical toolbox most appropriate for our problem is the theory of bifurcations [7], of which we give a rudimentary overview in Appendix A. Since we only have one equation to relate q_1 and q_2, one of these two variables will be treated as the state variable and the other as the bifurcation parameter. We show in Appendix B that, if g and its first two partial derivatives with respect to q_1 are null, then all partial derivatives of arbitrarily high order of g with respect to q_1 are null as well.

We will therefore rather study here what happens if we use $x = q_2$ as the state variable and $\lambda = q_1$ as the bifurcation parameter and we decompose the study into cases based on the Denavit-Hartenberg parameters a_1 and d_2. This means that we study the bifurcations of the family of functions $H(x, \lambda; \mathbf{p}) = H(q_2, q_1; \mathbf{p}) = G(q_1, q_2; \mathbf{p})$.

5.1.2 Notation

In order to facilitate the study of $h(x, \lambda) = h(q_2, q_1)$, we factor it so as to separate as much as possible the terms that depend solely on q_1 and those that depend on q_2:

$$h(q_2, q_1) = (a_1 + a_2 C_2) \cdot (k_3(q_2) - C_2 \cdot k_2(q_1)) + d_2 C_2 \cdot k_1(q_1),$$

where
- $k_1(q_1) = d_2 + X_c \cdot S_1 - Y_c \cdot C_1,$
- $k_2(q_1) = X_c \cdot C_1 + Y_c \cdot S_1,$
- $k_3(q_2) = a_2 + a_1 \cdot C_2 + Z_c \cdot S_2.$

We note in particular that $k_1'(q_1) = k_2(q_1)$, $k_2'(q_1) = d_2 - k_1(q_1)$, and $k_3''(q_1) = a_2 - k_3(q_2)$.

Another important property of our problem is its cylindrical symmetry with respect to the first joint axis, $\vec{z}_0$ (Figure 13(a)). This means that we can simplify the problem by using the distance between the observer and the first joint, $R_c = (X_c^2 + Y_c^2)^{1/2}$, rather than coordinates X_c and Y_c, as long as we use a relative angle to represent the state of the the first joint. Let us consider Figure 13(b), which is drawn in the horizontal plane of the manipulator's reference frame (that is, perpendicular to $\vec{z}_0$). The polar coordinates of the observer's projection onto this plane are therefore (R_c, θ_c), with $X_c = R_c \cos \theta_c$ and $Y_c = R_c \sin \theta_c$.

Substituting for X_c and Y_c in the expressions of k_1 and k_2, we obtain

$$\begin{aligned} k_1(q_1) &= d_2 + R_c \cdot (\cos \theta_c \cdot \sin q_1 - \sin \theta_c \cdot \cos q_1) \\ &= d_2 + R_c \cdot \sin(q_1 - \theta_c) \end{aligned}$$

$$\begin{aligned} k_2(q_1) &= R_c \cdot (\cos \theta_c \cdot \cos q_1 + \sin \theta_c \cdot \sin q_1) \\ &= R_c \cdot \cos(q_1 - \theta_c). \end{aligned}$$
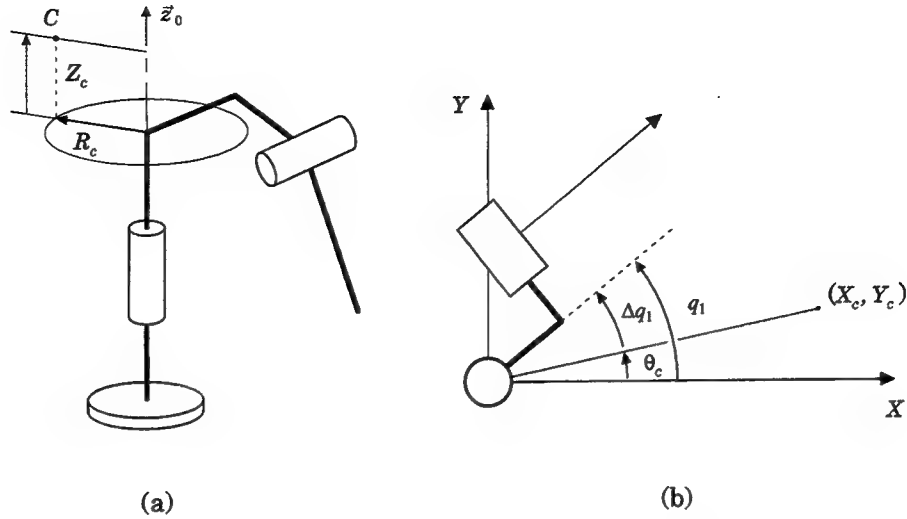
Figure 13 — (a) Cylindrical symmetry of the problem. (b) Representation in the horizontal plane passing through the origin O_0.

The absolute value of the first joint angle only matters in terms of the joint travel, which is not relevant to this study. We can therefore assume without loss of generality that $\theta_c = 0$,[11] so that we obtain

$$k_1(q_1) = d_2 + R_c \cdot \sin q_1$$
$$k_2(q_1) = R_c \cdot \cos q_1.$$

Since, for any pair of real numbers $(K_1, K_2) \neq (0, 0)$, there exists a unique pair of real numbers, $(R_c, q_1) \in \mathbb{R} \times [0, 2\pi]$, such that $k_1(q_1) = K_1$ and $k_2(q_1) = K_2$, we can treat $k_1(q_1)$ and $k_2(q_1)$ as the unknowns of the linear equations $h = 0$ and $h_x = 0$.

5.1.3 Underlying philosophy of the approach

The underlying philosophy of the approach we are following here is that of the theory of singularities, applied to the study of bifurcation problems [7] and in particular to the concept of an *organizing center*. It is probably best to reproduce here the loose description of this "very suggestive, but somewhat vague," term (characteristics shared by most names coined by René Thom) proposed by Golubitsky and Schaeffer:

> "Consider a problem which exhibits a variety of qualitatively different behaviors, depending on various parameters. An organizing center is associated with the distinguished set of values for the parameters such that all (or at least many) of the different behaviors occur for parameter values in a small neighborhood of the distinguished values. Typically at an organizing center the system exhibits its most singular behavior. [...] In particular, quasi-global results may often be obtained by the application of local analysis near an appropriately chosen organizing center."

---

[11] Alternatively, we could pose $\Delta q_1 = q_1 - \theta_c$ and study $h(q_2, \Delta q_1)$, but this leads to cumbersome formulas for the derivatives of h.

23

The various parameters of the system can therefore be treated as *perturbation* terms in the neighborhood of the organizing center. This introduces the second important concept of the approach, that of the *codimension* of a bifurcation problem, which is defined to be the minimum number of parameters necessary to represent all possible perturbations of the organizing center, up to smooth (C^∞) equivalence.

For example, only two parameters suffice to represent (up to smooth equivalence) all possible perturbations of the "pitchfork" bifurcation problem $x^3 - \lambda x = 0$ in the neighborhood of the bifurcation point $(x_0, \lambda_0) = (0, 0)$. Indeed, for any function $g(x, \lambda)$ smooth-equivalent to $x^3 - \lambda x$ in a neighborhood of $(0, 0)$ and any appropriately small perturbation term $p(x, \lambda)$, there exists a pair $(\alpha, \beta) \in \mathbb{R}^2$ such that $g(x, \lambda) + p(x, \lambda)$ is smooth-equivalent to $x^3 + \lambda x + \alpha + \beta x^2$ in a neighborhood of $(0, 0)$. In other words, if n is the codimension of the bifurcation problem under study, it is sufficient to study the perturbations of the organizing center by choosing perturbations in a set $W \subset \mathbb{R}^n$ that is often of finite, small dimension, while the original set of perturbation functions was of infinite, non-denumerable, dimension.

The last important concept of the approach is that of the *transition set*, Σ, of a bifurcation problem, that is, of the subset of $W \subset \mathbb{R}^n$ composed of those n-tuples of perturbation parameters for which one of the basic elementary phenomena—bifurcation, hysteresis, and double limit point (see details in Appendix A or [7])—are observed. Except in the most degenerate cases of bifurcation problems, Σ defines a segmentation of W into connected components (typically, for a bifurcation problem of codimension n, Σ is a set of dimension $n - 1$, for example a set of planar curves when $W = \mathbb{R}^2$).

We now have defined the rudimentary background necessary for understanding the main theorem of the approach [7]:

Main geometric theorem:

> Let $G : U \times L \times W \longrightarrow \mathbb{R}$ be a family of bifurcation problems satisfying
>
> $$G(x, \lambda; \alpha) \neq 0 \quad \forall (x, \lambda, \alpha) \in \partial U \times L \times W.$$
>
> Let α and β be in the same connected component of $W \sim \Sigma$. Then $G(\,\cdot\,, \,\cdot\,; \alpha)$ and $G(\,\cdot\,, \,\cdot\,; \beta)$ are globally equivalent on $U \times L$.

Let us quote from [7] one last time: "In other words, the persistent bifurcation diagrams in the unfolding G are enumerated by the connected components of $W \sim \Sigma$. A priori it is possible that equivalent diagrams could occur in two different components of $W \sim \Sigma$, but we have not found any example where this actually occurs."

Although these results apply regardless of the codimension of the bifurcation problem, only the space of bifurcation problems of codimension ≤ 3 has been completely charted so far. An obvious reason for this limit is that the complexity of topological behavior increases with the codimension of the bifurcation. Another reason is that a geometric interpretation of the results becomes almost impossible when the codimension of the bifurcation (that is, the dimension of W) is greater than 3.

5.1.4 Application to the singularities of the PKM

The family of bifurcation problems that we are studying here is defined by the condition for the nullity of the Jacobian J, for which our model admits four parameters, two of which are active (the camera pose parameters, Z_c and R_c), and two of which are fixed (Denavit-Hartenberg parameters a_1 and d_2).

Ideally, we would like to study the organizing center for this general system. It turns out, unfortunately, that it is possible to pick values for a_1, d_2, Z_c, and R_c that result in an organizing center of very high codimension. It follows that our study of the bifurcations of $h(q_2, q_1)$ must be decomposed into cases, based on the geometry of the manipulator, that is, on the relative values of its Denavit-Hartenberg a_1, a_2, and d_2 (Figure 14).
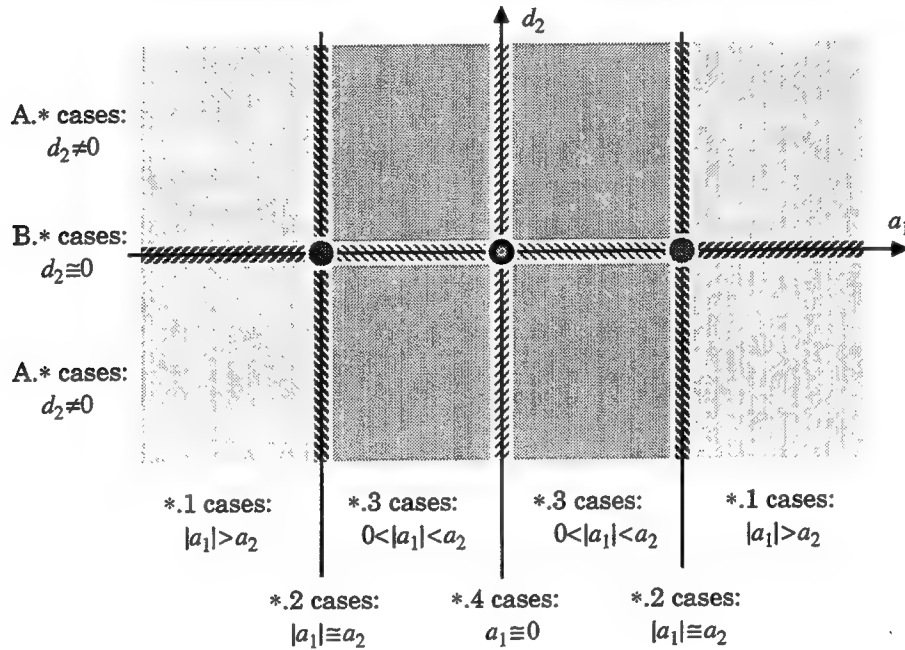

Figure 14 — Decomposition into cases, based on the geometry of the manipulator

For some cases of manipulator geometry, the "disappearing" organizing center will then be replaced by another, simpler organizing center. In some other cases, the "disappearance" of the underlying organizing center will result in the emergence of several competing, simpler organizing centers.

In order to illustrate this comment, let us consider the case of a system whose underlying organizing center is a pitchfork bifurcation (see Appendix A), but for which only one parameter is available (through the model) to perturb the bifurcation equation. Let us first consider the simple case where $\alpha = \alpha_1 \neq 0$ is fixed and β is the parameter that can be controlled. In other words, we are restricting the study to the subset $\{\alpha_1\} \times \mathbb{R} \subset W$ (Figure 15). In this case, as β varies from β_1 to β_2, a modification of the topology of the bifurcation diagram is observed, for $\beta = \beta_0$, that can be satisfactorily explained in terms of the *hysteresis* bifurcation $x^3 - \lambda = 0$. In this case, we can say that a simpler organizing center has "emerged" once the "true" organizing center had been removed.

Note, however, that this "emerging" organizing center does not tell us anything about the parabolic branch of the bifurcation diagram.
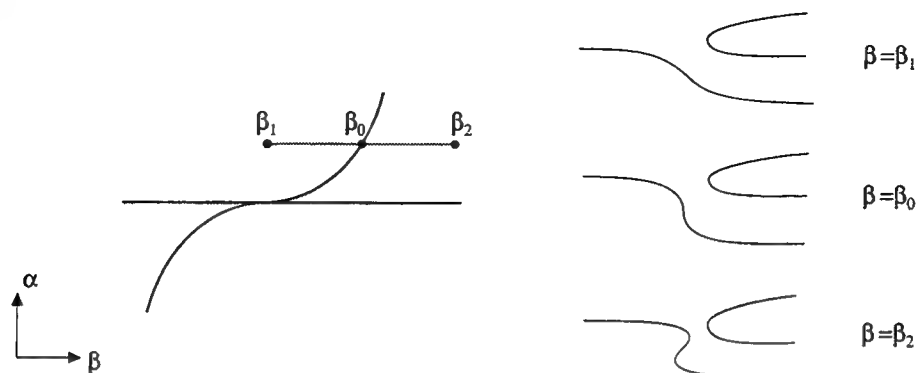

Figure 15 — A simple path across the space of perturbations

The problem is much more complex if a more general path is chosen. Let us for example consider the parametric path $(\alpha(\delta), \beta(\delta))$ across W shown in Figure 16.[12] This time, as δ varies from δ_1 to δ_2, two different changes can be observed, which can be explained *separately* in terms of the *hysteresis* bifurcation $x^3 - \lambda = 0$ and of the *simple bifurcation* $x^2 - \lambda^2 = 0$. It is clear that whatever explanation we could present, based on the plots obtained as δ varies, would not provide the sort of global view of the problem (in particular, regarding the changes observed between δ_0 and δ_0') that the pitchfork organizing center does.
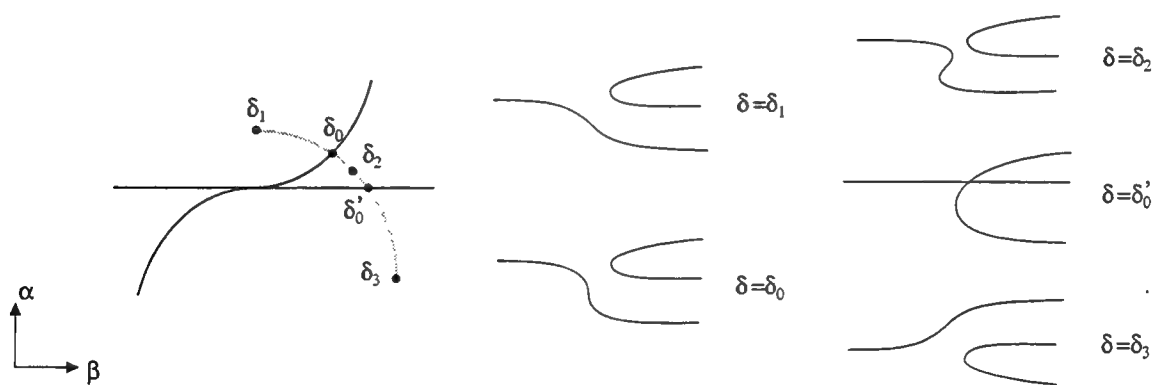
Figure 16 — A more complex path across the space of perturbations

Sometimes, recognizing the perturbed bifurcation diagrams of these "emerging" organizing centers requires some practice. A reason for that is that the branches of the bifurcation diagrams then rarely continue cleanly to infinity. Instead, separate branches join and there will sometimes be another bifurcation to consider at the junction point. Again, both bifurcations would be explained as part of the same phenomenon if the "true"

---

[12] Of course, the actual physical parameters accessible to the experimenter may generate any kind of path in W, for example one containing several loops that all intersect the transition set.

organizing center were accessible to analysis. Let us consider for example the bifurcation diagrams shown in Figure 17. All correspond to perturbed diagrams of the pitchfork bifurcation that appear as a part of the *winged cusp* elementary bifurcation (codimension 3).[13]

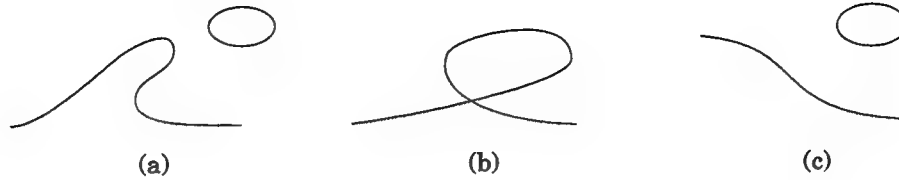(a)   (b)   (c)

Figure 17 — Perturbed forms of the pitchfork appearing as a part of the *winged cusp* bifurcation

For some cases of manipulator geometry, the bifurcation problem will still contain an organizing center of codimension greater than 3.[14] On can therefore wonder if the displacements of the observer could not be restricted so as to remain in the neighborhood of one of the simpler organizing centers, and avoid the most degenerate ones. This suggestion is not completely groundless: after all, with most practical hand/eye systems, the observer cannot move freely with respect to the manipulator, as it is constrained by the mechanism that activates it (in particular, it is fairly frequent that Z_c is constrained to be positive, as in the case of the human hand/eye system, or negative, but cannot cross the plane $Z_c = 0$). In this case, we might be able to describe the topological changes happening *within a few branches of the bifurcation diagram, and for small camera displacements*. We would still, however, be unable to indicate *a priori* what the other branches of the bifurcation diagram may look like. Even if we we plot bifurcation diagrams for a very large number of poses of the camera, we would be unable to guarantee that we have not missed some local phenomenon.

5.1.5 Symmetry and periodicity of the PKM

We notice that S_2 and Z_c appear in the expression of H only when multiplied by each other so that $H(q_2, q_1; Z_c, R_c) = H(-q_2, q_1; -Z_c, R_c)$. As a consequence, we can restrict our study of the perturbed bifurcations of h to the half of the perturbation space corresponding to $Z_c \geq 0$,[15] knowing that the topology for the other half can be built by simple symmetry.

Since q_1 only appears in the expression of h and its derivatives in terms that are multiplied by R_c (i.e. $R_c \cos q_1$ and $R_c \sin q_1$), setting $R_c = 0$ would effectively eliminate

---

[13] There is obviously something artificial in my saying "Let us imagine we knew nothing of the winged cusp bifurcation (resp. pitchfork bifurcation) and then looked at this diagram; wouldn't it be hard then to figure out what is going on?" The point here is that, for some geometries of manipulators that we will have to study, the underlying organizing center is not available to us, since it is deep in uncharted mathematical territory.

[14] One of these cases will produce *the* organizing center of the entire system, regardless of whether the pose of the camera that it calls for is actually reachable or not: For many cases in our study of the PKM, the bifurcation of highest codimension is obtained when $Z_c = 0$ and/or $R_c = 0$, when the corresponding point in fact belongs to the physical manipulator itself, and cannot therefore be reached by the camera.

[15] Alternatively, we could restrict our study to one half of the Joint Space: $(q_2, q_1) \in [0, \pi] \times [0, 2\pi[$, which leads to simpler individual cases, but a more complex task of pasting the symmetric halves together.

the first joint angle, thus resulting in a very degenerate topology. We will therefore only consider the case $R_c > 0$ in our study.

Finally, we should mention that, since we ignore here the constraints imposed by joint travel, all branches of the bifurcation diagram "wrap around" to form closed curves anyway. This takes care of the the non-nullity condition on the boundary $\partial U \times L \times W$, since U is in fact a Jordan curve and has no boundary proper ($U \times L$ is simply a torus).

5.2 Manipulator Geometry Type A.1: $d_2 \neq 0$ and $|a_1| > a_2$

In this case, we have a fairly interesting behavior of function h, with no less than four "emerging organizing centers," plus a simple bifurcation and two "type 0" bifurcations that are connected to—but not directly related to—some of these centers.

5.2.1 Identification of the bifurcations

Proposition 1:

For any 2-dof manipulator such that its Denavit-Hartenberg parameters satisfy $d_2 \neq 0$ and $|a_1| > a_2$, there exist a unique triple of configurations of the hand/eye system, $\mathcal{H}_{1-} = (x_{1-}, \lambda_{1-}; Z_{c_{1-}}, R_{c_{1-}})$, $\mathcal{H}_{1+} = (x_{1+}, \lambda_{1+}; Z_{c_{1+}}, R_{c_{1+}})$, and $\mathcal{H}_2 = (x_2, \lambda_2; Z_{c_2}, R_{c_2})$, such that

$$H(x, \lambda; Z_{c_{1-}}, R_{c_{1-}}), \text{ in a neighborhood of } (x_{1-}, \lambda_{1-}),$$
$$H(x, \lambda; Z_{c_{1+}}, R_{c_{1+}}), \text{ in a neighborhood of } (x_{1+}, \lambda_{1+}), \text{ and}$$
$$H(x, \lambda; Z_{c_2}, R_{c_2}), \quad \text{ in a neighborhood of } (x_2, \lambda_2),$$

are all equivalent to the *quartic fold* bifurcation (type 7):

$$x^4 + \delta\lambda = 0, \quad \text{with } \delta_{1-} = \operatorname{Sgn} d_2, \ \delta_{1+} = -\operatorname{Sgn} d_2, \text{ and } \delta_2 = -\operatorname{Sgn}(a_1 d_2).$$

These hand/eye configurations are defined as follows:

A dual solution ($\mathcal{H}_{1-}$ and $\mathcal{H}_{1+}$):

$$x_{1-} = \pi \quad \lambda_{1-} = -\operatorname{Sgn}(d_2) \cdot \pi/2 \quad Z_{c_{1-}} = 0 \quad R_{c_{1-}} = \frac{d_2^2 + (a_1 - a_2)^2}{|d_2|} \qquad (16)$$

$$x_{1+} = 0 \quad \lambda_{1+} = -\operatorname{Sgn}(d_2) \cdot \pi/2 \quad Z_{c_{1+}} = 0 \quad R_{c_{1+}} = \frac{d_2^2 + (a_1 + a_2)^2}{|d_2|} \qquad (17)$$

An isolated solution ($\mathcal{H}_2$):

$$\cos x_2 = -a_2/a_1 \qquad \sin x_2 = -\frac{\sqrt{a_1^2 - a_2^2}}{|a_1|}, \qquad (18)$$

$$Z_{c_2} = \frac{2|a_1|a_2\sqrt{a_1^2 - a_2^2}}{2a_1^2 - a_2^2},$$

$$K_1^* = d_2 + R_{c_2}\sin\lambda_2 = \frac{(a_1^2 - a_2^2)^2}{d_2(2a_1^2 - a_2^2)}$$

$$K_2^* = R_{c_2}\cos\lambda_2 = \frac{3a_1(a_1^2 - a_2^2)}{2a_1^2 - a_2^2}.$$

28

Proposition 2:

For any 2-dof manipulator such that its Denavit-Hartenberg parameters satisfy $d_2 \neq 0$ and $|a_1| > a_2$, then *for the same values of the second joint angle and poses of the camera that give the dual quartic fold bifurcations*, $(x_{1-}, Z_{c_{1-}}, R_{c_{1-}})$ and $(x_{1+}, Z_{c_{1+}}, R_{c_{1+}})$, there exists a unique pair of values of the first joint angle, $(\lambda_{1'-}, \lambda_{1'+})$, to which corresponds a unique pair of hand/eye configurations, $\mathcal{H}_{1'-} = (x_{1-}, \lambda_{1'-}, Z_{c_{1-}}, R_{c_{1-}})$ and $\mathcal{H}_{1'+} = (x_{1+}, \lambda_{1'+}, Z_{c_{1+}}, R_{c_{1+}})$, such that

$$H(x, \lambda; Z_{c_{1-}}, R_{c_{1-}}), \text{ in a neighborhood of } (x_{1-}, \lambda_{1'-}), \text{ and}$$
$$H(x, \lambda; Z_{c_{1+}}, R_{c_{1+}}), \text{ in a neighborhood of } (x_{1+}, \lambda_{1'+}),$$

are equivalent to the type 0 bifurcation:

$$x^2 + \delta\lambda = 0 \quad \text{with } \delta_{1'-} = -\text{Sgn } d_2 \text{ and } \delta_{1'+} = \text{Sgn } d_2.$$

The values of the first joint angle corresponding to these bifurcations are defined as follows:

$$\cos \lambda_{1'-} = \frac{2|d_2| \cdot (a_1 - a_2)}{(a_1 - a_2)^2 + d_2^2} \quad \text{and} \quad \sin \lambda_{1'-} = \frac{\text{Sgn } d_2 \cdot \left((a_1 - a_2)^2 - d_2^2\right)}{(a_1 - a_2)^2 + d_2^2} \qquad (19)$$

$$\cos \lambda_{1'+} = \frac{2|d_2| \cdot (a_1 + a_2)}{(a_1 + a_2)^2 + d_2^2} \quad \text{and} \quad \sin \lambda_{1'+} = \frac{\text{Sgn } d_2 \cdot \left((a_1 + a_2)^2 - d_2^2\right)}{(a_1 + a_2)^2 + d_2^2} \qquad (20)$$

Proposition 3:

For any 2-dof manipulator such that its Denavit-Hartenberg parameters satisfy $d_2 \neq 0$ and $|a_1| > a_2$, then there exists a unique hand/eye configuration $\mathcal{H}_0 = (x_0, \lambda_0; Z_{c_0}, R_{c_0})$ such that $H(x, \lambda; Z_{c_0}, R_{c_0})$ is equivalent in a neighborhood of (x_0, λ_0) to the *pitchfork* bifurcation (type 6):

$$x^3 + \delta\lambda x = 0, \quad \text{with } \delta = \text{Sgn}(a_1 d_2)$$

The hand eye configuration corresponding to this organizing center is defined as follows:

$$x_0 = q_2^* = -\pi/2,$$

$$Z_{c_0} = a_2,$$

$$R_{c_0} = \frac{\sqrt{\left(a_1^2 - 2d_2^2\right)^2 + 9a_1^2 d_2^2}}{2|d_2|}, \qquad (21)$$

$$\sin \lambda_0 = \frac{a_1^2 - 2d_2^2}{2d_2 R_{c_0}}, \quad \text{and} \quad \cos \lambda_0 = \frac{3a_1}{2R_{c_0}} \qquad (22)$$

29

<u>Proposition 4:</u>

For any 2-dof manipulator such that its Denavit-Hartenberg parameters satisfy $d_2 \neq 0$ and $|a_1| > a_2$, then *for the same pose of the camera*, (Z_{c_0}, R_{c_0}), *and value of the second joint angle*, $q_2 = x_0$, *that give the pitchfork bifurcation*, there exists a unique value of the first joint angle, $\lambda_{0'}$, defining a unique hand/eye configuration $\mathcal{H}_{0'} = (x_0, \lambda_{0'}, Z_{c_0}, R_{c_0})$, such that $H(x, \lambda; Z_{c_0}, R_{c_0})$ is equivalent in a neighborhood of $(x_0, \lambda_{0'})$ to the *simple bifurcation* (type 2):

$$x^2 - \lambda^2 = 0.$$

The value of the first joint angle corresponding to this organizing center is defined as follows:

$$\cos \lambda_{0'} = \frac{a_1}{2R_{c_0}} \quad \text{and} \quad \sin \lambda_{0'} = -\frac{a_1^2 + 2d_2^2}{2d_2 R_{c_0}}. \tag{23}$$

5.2.2 Proof of these propositions

All possible organizing centers for this geometry of manipulator are covered by three cases studied in Appendix B: Cases 3.2.2 (configurations $\mathcal{H}_{1-}$, $\mathcal{H}_{1+}$, $\mathcal{H}_{1'-}$, and $\mathcal{H}_{1'+}$), 4.2 (configuration $\mathcal{H}_2$), and 2.2 (configurations $\mathcal{H}_0$ and $\mathcal{H}_{0'}$).

<u>Proof of Proposition 1:</u>

The *quartic fold* bifurcation $\zeta x^4 + \xi \lambda = 0$ is observed when the following three conditions are satisfied:

One defining condition:
1. $h = h_x = h_{xx} = h_{xxx} = 0$.

Two nondegeneracy conditions:
2. $\zeta = \mathrm{Sgn}\, h_{xxxx} \neq 0$
3. $\xi = \mathrm{Sgn}\, h_\lambda \neq 0$.

We deal separately with the case of the "isolated" bifurcation and of the "dual" bifurcation, which we treat here first.

From Appendix B, Case 3.2.2, we know that if $Z_c = 0$ and $q_2^* = (1 - \varepsilon)\pi/2$, with $\varepsilon = \pm 1$, then all odd-order partial derivatives of h with respect to q_2 are null. The expressions for the first even-order derivatives are

$$h(q_2^*, q_1) = \varepsilon \left((a_1 + \varepsilon a_2)^2 + d_2 \cdot K_1 - (a_1 + \varepsilon a_2) \cdot K_2 \right)$$

$$\frac{\partial^2 h}{\partial q_2^2}(q_2^*, q_1) = -\frac{\varepsilon}{2} \left((a_1 + \varepsilon a_2)^2 + d_2 \cdot K_1 - (a_1 + 2\varepsilon a_2) \cdot K_2 \right)$$

$$= -\frac{\varepsilon}{2} h(q_2^*, q_1) + \frac{a_2}{2} \cdot K_2.$$

30

One has to choose $K_2 = 0$ in order for the second derivative to be zero, and this in turn implies that $K_1 = -(a_1 + \varepsilon a_2)^2/d_2$ if we want $h = 0$ as well. From these values of K_1 and K_2, we get equations for R_c^* and $\lambda = q_1^*$:

$$R_c^* \cos q_1^* = K_2^* = 0$$

$$R_c^* \sin q_1^* = K_1^* - d_2 = -\frac{d_2^2 + (a_1 + \varepsilon a_2)^2}{d_2}.$$

It is then easy enough to verify that the values of R_c^* and $\lambda = q_1^*$ are indeed the ones given by (16) and (17). On the other hand,

$$\frac{\partial^4 h}{\partial q_2^4}(q_2^*, q_1) = 6a_1 a_2 \neq 0,$$

so that for both configurations $\mathcal{H}_{1-}$ and $\mathcal{H}_{1+}$, $\zeta = \text{Sgn } a_1$. It just remains to verify that $h_\lambda \neq 0$, which is easy enough, as

$$h_\lambda = -\frac{\varepsilon(a_1 + \varepsilon a_2) \cdot \left(d_2^2 + (a_1 + \varepsilon a_2)^2\right)}{d_2} \neq 0.$$

Finally, $\text{Sgn}(a_1 + \varepsilon a_2) = \text{Sgn } a_1$, so that $\xi = \text{Sgn } h_\lambda = -\varepsilon \cdot \text{Sgn}(a_1 d_2)$.

In conclusion:
- * If $\varepsilon = -1$ (configuration $\mathcal{H}_{1-}$), then $\zeta = \text{Sgn } a_1$ and $\xi = \text{Sgn}(a_1 d_2)$, so that the bifurcation observed is equivalent to $x^4 + \text{Sgn}(d_2) \cdot \lambda = 0$.
- * If $\varepsilon = +1$ (configuration $\mathcal{H}_{1+}$), then $\zeta = \text{Sgn } a_1$ and $\xi = -\text{Sgn}(a_1 d_2)$, so that the bifurcation observed is equivalent to $x^4 - \text{Sgn}(d_2) \cdot \lambda = 0$. $\blacksquare$

From Appendix B, Case 4.2, we know that, if $Z_c = 2|a_1|a_2\sqrt{a_1^2 - a_2^2}/(2a_1^2 - a_2^2)$ (which, since $|a_1| > a_2$ always lies between 0 and a_2), there exists a unique joint angle $q_2^* \in [0, 2\pi[$ such that $\cos q_2^* = -a_2/a_1$ and $\sin q_2^* = -\sqrt{a_1^2 - a_2^2}/|a_1|$. Then, there exists a unique pair $(R_c^*, q_1^*) \in [0, 2\pi[\times \mathbb{R}$ such that

$$K_1^* = d_2 + R_c^* \cdot \sin q_1^* = -\frac{\left(a_1^2 - a_2^2\right)^2}{2a_1^2 - a_2^2} \tag{24}$$

$$K_2^* = R_c^* \cdot \cos q_1^* = \frac{3a_1\left(a_1^2 - a_2^2\right)}{d_2\left(2a_1^2 - a_2^2\right)} \tag{25}$$

In this case, h and its first three partial derivatives with respect to q_2 are zero, but the fourth order derivative is $h_{xxxx} = 6a_1^3 a_2/(2a_1^2 - a_2^2)$, which cannot be equal to zero. Then, $\zeta = \text{Sgn } h_{xxxx} = \text{Sgn } a_1 \neq 0$. $\blacksquare$

31

Next, we prove that condition 3 applies

$$h_\lambda = d_2 K_2 C_2 - (d_2 - K_1)C_2 \cdot (a_1 + a_2 C_2).$$

Replacing K_1 and K_2 by the expressions given in (24) and (25), we get:

$$h_\lambda = \frac{-3a_2 d_2(a_1^2 - a_2^2)}{2a_1^2 - a_2^2} - \frac{a_2(a_1^2 - a_2^2)\left((a_1^2 - a_2^2)^2 + d_2^2(a_2^2 - 2a_1^2)\right)}{a_1^2 d_2(2a_1^2 - a_2^2)}$$

$$= -\frac{a_2(a_1^2 - a_2^2)\left((a_1^2 - a_2^2)^2 + d_2^2(a_1^2 + a_2^2)\right)}{a_1^2 d_2(2a_1^2 - a_2^2)},$$

so that we get $\xi = \text{Sgn } h_\lambda = -\text{Sgn } d_2$ and therefore $\delta_2 = \zeta \cdot \xi = -\text{Sgn }(a_1 d_2)$, which concludes our proof. $\qquad\square$

Proof of Proposition 2:

The type 0 bifurcation $\zeta\left(x^2 + \xi\lambda\right) = 0$ is observed when the following three conditions are satisfied:

One defining condition:
1. $h = h_x = 0$

Two nondegeneracy conditions:
2. $\zeta = \text{Sgn } h_{xx} \neq 0$
3. $\xi = \text{Sgn }(h_\lambda) \neq 0$.

The codimension of this bifurcation is zero, which means that it is always present, whatever the pose of the camera may be. Its shape is that of a horizontal hyperbola and its "role," in the complete bifurcation diagram, is to connect branches that are produced by other, more singular bifurcations.

We show in Appendix B, Case 3.2.2 that, for $\varepsilon = -1$ and for $\varepsilon = +1$, the equation $h = 0$,

$$(a_1 + \varepsilon a_2)^2 + d_2 \cdot K_1 - (a_1 + \varepsilon a_2) \cdot K_2 = 0,$$

admits two solutions sharing the same value for R_c. The first solution gives rise to one of the dual quartic fold bifurcations, which we just studied. The second solution corresponds to

$$K_1^{**} = \frac{(a_1 + \varepsilon a_2)^2}{d_2} \quad \text{and} \quad K_2^{**} = 2(a_1 + \varepsilon a_2), \tag{26}$$

and it is easy to verify that this solution is obtained for the values of R_c and λ given in (16) and (20), and in (17) and (20).

Since the hand/eye configurations for this bifurcation only differ from the one that gives rise to the quartic folds in the values of the first joint angle, $\lambda = q_1$, most of the last proof corresponding to these solutions applies here as well. In particular, we have already

established that $h = 0$, $h_x = 0$ and $h_{xx} \neq 0$, although we have yet to check its sign. We must also verify the sign of h_λ:

$$h_{xx} = 3a_1a_2 - 2a_2K_2,$$
$$h_\lambda = d_2K_2C_2 - (d_2 - K_1)C_2 \cdot (a_1 + a_2C_2),$$

so that, if we replace K_1 and $K2$ by the values given in (26), we get

$$h_{xx} = 2a_2(a_1 + \varepsilon a_2) \neq 0$$

$$h_\lambda = \frac{\varepsilon \cdot (a_1 + \varepsilon a_2) \cdot \left((a_1 + \varepsilon a_2)^2 + d_2^2\right)}{d_2} \neq 0.$$

Therefore, $\zeta = \operatorname{Sgn} h_{xx} = \operatorname{Sgn} a_1$ and, since $|a_1| > a_2$ $\xi = \operatorname{Sgn} h_\lambda = \varepsilon \operatorname{Sgn}(a_1 d_2)$, so that $\delta = \zeta \cdot \xi = \varepsilon \cdot \operatorname{Sgn} d_2$. In conclusion, $\delta_{1'-} = -\operatorname{Sgn} d_2$ and $\delta_{1'+} = \operatorname{Sgn} d_2$, which concludes our proof. $\qquad\square$

Proof of Proposition 3:

The pitchfork bifurcation $\zeta x^3 + \xi\lambda x = 0$ is observed when the following three conditions are satisfied:

Two defining conditions:
1. $h = h_x = h_{xx} = 0$
2. $h_\lambda = 0$

Two nondegeneracy conditions:
3. $\zeta = \operatorname{Sgn} h_{xxx} \neq 0$
4. $\xi = \operatorname{Sgn} h_{x\lambda} \neq 0$.

Points 1 and 3 were essentially covered in Appendix B, Case 2.2. There, we saw that, for $Z_c = a_2$ and $q_2^* = -\pi/2$, $h = 0$ for all values of q_1, and that the condition $h_x = 0$ simplifies to

$$d_2 \cdot K_1 - a_1 \cdot K_2 = -a_1^2. \tag{27}$$

Since the second order derivative of h with respect to q_2 is also a linear function of K_1 and K_2, $h_{xx} = 3a_1a_2 - 2a_2K_2$, we can calculate K_1 and K_2 such that $h = h_x = h_{xx} = 0$:

$$K_1^* = d_2 + R_c^* \sin q_1^* = \frac{a_1^2}{2d_2} \quad \text{and} \quad K_2^* = R_c^* \cos q_1^* = 3a_1/2 \tag{28}$$

It is then easy to verify that the values of $\lambda = q_1^*$ and R_c^* corresponding to (28) are the ones given in (21) and (22). In this case, $h_{xxx} = 3a_2^2 > 0$, so $\zeta = 1$. $\qquad\blacksquare$

The proof of point 2 is straightforward, since C_2 is a factor of h_λ:

$$h_\lambda = -(a_1 + a_2C_2) \cdot C_2 \cdot (d_2 - K_1) + d_2K_2C_2.$$

For $q_2 = \lambda_0 = -\pi/2$, we therefore get $h_\lambda = 0$. $\qquad\blacksquare$

Finally, we prove that point 4 applies as well:

$$h_{x\lambda} = -d_2 K_2 S_2 + a_2(d_2 - K_1)C_2 S_2 + (d_2 - K_1) \cdot (a_1 + a_2 C_2)S_2,$$

so that, if we replace K_1 and $K2$ by the values given in (28),

$$h_{x\lambda} = \frac{3a_1 d_2}{2} - \left(d_2 - \frac{a_1^2}{2d_2}\right) = \frac{a_1 \cdot \left(a_1^2 + d_2^2\right)}{2d_2} \neq 0.$$

Therefore, $\xi = \text{Sgn } h_{x\lambda} = \text{Sgn} (a_1 d_2)$ and $\delta = \zeta \cdot \xi = \text{Sgn} (a_1 d_2)$, which concludes our proof. $\qquad\square$

Proof of Proposition 4:

The simple bifurcation or the isola $\zeta \left(x^2 + \xi\lambda^2\right) = 0$ are observed when the following three conditions are satisfied:

Two defining conditions:
1. $h = h_x = 0$
2. $h_\lambda = 0$

Two nondegeneracy conditions:
3. $\zeta = \text{Sgn } h_{xx} \neq 0$
4. $\xi = \text{Sgn} (\det d^2 h) \neq 0$.

If $\xi = +1$, the bifurcation is an isola; if $\xi = -1$, it is a simple bifurcation.

We show in Appendix B, Case 2.2 that (27) admits two solutions sharing the same value for R_c. The first solution gives rise to the pitchfork bifurcation, which we just studied. The second solution corresponds to

$$K_1^* = -a_1^2/2d_2 \quad \text{and} \quad K_2^* = a_1/2, \tag{29}$$

and it is easy to verify that this solution is obtained for the values of R_c and λ given in (21) and (23).

Since the hand/eye configuration for this bifurcation only differs from the one that gives rise to the pitchfork in the value of the first joint angle, $\lambda = q_1$, most of the last proof applies here as well. In particular, we have already established that $h = 0$, $h_x = 0$, $h_\lambda = 0$. We also know that $h_{xx} \neq 0$, although we have yet to check its sign. Finally, we must verify that $\det(d^2 h) \neq 0$ and check its sign.

$$h_{xx} = 2a_1 a_2 - a_1^2 C_2 - a_2^2 C_2 - 4a_1 a_2 C_2^2 - C_2 d_2 K_1 - 2a_2 K_2 +$$
$$a_1 C_2 K_2 + 4a_2 C_2^2 K_2 - a_1 a_2 S_2 - 4a_2^2 C_2 S_2,$$

so that, if we set $q_2 = -\pi/2$ and replace K_1 and $K2$ by the values given in (29), we get

$$h_{xx} = 2a_1 a_2 \neq 0.$$

34

Replacing in the expression of the Hessian matrix, $\det(d^2 h)$, we get

$$\det(d^2 h) = \begin{vmatrix} 2a_1 a_2 & \dfrac{-a_1(a_1^2 + d_2^2)}{2d_2} \\[2ex] \dfrac{-a_1(a_1^2 + d_2^2)}{2d_2} & 0 \end{vmatrix} = -\dfrac{a_1^2(a_1^2 + d_2^2)^2}{4d_2^2} < 0.$$

Therefore, $\zeta = \operatorname{Sgn} h_{xx} = \operatorname{Sgn} a_1$ and $\xi = \operatorname{Sgn}\left(\det(d^2 h)\right) = -1$, so that the bifurcation observed will always be a simple bifurcation. $\qquad\square$

5.3 Manipulator Geometry Type A.3: $d_2 \neq 0$ and $0 < |a_1| < a_2$

In this case, the behavior of function h is rather similar to that encountered with Type A.1 geometries. We encounter again the "dual" quartic fold bifurcations for hand/eye coordinations $\mathcal{H}_{1-}$ and $\mathcal{H}_{1+}$, as well as the pitchfork bifurcation at $\mathcal{H}_0$. The orientation of the bifurcation diagrams about these organizing centers, however, may be different, since now $\operatorname{Sgn}(a_1 + a_2 C_2) = \operatorname{Sgn} C_2$, and not $\operatorname{Sgn} a_1$, as before. There is nevertheless an important difference between the topologies associated with type A.1 and type A.3 manipulators since one of the quartic folds encountered in Proposition 1 is being here "replaced" by two pitchfork bifurcations (Case 4.3).

5.3.1 Identification of the bifurcations

Proposition 5:

For any 2-dof manipulator such that its Denavit-Hartenberg parameters satisfy $d_2 \neq 0$ and $0 < |a_1| < a_2$, there exist two configurations of the hand/eye system, $\mathcal{H}_{1-} = (x_{1-}, \lambda_{1-}; Z_{c_1-}, R_{c_1-})$ and $\mathcal{H}_{1+} = (x_{1+}, \lambda_{1+}; Z_{c_1+}, R_{c_1+})$ such that

$$H(x, \lambda; Z_{c_1-}, R_{c_1-}), \text{ in a neighborhood of } (x_{1-}, \lambda_{1-}), \text{ and}$$
$$H(x, \lambda; Z_{c_1+}, R_{c_1+}), \text{ in a neighborhood of } (x_{1+}, \lambda_{1+}),$$

are equivalent to the *quartic fold* bifurcation (type 7):

$$x^4 + \delta\lambda = 0, \quad \text{with } \delta_{1-} = \delta_{1+} = -\operatorname{Sgn}(a_1 d_2).$$

These dual hand/eye configurations are defined as follows:

$$x_{1-} = \pi \quad \lambda_{1-} = -\operatorname{Sgn}(d_2) \cdot \pi/2 \quad Z_{c_1-} = 0 \quad R_{c_1-} = \dfrac{d_2^2 + (a_1 - a_2)^2}{|d_2|}$$

$$x_{1+} = 0 \quad \lambda_{1+} = -\operatorname{Sgn}(d_2) \cdot \pi/2 \quad Z_{c_1+} = 0 \quad R_{c_1+} = \dfrac{d_2^2 + (a_1 + a_2)^2}{|d_2|}$$

<u>Proposition 6:</u>

For any 2-dof manipulator such that its Denavit-Hartenberg parameters satisfy $d_2 \neq 0$ and $0 < |a_1| < a_2$, then *for the same values of the second joint angle and poses of the camera that give the "dual" quartic fold bifurcations,* $(x_{1-}, Z_{c_{1-}}, R_{c_{1-}})$ and $(x_{1+}, Z_{c_{1+}}, R_{c_{1+}})$, there exists a unique pair of values of the first joint angle, $(\lambda_{1'-}, \lambda_{1'+})$, which defines a pair of corresponding hand/eye configurations, $\mathcal{H}_{1'-} = (x_{1-}, \lambda_{1'-}, Z_{c_{1-}}, R_{c_{1-}})$ and $\mathcal{H}_{1'+} = (x_{1+}, \lambda_{1'+}, Z_{c_{1+}}, R_{c_{1+}})$, such that

$$H(x, \lambda; Z_{c_{1-}}, R_{c_{1-}}), \text{ in a neighborhood of } (x_{1-}, \lambda_{1'-}), \text{ and}$$

$$H(x, \lambda; Z_{c_{1+}}, R_{c_{1+}}), \text{ in a neighborhood of } (x_{1+}, \lambda_{1'+}),$$

are equivalent to the type 0 bifurcation:

$$x^2 + \delta\lambda = 0 \quad \text{with } \delta_{1'-} = -\text{Sgn}\, d_2 \text{ and } \delta_{1'+} = \text{Sgn}\, d_2.$$

The values of the first joint angle corresponding to these bifurcations are defined as follows:

$$\cos\lambda_{1'-} = \frac{2|d_2| \cdot (a_1 - a_2)}{(a_1 - a_2)^2 + d_2^2} \quad \text{and} \quad \sin\lambda_{1'-} = \frac{\text{Sgn}\, d_2 \cdot \left((a_1 - a_2)^2 - d_2^2\right)}{(a_1 - a_2)^2 + d_2^2}$$

$$\cos\lambda_{1'+} = \frac{2|d_2| \cdot (a_1 + a_2)}{(a_1 + a_2)^2 + d_2^2} \quad \text{and} \quad \sin\lambda_{1'+} = \frac{\text{Sgn}\, d_2 \cdot \left((a_1 + a_2)^2 + d_2^2\right)}{(a_1 + a_2)^2 + d_2^2}$$

<u>Proposition 7:</u>

For any 2-dof manipulator such that its Denavit-Hartenberg parameters satisfy $d_2 \neq 0$ and $0 < |a_1| < a_2$, then there exists a unique triple of configurations of the hand/eye system, $\mathcal{H}_0 = (x_0, \lambda_0; Z_{c_0}, R_{c_0})$, $\mathcal{H}_8 = (x_8, \lambda_8; Z_{c_8}, R_{c_8})$, and $\mathcal{H}_9 = (x_9, \lambda_9; Z_{c_9}, R_{c_9})$, such that

$$H(x, \lambda; Z_{c_0}, R_{c_0}), \text{ in a neighborhood of } (x_0, \lambda_0),$$

$$H(x, \lambda; Z_{c_8}, R_{c_8}), \text{ in a neighborhood of } (x_8, \lambda_8), \text{ and}$$

$$H(x, \lambda; Z_{c_9}, R_{c_9}), \text{ in a neighborhood of } (x_9, \lambda_9),$$

are all equivalent to the *pitchfork* bifurcation (type 6):

$$x^3 + \delta\lambda x = 0, \quad \text{with } \delta_0 = \delta_8 = \delta_9 = \text{Sgn}\,(a_1 d_2).$$

Hand eye configuration $\mathcal{H}_0$ is defined as follows:

$$x_0 = q_2^* = -\pi/2,$$

$$\sin\lambda_0 = \frac{a_1^2 - 2d_2^2}{2d_2 R_{c_0}} \qquad \cos\lambda_0 = \frac{3a_1}{2R_{c_0}},$$

$$Z_{c_0} = a_2, \quad \text{and} \quad R_{c_0} = \frac{\sqrt{\left(a_1^2 - 2d_2^2\right)^2 + 9a_1^2 d_2^2}}{2|d_2|}.$$

Hand/eye configuration $\mathcal{H}_8$ is defined in terms of the *unique* real solution C_2^* of the following cubic equation:

$$(a_1 + a_2 \cdot X)^3 + d_2^2 (a_1 + a_2 \cdot X^3).$$

$$\cos x_8 = C_2^* \quad \text{and} \quad \sin x_8 = S_2^* = -\sqrt{1 - C_2^{*2}},$$

$$Z_{c8} = \frac{-2a_1 a_2 S_2^{*3}}{2a_1 - 3a_1 C_2^{*2} - a_2 C_2^{*3}},$$

$$K_1^* = d_2 + R_{c8} \sin \lambda_8 = \frac{(a_1 + a_2 \cdot C_2^*)^3}{d_2 \left(2a_1 - 3a_1 C_2^{*2} - a_2 C_2^{*3}\right)}, \quad \text{and} \tag{30}$$

$$K_2^* = R_{c8} \cos \lambda_8 = \frac{3a_1(a_1 + a_2 \cdot C_2^*)S_2^{*2}}{2a_1 - 3a_1 C_2^{*2} - a_2 C_2^{*3}}.$$

Finally, hand/eye configuration $\mathcal{H}_9$ is defined as follows:

$$\cos x_9 = -a_1/a_2, \qquad \sin x_9 = \frac{-\sqrt{a_2^2 - a_1^2}}{a_2},$$

$$\lambda_9 = -\mathrm{Sgn}\, d_2 \cdot \pi/2, \quad Z_{c9} = \sqrt{a_2^2 - a_1^2}, \quad \text{and} \quad R_{c9} = |d_2|. \tag{31}$$

<u>Proposition 8:</u>

For any 2-dof manipulator such that its Denavit-Hartenberg parameters satisfy $d_2 \neq 0$ and $|a_1| > a_2$, then *for the same pose of the camera,* (Z_{c0}, R_{c0}), *and value of the second joint angle,* $q_2 = x_0$, *that give the pitchfork bifurcation,* there exists a unique value of the first joint angle, $\lambda_{0'}$, defining a unique hand/eye configuration $\mathcal{H}_{0'} = (x_0, \lambda_{0'}, Z_{c0}, R_{c0})$, such that $H(x, \lambda; Z_{c0}, R_{c0})$ is equivalent in a neighborhood of $(x_0, \lambda_{0'})$ to the *simple bifurcation* (type 2):

$$x^2 - \lambda^2 = 0.$$

The value of the first joint angle corresponding to this organizing center is defined as follows:

$$\cos \lambda_{0'} = \frac{a_1}{2R_{c0}} \quad \text{and} \quad \sin \lambda_{0'} = -\frac{a_1^2 + 2d_2^2}{2d_2 R_{c0}}.$$

5.3.2 Proof of these propositions

All possible organizing centers for this geometry of manipulator are covered by three cases studied in Appendix B: Cases 3.2 (configurations $\mathcal{H}_{1-}$ and $\mathcal{H}_{1+}$), Case 2.2, which corresponds to the pitchfork bifurcation observed at configuration $\mathcal{H}_0$, and Case 4.3, which corresponds to the pitchfork bifurcations observed at configurations $\mathcal{H}_8$ and $\mathcal{H}_9$.

Proof of Proposition 5:

The proof of this proposition is almost identical to that of Proposition 1, regarding dual hand/eye configurations $\mathcal{H}_{1-}$ and $\mathcal{H}_{1+}$. The only differences involve the signs of non-zero derivatives:

$$h_{xxxx} = 6\,a_1 a_2 \neq 0$$

$$h_\lambda = \frac{-\varepsilon\,(a_1 + \varepsilon a_2) \cdot \left((a_1 + \varepsilon a_2)^2 + d_2^2\right)}{d_2} \neq 0.$$

Therefore, $\zeta = \mathrm{Sgn}\,h_{xxxx} = \mathrm{Sgn}\,a_1$, as with manipulator type A.1. On the other hand, since $|a_1| < a_2$, $\mathrm{Sgn}\,(a_1 + \varepsilon a_2) = \varepsilon$, so that $\xi = \mathrm{Sgn}\,h_\lambda = -\mathrm{Sgn}\,d_2$. Finally, we get $\delta = \zeta \cdot \xi = -\mathrm{Sgn}\,(a_1 d_2)$. □

Proof of Proposition 6:

The proof for the type 0 bifurcations observed for configurations $\mathcal{H}_{1'-}$ and $\mathcal{H}_{1'+}$ is identical to the one given for manipulator geometry type A.1.

Proof of Proposition 7:

The proof for the pitchfork observed for configuration $\mathcal{H}_0$ is identical to the one given for manipulator configuration type A.1.

Hand/eye configurations $\mathcal{H}_8$ and $\mathcal{H}_9$ both correspond to Case 4.3 of Appendix B, that is, for values of the second joint angle, q_2, such that $C_2 \neq 0$, $S_2 \neq 0$, and $2a_1 - 3a_1 C_2^2 - a_2 C_2^3 \neq 0$. Then, if Z_c, R_c, and λ_1 can be expressed as functions of q_2 as shown in (B.16) (of which (30) and (31) are just particular instances), we get $h = h_x = h_{xx} = 0$. Furthermore, since $0 < |a_1| < a_2$, the term $a_2 + a_1 C_2$ cannot be null, which implies that $h_{xxx} \neq 0$. We have therefore already verified part of the conditions determining the type of these organizing centers.

The pitchfork bifurcation $\zeta x^3 + \xi \lambda x = 0$ is observed when the following four conditions are satisfied:

Two defining conditions:
1. $h = h_x = h_{xx} = 0$
2. $h_\lambda = 0$

Two nondegeneracy conditions:
3. $\zeta = \mathrm{Sgn}\,h_{xxx} \neq 0$
4. $\xi = \mathrm{Sgn}\,h_{x\lambda} \neq 0$.

As we just mentioned, point 1 was verified for both $\mathcal{H}_8$ and $\mathcal{H}_9$ in Appendix B, Case 4.3, and we just have to check the sign of h_{xxx} in order to complete the proof of point 3. We will be able do that once we have obtained a condition for q_2, by verifying that condition 2 applies.

$$h_\lambda = d_2 K_2 C_2 - (d_2 - K_1)C_2 \cdot (a_1 + a_2 C_2), \tag{32}$$

so that, if we replace Z_c, K_1, and $K2$ by the values given in (B.16), we get

$$h_\lambda = \frac{-C_2(a_1 + a_2C_2) \cdot \left((a_1 + a_2C_2)^3 + d_2^2 \cdot (a_1 + a_2C_2^3)\right)}{d_2 \left(2a_1 - 3a_1C_2^2 - a_2C_2^3\right)}.$$

Since here $C_2 \neq 0$, $h_\lambda = 0$ if and only if q_2 is a solution to one of the following equations:

$$a_1 + a_2C_2 = 0 \quad \text{or} \tag{33}$$

$$(a_1 + a_2C_2)^3 + d_2^2 \cdot (a_1 + a_2C_2^3) = 0, \tag{34}$$

Let us first deal with the case where (34) applies, which corresponds to hand/eye configuration $\mathcal{H}_8$ in this study. We need to get the solutions of (34), which means that we must study the values taken by the following function:

$$F : [-1, 1] \longrightarrow \mathbb{R}$$

$$X \longmapsto \frac{(a_1 + a_2X)^3}{a_1 + a_2X^3}.$$

The first derivative of $F(X)$ is

$$F'(X) = \frac{3a_1a_2(a_1 + a_2X)^2(1 - X^2)}{(a_1 + a_2X^3)^2}.$$

Therefore, $F'(X) = 0$ if and only if $X = \pm 1$ or $X = -a_1/a_2$, and F will vary on $[-1, 1]$ as indicated in Table 1, in the case $a_1 > 0$ (the table for $-a_1$ would simply be built by symmetry with respect to the Y axis). Figure 18 gives examples of typical graphs for $F(X)$ both when $a_1 < 0$ and when $a_1 > 0$.

Table 1 — Evolution table for F on $[-1, 1]$ (when $a_1 > 0$)

X	-1		$(-a_1/a_2)^{1/3}$		$-a_1/a_2$		1
$F'(X)$	0	$+$	$+\infty$	$+$	0	$+$	0
$F(X)$	$(a_1 - a_2)^2$ ↗		$+\infty$ $-\infty$	↗	0	↗	$(a_1 - a_2)^2$

We can see in Table 1 that the reduction of F to $](-a_1/a_2)^{1/3}, -a_1/a_2]$ bijectively maps that interval onto $\mathbb{R}^-$. As a consequence, for any value of d_2, there exists a unique $X^* \in](-a_1/a_2)^{1/3}, -a_1/a_2]$ such that $F(X^*) = -d_2^2$. Furthermore, since F admits no extrema outside of $[-1, 1]$ and $\lim_{X \to -\infty} F(X) = \lim_{X \to +\infty} F(X) = a_2^2 > 0$, X^* is, as we claimed in proposition 7, the unique real solution of the cubic equation

$$(a_1 + a_2X)^3 + d_2^2 (a_1 + a_2X^3).$$
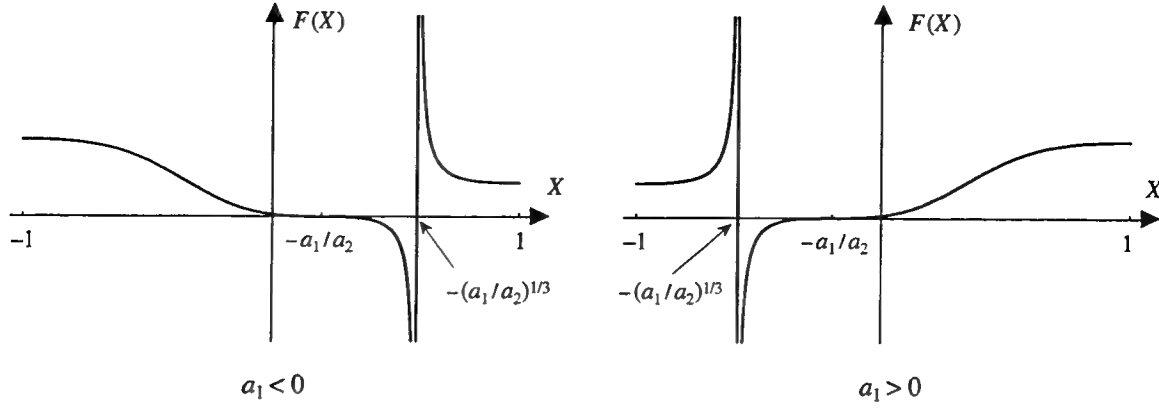
Figure 18 — Examples of typical graphs for $F(X)$ when $a_1 < 0$ and when $a_1 > 0$.

We choose $C_2^* = \cos x_8 = X^*$. The sign of $\sin x_8$ is determined by the expression for Z_c in (30): $\operatorname{Sgn} Z_c = -\operatorname{Sgn} a_1 \cdot \operatorname{Sgn} S_2^* \cdot \operatorname{Sgn}(2a_1 - 3a_1 C_2^{*2} - a_2 C_2^{*3})$. Since $Z_c > 0$, we must have $\operatorname{Sgn} S_2^* = -\operatorname{Sgn} a_1 \cdot \operatorname{Sgn}(2a_1 - 3a_1 C_2^{*2} - a_2 C_2^{*3})$. We know from our analysis of F that C_2^* lies between $(-a_1/a_2)^{1/3}$ and $-a_1/a_2$, it is therefore easy to verify, by adding up inequalities, that $\operatorname{Sgn}(2a_1 - 3a_1 C_2^{*2} - a_2 C_2^{*3}) = \operatorname{Sgn} a_1$, which imposes that $\operatorname{Sgn} S_2^* = -1$. We apply this information to determine the sign of h_{xxx}:

$$h_{xxx} = \frac{-6\, a_1 a_2\, (a_2 + a_1 C_2^*)\, S_2^*}{2a_1 - 3a_1 C_2^{*2} - a_2 C_2^{*3}}, \tag{35}$$

so that $\zeta = \operatorname{Sgn} h_{xxx} = -(\operatorname{Sgn} a_1)^2 \cdot \operatorname{Sgn} S_2^* = +1$. We have now proven that conditions 1 through 3 apply. ∎

It just remains to verify that $h_{x\lambda} \neq 0$ and check for its sign. The general expression for this derivative is

$$h_{x\lambda} = -d_2 K_2 S_2 + a_2(d_2 - K_1)C_2 S_2 + (d_2 - K_1)\cdot(a_1 + a_2 C_2)S_2. \tag{36}$$

First, we can use the condition $(a_1 + a_2 \cdot C_2^*)^3 + d_2^2(a_1 + a_2 C_2^{*3}) = 0$ together with (B.16) and (30) to get simpler expressions for K_1 and for K_2 and Z_c as functions of K_1:

$$K_1^* = \frac{d_2(a_1 + a_2 C_2^*)^3}{(a_1 + a_2 C_2^*)^3 + 3a_1 d_2^2 S_2^{*2}}$$

$$K_2^* = \frac{(a_1 + a_2 C_2^*)\cdot(d_2 - K_1^*)}{d_2}$$

$$Z_{c8} = \frac{-2a_2 S_2 \cdot (d_2 - K_1^*)}{3d_2}$$

Substituting for K_2 and Z_c in (36), we get

$$h_{x\lambda} = a_2 C_2^* S_2^* \cdot (d_2 - K_1^*).$$

40

Since $C_2^* S_2^* \neq 0$, $h_{x\lambda}$ is null if and only if $d_2 - K_1^* = 0$.

$$d_2 - K_1^* = \frac{3a_1 d_2 S_2^{*2}}{2a_1 - 3a_2 C_2^{*2} - a_2 C_2^{*3}} \neq 0.$$

We already know that

$$\begin{aligned}
\text{Sgn}\,(2a_1 - 3a_2 C_2^{*2} - a_2 C_2^{*3}) &= \text{Sgn}\, a_1, \\
\text{Sgn}\, C_2^* &= -\text{Sgn}\, a_1, \text{ and} \\
\text{Sgn}\, S_2^* &= -1,
\end{aligned}$$

so $\text{Sgn}\,(d_2 - K_1) = \text{Sgn}\, d_2$ and therefore

$$\begin{aligned}
\xi = \text{Sgn}\, h_{x\lambda} &= \text{Sgn}\, C_2^* \cdot \text{Sgn}\, S_2^* \cdot \text{Sgn}\,(d_2 - K_1) \\
&= \text{Sgn}\,(a_1 d_2).
\end{aligned}$$

In conclusion, $\delta_8 = \zeta \cdot \xi = \text{Sgn}\,(a_1 d_2)$. ∎

The proof for $\mathcal{H}_9$ is fortunately much simpler. We return to (32) and get $h_\lambda = 0$ by choosing $C_2^* = -a_1/a_2$. Substituting for C_2 in (B.16), we obtain

$$K_1 = 0, \quad K_2 = 0, \quad \text{and}\, Z_c = -\text{Sgn}\, S_2^* \cdot \sqrt{a_2^2 - a_1^2}.$$

Since we have imposed here $Z_c \geq 0$, we must therefore choose $S_2^* < 0$. Similarly, from $K_1 = K_2 = 0$, it is easy to deduce that $R_c = |d_2|$ and $\lambda_9 = -\text{Sgn}\, d_2 \cdot \pi/2$, which completes our determination of $\mathcal{H}_9$, as given in (31).

We only have now to determine the sign of h_{xxx}, prove that $h_{x\lambda}$ is not null, and check for its sign. The expression for h_{xxx} is the same as in (35) and, after substituting for C_2, simplifies to $h_{xxx} = -3a_2^2 S_2^*$. So, $\zeta = \text{Sgn}\, h_{xxx} = +1$. ∎

The expression for $h_{x\lambda}$ is still (36). At organizing center $\mathcal{H}_9$, this derivative is equal to

$$h_{x\lambda} = -a_1 d_2 S_2^* = a_1 d_2 \sqrt{a_2^2 - a_1^2}/a_2 \neq 0.$$

Therefore, $\xi = \text{Sgn}\, h_{x\lambda} = \text{Sgn}\,(a_1 d_2)$ and $\delta_9 = \zeta \cdot \xi = \text{Sgn}\,(a_1 d_2)$. □

Proof of Proposition 8:

The proof for the simple bifurcation or isola observed for hand/eye configuration $\mathcal{H}_{0'}$ is identical to the one given for manipulator geometry type A.1.

5.4 Manipulator Geometry Type A.2: $d_2 \neq 0$ and $|a_1| = a_2$

Since this type of manipulator geometry is in fact a "boundary" between types A.1 and A.3, it should not come as a surprise that some of the organizing centers we encountered in the two previous subsections exist for A.2-type manipulators as well. On the other hand, one of the "dual" quartic folds, either $\mathcal{H}_{1-}$ or $\mathcal{H}_{1+}$, and its associated type 0 bifurcation, merge together to form an organizing center of codimension greater than 3 that did not exist for either type A.1 or type A.3 manipulators.

5.4.1 Identification of the bifurcations

<u>Proposition 9:</u>

For any 2-dof manipulator such that its Denavit-Hartenberg parameters satisfy $d_2 \neq 0$ and $|a_1| = a_2$, then there exists a unique configuration of the hand/eye system, $\mathcal{H}_3 = (x_3, \lambda_3, Z_{c3}, R_{c3})$, with

$$x_3 = (1 + \text{Sgn}(a_1)) \cdot \pi/2 \qquad \lambda_3 = -\text{Sgn}\, d_2 \cdot \pi/2$$

$$Z_{c3} = 0 \qquad R_{c3} = |d_2|,$$

such that $H(x, \lambda; Z_{c3}, R_{c3})$ is equivalent, in a neighborhood of (x_3, λ_3), to a bifurcation of codimension ≥ 4.

<u>Proposition 10:</u>

For any 2-dof manipulator such that its Denavit-Hartenberg parameters satisfy $d_2 \neq 0$ and $0 < |a_1| < a_2$, there exist a unique hand/eye configuration, $\mathcal{H}_{1\varepsilon} = (x_{1\varepsilon}, \lambda_{1\varepsilon}; Z_{c_{1\varepsilon}}, R_{c_{1\varepsilon}})$, such that $H(x, \lambda; Z_{c_{1\varepsilon}}, R_{c_{1\varepsilon}})$, in a neighborhood of $(x_{1\varepsilon}, \lambda_{1\varepsilon})$ is equivalent to the *quartic fold* bifurcation (type 7):

$$x^4 + \delta\lambda = 0, \quad \text{with } \delta = -\text{Sgn}(a_1 d_2).$$

This hand/eye configuration is defined as follows:

$$
\begin{aligned}
\varepsilon &= \text{Sgn}\, a_1, \\
x_{1\varepsilon} &= (1 - \varepsilon) \cdot \pi/2, \quad \lambda_{1\varepsilon} = -\text{Sgn}(d_2) \cdot \pi/2, \\
Z_{c_{1\varepsilon}} &= 0, \quad \text{and} R_{c_{1\varepsilon}} = \frac{d_2^2 + 4a_2^2}{|d_2|}
\end{aligned}
$$

<u>Proposition 11:</u>

For any 2-dof manipulator such that its Denavit-Hartenberg parameters satisfy $d_2 \neq 0$ and $0 < |a_1| < a_2$, then *for the same values of the second joint angle and pose of the camera as in configuration* $\mathcal{H}_{1\varepsilon}$, $(x_{1\varepsilon}, Z_{c_{1\varepsilon}}, R_{c_{1\varepsilon}})$there exists a unique value of the first joint angle, $(\lambda_{1'\varepsilon}$, which defines a corresponding hand/eye configuration, $\mathcal{H}_{1'\varepsilon} = (x_{1\varepsilon}, \lambda_{1'\varepsilon}, Z_{c_{1\varepsilon}}, R_{c_{1\varepsilon}})$, such that $H(x, \lambda; Z_{c_{1\varepsilon}}, R_{c_{1\varepsilon}})$, in a neighborhood of $(x_{1\varepsilon}, \lambda_{1'\varepsilon})$, is equivalent to the type 0 bifurcation:

$$x^2 + \delta\lambda = 0, \quad \text{with } \delta = -\text{Sgn}(a_1 d_2).$$

The value of the first joint angle corresponding to this bifurcation is defined as follows:

$$
\cos\lambda_{1'\varepsilon} = \frac{2|d_2| \cdot (a_1 + \varepsilon a_2)}{(a_1 + \varepsilon a_2)^2 + d_2^2} \quad \text{and} \quad \sin\lambda_{1'\varepsilon} = \frac{\text{Sgn}\, d_2 \cdot \left((a_1 + \varepsilon a_2)^2 - d_2^2\right)}{(a_1 + \varepsilon a_2)^2 + d_2^2}
$$

<u>Proposition 12:</u>

For any 2-dof manipulator such that its Denavit-Hartenberg parameters satisfy $d_2 \neq 0$ and $|a_1| < a_2$, then there exists a unique hand/eye configuration $\mathcal{H}_0 = (x_0, \lambda_0; Z_{c_0}, R_{c_0})$ such that $h(x, \lambda; Z_{c_0}, R_{c_0})$ is equivalent in a neighborhood of (x_0, λ_0) to the *pitchfork* bifurcation (type 6):

$$x^3 + \delta \lambda x = 0 \quad \text{with } \delta = \text{Sgn}(a_1 d_2)$$

The hand eye configuration corresponding to this organizing center is defined as follows:

$$x_0 = q_2^* = -\pi/2,$$
$$Z_{c_0} = a_2,$$
$$R_{c_0} = \frac{\sqrt{\left(a_1^2 - 2d_2^2\right)^2 + 9a_1^2 d_2^2}}{2|d_2|}$$
$$\sin \lambda_0 = \frac{a_1^2 - 2d_2^2}{2d_2 R_{c_0}} \qquad \cos \lambda_0 = \frac{3a_1}{2R_{c_0}}$$

<u>Proposition 13:</u>

For any 2-dof manipulator such that its Denavit-Hartenberg parameters satisfy $d_2 \neq 0$ and $|a_1| > a_2$, then *for the same pose of the camera, (Z_{c_0}, R_{c_0}), and value of the second joint angle, $q_2 = x_0$, that give the pitchfork bifurcation*, there exists a unique value of the first joint angle, $\lambda_{0'}$, defining a unique hand/eye configuration $\mathcal{H}_{0'} = (x_0, \lambda_{0'}, Z_{c_0}, R_{c_0})$, such that $H(x, \lambda; Z_{c_0}, R_{c_0})$ is equivalent in a neighborhood of $(x_0, \lambda_{0'})$ to the *simple bifurcation* (type 2):

$$x^2 - \lambda^2 = 0.$$

The value of the first joint angle corresponding to this organizing center is defined as follows:

$$\cos \lambda_{0'} = \frac{a_1}{2R_{c_0}} \quad \text{and} \quad \sin \lambda_{0'} = -\frac{a_1^2 + 2d_2^2}{2d_2 R_{c_0}}.$$

5.4.2 Proof of these propositions

All possible organizing centers for this geometry of manipulator are covered by two cases studied in Appendix B: Cases 3.1 (configuration $\mathcal{H}_3$), 3.2 (configuration $\mathcal{H}_{1\epsilon}$), and 2.2, which corresponds to the pitchfork bifurcation (configuration $\mathcal{H}_0$) and its associated simple bifurcation or isola bifurcation (configuration $\mathcal{H}_{0'}$).

<u>Proof of Proposition 9:</u>

Hand/eye configuration $\mathcal{H}_3$ in fact represents a degenerate form of one of the "dual" configurations, $\mathcal{H}_{1-}$ and $\mathcal{H}_{1+}$ giving rise to quartic fold bifurcations for type A.1 and type A.3 manipulators. For the type A.2 manipulators that we are considering here, $a_1 = \varepsilon a_2$, with $\varepsilon = \text{Sgn}\, a_1$, and hand/eye configurations $\mathcal{H}_{1-\epsilon}$ and $\mathcal{H}_{1'-\epsilon}$ coincide (at $\mathcal{H}_3$), thus giving rise to a very singular bifurcation.

43

We see in Appendix B, Case 3.1 that, if $q_2 = (1 + \text{Sgn}\, a_1) \cdot \pi/2$, $Z_c = 0$, and $K_1 = K_2 = 0$, then

$$h = h_x = h_{xx} = h_{xxx} = 0, \quad \text{but} \quad h_{xxxx} = 6a_1a_2 \neq 0.$$

There are only two elementary bifurcations of codimension ≤ 3 that satisfy these conditions: the quartic fold $\zeta x^4 + \xi \lambda = 0$, which we have already seen, and the "type 10" bifurcation $\zeta x^4 + \xi \lambda x = 0$.

It is easy to verify that, for the hand/eye configuration we have here,

$$h_\lambda = (a_1 + a_2 C_2) \cdot C_2 \cdot (d_2 - K_1) + d_2 K_2 C_2 = 0,$$

since $C_2 = -\text{Sgn}\, a_1$ and $K_2 = 0$. The bifurcation observed here is therefore not a quartic fold. Similarly,

$$h_{x\lambda} = (-a_1 S_2 - 2a_2 C_2 S_2) \cdot (d_2 - K_1) - d_2 K_2 S_2 = 0,$$

since $S_2 = 0$. The bifurcation corresponding to this hand/eye configuration is therefore not "type 10" either. Its codimension must then be greater than 3. $\qquad\square$

Proof of Proposition 10:

The proof of this proposition is almost identical to the proof of Proposition 1 regarding dual hand/eye configurations $\mathcal{H}_{1-}$ and $\mathcal{H}_{1+}$. The only differences involve the signs of non-zero derivatives:

$$h_{xxxx} = 6\,a_1 a_2 \neq 0$$

$$h_\lambda = \frac{-\varepsilon\,(a_1 + \varepsilon a_2) \cdot \left((a_1 + \varepsilon a_2)^2 + d_2^2\right)}{d_2} \neq 0.$$

Therefore, $\zeta = \text{Sgn}\, h_{xxxx} = \text{Sgn}\, a_1$, as with Configuration A.1. On the other hand, since $a_1 = \varepsilon a_2$, we get $\text{Sgn}\,(a_1 + \varepsilon a_2) = \text{Sgn}\,(2\varepsilon a_2) = \varepsilon$, so that $\xi = \text{Sgn}\, h_\lambda = -\text{Sgn}\, d_2$ and therefore $\delta = \zeta \cdot \xi = -\text{Sgn}\,(a_1 d_2)$. $\qquad\square$

Proof of Proposition 11:

The proof for the type 0 bifurcation observed for configuration $\mathcal{H}_{1'\varepsilon}$ is identical to the one given for manipulator geometry type A.1.

Proof of Proposition 12:

The proof for the pitchfork observed for configuration $\mathcal{H}_0$ is identical to the one given for manipulator configuration types A.1 and A.3.

Proof of Proposition 13:

The proof for the simple bifurcation or isola observed for configuration $\mathcal{H}_{0'}$ is identical to the one given for manipulator configuration types A.1 and A.3.

5.5 Manipulator Geometry Type A.4: $d_2 \neq 0$ and $a_1 = 0$

The most common geometry among manipulator arms unfortunately also seems to be the least suitable for hand/eye coordination purposes.

Proposition 14:

For any 2-dof manipulator such that its Denavit-Hartenberg parameters satisfy $d_2 \neq 0$ and $a_1 = 0$, then for

$$\lambda_4 = -\mathrm{Sgn}\,(d_2) \cdot \pi/2, \quad Z_{c_4} = 0, \quad \text{and} \quad R_{c_4} = \frac{a_2^2 + d_2^2}{d_2},$$

$H(x, \lambda; Z_{c_4}, R_{c_4})$ is equivalent, for any $x_4 \in \mathbb{R}$, in a neighborhood of (x_4, λ_4) to a bifurcation of infinite codimension.

Proof of Proposition 14:

Setting $a_1 = Z_c^* = 0$ and $R_c^* = (a_2^2 + d_2^2)/d_2$ in the expression of $h(q_2, q_1)$, we obtain

$$h(q_2, q_1) = (a_2^2 + d_2^2) \cdot (1 + S_1) \cdot C_2 - \frac{a_2(a_2^2 + d_2^2)}{d_2} \cdot C_1 C_2^2.$$

It is then trivial to check that, for $\lambda_4 = q_1^* = (2k+1)\pi$, then $H(\,\cdot\,, \lambda_4, Z_c^*, R_c^*)$ is the null function. □

5.6 Manipulator Geometry Type B.1: $d_2 = 0$ and $|a_1| > a_2$

This—admittedly rather uncommon—manipulator geometry produces the only codimension 3 bifurcation that we will encounter during this study.

Proposition 15:

For any 2-dof manipulator such that its Denavit-Hartenberg parameters satisfy $d_2 = 0$ and $|a_1| > a_2$, there exists a unique hand/eye configuration $\mathcal{H}_5 = (x_5, \lambda_5, Z_{c_5}, R_{c_5})$, with

$$x_5 = -\pi/2, \quad \lambda_5 = (1 - \mathrm{Sgn}\, a_1) \cdot \pi/2, \quad Z_{c_5} = a_2 \quad R_{c_5} = |a_1|, \tag{37}$$

such that $H(x, \lambda; Z_{c_5}, R_{c_5})$ is equivalent, in a neighborhood of (x_5, λ_5), to the following elementary bifurcation (type 8^- or type 8^+):

$$x^2 + \delta_5 \cdot \lambda^4 = 0, \quad \text{with } \delta_5 = -\mathrm{Sgn}\, a_1.$$

Proof of Proposition 15:

The elementary bifurcation $\zeta x^2 + \xi \lambda^4 = 0$ is observed when the following four conditions are satisfied:

    Two defining conditions:
    1. $h = h_x = 0$
    2. $h_\lambda = \det(d^2 h) = h_{vvv} = 0$, where v is any vector such that $h_{vv} \neq 0$.

Two nondegeneracy conditions:

3. $\zeta = \mathrm{Sgn}\, h_{xx} \neq 0$

4. $\xi = \mathrm{Sgn}\, q \neq 0$, where $q = h_{vvvv} \cdot h_{xx} - 3h_{vxx}^2$.

First, we prove that condition 1 applies.

For all Z_c such that $Z_c \leq a_2$, there exists a unique pair of numbers $(q_2^*, q_2^{**}) \in [0, \pi]^2$ such that

$$\sin q_2^* = \sin q_2^{**} = -Z_c/a_2$$

$$\cos q_2^* = -\cos q_2^{**} = \sqrt{a_2^2 - Z_c^2}/a_2.$$

Obviously, $q_2^{**} = \pi - q_2^*$. Then, from Appendix B, Case 1.2, we have the following:

- For all $R_c \geq \left| a_1 + \left(a_2^2 - Z_c^2\right)^{1/2} \right|$, there exists a unique $q_1^* \in [0, \pi]$ such that

$$K_2 = R_c \cdot \cos q_1^* = a_1 + a_2 C_2^* = a_1 + \left(a_2^2 - Z_c^2\right)^{1/2}.$$

Then, at (q_1^*, q_2^*) and $(-q_1^*, q_2^*)$, $h = h_x = 0$, but $h_{xx} = a_2\left(a_1 + a_2 C_2^*\right) \neq 0$. In this case, $\zeta = \mathrm{Sgn}\, h_{xx} = \mathrm{Sgn}\, a_1$.

- For all $R_c \geq \left| a_1 - \left(a_2^2 - Z_c^2\right)^{1/2} \right|$, there exists a unique $q_1^{**} \in [0, \pi]$ such that

$$K_2 = R_c \cdot \cos q_1^{**} = a_1 + a_2 C_2^{**} = a_1 - \left(a_2^2 - Z_c^2\right)^{1/2}.$$

Then, at (q_1^{**}, q_2^{**}) and $(-q_1^{**}, q_2^{**})$, $h = h_x = 0$, but $h_{xx} = a_2\left(a_1 + a_2 C_2^{**}\right) \neq 0$. In this case, $\zeta = \mathrm{Sgn}\, h_{xx} = \mathrm{Sgn}\, a_1$.

The value of R_c will be determined next, but $\forall R_c$, $\zeta = \mathrm{Sgn}\, a_1$. ∎

Next, we prove that conditions 2 and 3 apply.

In its expanded form, $h(q_2, q_1) = (a_1 + a_2 C_2) \cdot (a_2 + a_1 C_2 - R_c C_1 C_2 + Z_c S_2)$, so that its partial derivative with respect to λ, $h_\lambda = R_c S_1 C_2 \cdot (a_1 + a_2 C_2)$ is null if and only if $R_c = 0$, $S_1 = 0$ or $C_2 = 0$.

The determinant of the Hessian matrix of $h(x, \lambda)$ is

$$\det(d^2 h) = \begin{vmatrix} h_{xx} & h_{x\lambda} \\ h_{x\lambda} & h_{\lambda\lambda} \end{vmatrix} = h_{xx} \cdot h_{\lambda\lambda} - h_{x\lambda}^2, \tag{38}$$

with

$$h_{\lambda\lambda} = R_c C_1 C_2 \cdot (a_1 + a_2 C_2) \quad \text{and}$$
$$h_{x\lambda} = -R_c S_1 C_2 \cdot (a_1 + a_2 C_2).$$

We now study separately the three cases that give $h_\lambda = 0$ and study them in terms of the results gathered in proving conditions 1 and 3 and then in terms of the condition $\det(d^2 h) = 0$.

- $R_c = 0$ is impossible since we just saw that in order to get $h = h_x = 0$, we must have $K_2 = R_c C_1 = a_1 + a_2 C_2 \neq 0$

- $S_1 = 0 \Rightarrow h_{xx} = a_2 \cdot (a_1 + a_2 C_2)$, $h_{\lambda\lambda} = \pm R_c C_2 \cdot (a_1 + a_2 C_2)$, and $h_{x\lambda} = 0$. Then, from (38), we see that $\det(d^2 h) = \pm R_c a_2 C_2 \cdot (a_1 + a_2 C_2)^2$ is null if and only if $R_c = 0$ or $C_2 = 0$. We already know that the former is not possible and, since the latter happens to be the third and final case of our initial condition, we will now study it regardless of the value of q_1.

- $C_2 = 0$ and $Z_c = -a_2 S_2 = a_2$ implies that $q_2^* = q_2^{**} = -\pi/2$. Then $h_{xx} = a_1 a_2$, $h_{\lambda\lambda} = 0$, $h_{x\lambda} = -R_c a_1 S_1$, and $\det(d^2 h) = -h_{x\lambda}^2 = R_c^2 a_1^2 S_1^2$, which, since $R_c \neq 0$ and $a_1 \neq 0$, can be null only if $S_1 = 0$. Returning to the value that we found earlier for K_2, we see that $K_2 = R_c C_1^* = a_1$ implies that $C_1^* = \mathrm{Sgn}\, a_1$, that is, $q_1^* = (1 - \mathrm{Sgn}\, a_1) \cdot \pi/2$.

In conclusion, the only hand/eye configuration that gives us $h_\lambda = \det(d^2 h) = 0$ (in addition to the conditions for the existence of a bifurcation, $h = h_x = 0$) is

$$Z_c^* = a_2, \quad R_c^* = |a_1|, \quad q_2^* = -\pi/2, \quad \text{and} \quad q_1^* = (1 - \mathrm{Sgn}\, a_1) \cdot \pi/2,$$

which means that the nondegeneracy term in condition 3 is $\zeta = \mathrm{Sgn}\, a_1$. ∎

Finally, we take care of nondegeneracy condition 4.
Replacing in the expression of the Hessian matrix, $\det(d^2 h)$, for all the variables and parameters that we have determined, we get

$$\det(d^2 h) = \begin{vmatrix} a_1 a_2 & 0 \\ 0 & 0 \end{vmatrix}.$$

We can select $v = (0, 1)'$ as a non-zero vector of $\mathrm{Ker}\, d^2 h$ and we can trivially verify that $h_{vvvv} = h_{\lambda\lambda\lambda\lambda} = -R_c C_1 C_2 \cdot (a_1 + a_2 C_2) = 0$. The expression for the differential form q is therefore

$$q = h_{vvvv} \cdot h_{xx} - 3 h_{vvx}^2 = 0 - 3 h_{vvx}^2$$
$$= -3 \left(R_c C_1 S_2 a_1 \right)^2 = -3 a_1^2 R_c^2 < 0,$$

and therefore $\xi = -1$, so that $\delta_5 = \zeta \cdot \xi = -\mathrm{Sgn}\, a_1$, which concludes our proof. □

5.7 Manipulator Geometry Type B.3: $d_2 = 0$ and $0 < |a_1| < a_2$

We encounter the same organizing center as with configurations type B.1, plus another—particularly degenerate—one that is made possible since $a_1 + a_2 C_2$ can now be null. In fact, the true organizing center for this manipulator geometry would be observed for $R_c = 0$. We have decided to avoid studying this case, but it shows up here uninvited. What this means is that the neighborhood of $R_c = 0$ should be avoided for the observer, but that the influence of this organizing center will be felt even far away from it. This topic will be addressed in more detail in Part II.

5.7.1 Identification of the bifurcations
Proposition 16:

For any 2-dof manipulator such that its Denavit-Hartenberg parameters satisfy $d_2 = 0$ and $|a_1| > a_2$, there exists a unique configuration of the hand/eye system, $\mathcal{H}_5 = (x_5, \lambda_5, Z_{c_5}, R_{c_5})$, with

$$x_5 = -\pi/2, \quad \lambda_5 = (1 - \text{Sgn } a_1) \cdot \pi/2, \quad Z_{c_5} = a_2, \quad R_{c_5} = |a_1|,$$

such that $H(x, \lambda; Z_{c_5}, R_{c_5})$ is equivalent, in a neighborhood of (x_5, λ_5), to the following elementary bifurcation (type 8^- or type 8^+):

$$x^2 - \delta \cdot \lambda^4 = 0, \quad \text{where } \delta = \text{Sgn } a_1.$$

Proposition 17:

For any 2-dof manipulator such that its Denavit-Hartenberg parameters satisfy $d_2 = 0$ and $|a_1| > a_2$, there exists a unique 3-tuple $(x_6, \lambda_6; Z_{c_6})$ such that, for all values of R_{c_6}, $H(x, \lambda; Z_{c_6}, R_{c_6})$ is equivalent, in a neighborhood of (x_6, λ_6), and $(x_6, -\lambda_6)$, to the pitchfork bifurcation (type 6):

$$x^3 - \delta \lambda x = 0, \quad \text{where } \delta = \text{Sgn } a_1.$$

The values of x_6, λ_6 and Z_{c_6} are defined as follows:

$$\cos x_6 = -\frac{a_1}{a_2}, \quad \sin x_6 = -\frac{\sqrt{a_2^2 - a_1^2}}{a_2}$$
$$\lambda_6 = \pi/2$$
$$Z_{c_6} = \sqrt{a_2^2 - a_1^2}.$$

5.7.2 Proof of these propositions
Proof of Proposition 16:

The proof for the type 8 bifurcation observed for configuration $\mathcal{H}_5$ is identical to the one given for manipulator configuration type B.1.

Proof of Proposition 17:

The pitchfork bifurcation $\zeta x^3 + \xi \lambda x = 0$ is observed when the following three conditions are satisfied:

Two defining conditions:
1. $h = h_x = h_{xx} = 0$
2. $h_\lambda = 0$

Two nondegeneracy conditions:

3. $\zeta = \text{Sgn}\, h_{xxx} \neq 0$

4. $\xi = \text{Sgn}\, h_{x\lambda} \neq 0$.

1 and 3 directly follow from the results of Appendix B, Case 1.1.3, where we showed that, if $q_2 = x_6$, $Z_c = \sqrt{a_2^2 - a_1^2}$, and $K_2 = 0$, then

$$h = h_x = h_{xx} = 0$$

$$h_{xxx} = 3a_2 \sqrt{a_2^2 - a_1^2} \neq 0.$$

The condition $K_2 = 0$ implies that $\lambda = q_1 = \pm\pi/2$ since, as we explained earlier, we must exclude the case $R_c = 0$. In any case, $\zeta = \text{Sgn}\, h_{xxx} = 1$.

Proving that 2 and 4 hold is just as straightforward:

$$
\begin{aligned}
h_\lambda &= R_c S_1 C_2 \cdot (a_1 + a_2 C_2^*) \\
&= 0.
\end{aligned}
$$

$$
\begin{aligned}
h_{x\lambda} &= -R_c S_1^* S_2^* \cdot (a_1 + 2a_2 C_2^*) \\
&= -\frac{\text{Sgn}\,(\lambda) R_c a_1 \sqrt{a_2^2 - a_1^2}}{a_2},
\end{aligned}
$$

which cannot be null since $R_c \neq 0$. Then $\xi = \text{Sgn}\, h_{x\lambda} = -\text{Sgn}\,(\lambda_6 a_1)$. $\square$

5.8 Manipulator Geometry Type B.2: $d_2 = 0$ and $|a_1| = a_2$

As can often be expected with "boundary" configurations, we encounter degenerate solutions of the more general Cases B.1 and B.3.

Proposition 18:

For any 2-dof manipulator such that its Denavit-Hartenberg parameters satisfy $d_2 = 0$ and $|a_1| = a_2$, then there exists a unique 3-tuple (x_7, λ_7, Z_{c7}), with

$$x_7 = (1 + \text{Sgn}\, a_1) \cdot \pi/2 \quad \lambda_7 = \pi/2, \quad \text{and}\quad Z_{c7} = 0,$$

such that for any value of radius R_{c7}, $H(x, \lambda; Z_{c7}, R_{c7})$ is equivalent, in a neighborhood of (x_7, λ_7) and in a neighborhood of $(x_7, -\lambda_7)$, to a bifurcation of codimension ≥ 4.

Proof of Proposition 18:

Here we have $a_1 = \varepsilon \cdot a_2$ (with $\varepsilon = \pm 1$). From Appendix B, Case 1.1.2, we know that, if $Z_c = 0$, then for $q_2^* = (1 + \varepsilon) \cdot \pi/2$ (so that $C_2 = -a_1/a_2 = -\varepsilon$ and $S_2 = 0$) and $K_2 = R_c C_1 = 0$, then $h = h_x = h_{xx} = h_{xxx} = 0$, but $h_{xxxx} = 6\varepsilon a_2^2 \neq 0$.

We explained earlier why we want to avoid the case $R_c = 0$. The condition $K_2 = 0$ is therefore satisfied only if $C_1^* = 0$, that is, if $\lambda = q_1^* = \pm\pi/2$. The only elementary bifurcations of codimension ≤ 3 that contain the term x^4 are $x^4 \pm \lambda$ and $x^4 \pm \lambda x$. However,

it is easy to verify that

$$h_\lambda = K_1 \cdot C_2 \cdot (a_1 + a_2 C_2) = 0 \quad \text{and}$$
$$h_{\lambda x} = -K_1 \cdot S_2 \cdot (a_1 + 2a_2 C_2) = 0,$$

which implies that codim $h \geq 4$. □

5.9 Manipulator Geometry Type B.4: $d_2{=}0$ and $a_1{=}0$

This is another type of manipulator geometry that does not seem suitable for hand/eye coordination purposes. Unfortunately, this is also the most common geometry among small robot arms used today for hand/eye coordination projects.

Proposition 19:

For any 2-dof manipulator such that its Denavit-Hartenberg parameters satisfy $d_2 = 0$ and $a_1 = 0$, there exists a unique 3-tuple $(x_{10}, \lambda_{10}, Z_{c10})$,

$$x_{10} = -\pi/2, \quad \lambda_{10} = \pi/2, \quad \text{and} \quad Z_c 10 = a_2, \tag{39}$$

such that, for any value of R_c, $H(x, \lambda; Z_{c10}, R_c)$ is equivalent in a neighborhood of (x_{10}, λ_{10}) and in a neighborhood of $(x_{10}, -\lambda_{10})$ to a bifurcation of codimension greater than 3.

Proof of Proposition 19:

This bifurcation corresponds to Case 1.1.1 of Appendix B. Setting $a_1 = 0$, $d_2 = 0$, and $Z_c = a_2$ in the expression of $h(q_2, q_1)$, we obtain

$$h(q_2, q_1) = a_2 C_2 \cdot (a_2 + a_2 S_2 - R_c C_1 C_2).$$

It is then trivial to check that, for $q_2 = -\pi/2$ and $q_1 = \pm\pi/2$, we get $h = h_x = h_{xx} = 0$, but $h_{xxx} = 3a_2^2 > 0$. The only bifurcations of codimension ≤ 3 that contain the term x^3 are $x^3 \pm \lambda$ (codimension 1), $x^3 \pm \lambda x$ (codimension 2), and $x^3 \pm \lambda^2$ (codimension 3). However, since $C_2 = 0$, it is easy to verify that

$$h_\lambda = R_c S_1 a_2 C_2^2 = 0,$$
$$h_{x\lambda} = -2R_c S_1 a_2 C_2 S_2 = 0, \text{ and}$$
$$h_{\lambda\lambda} = R_c C_1 a_2 C_2^2 = 0,$$

which implies that codim $h \geq 4$. □

6. Discussion and Conclusions

There are two important aspects to the work that I have presented here. First, there is the role of the active observer in a visual navigation problem, in terms of the low-level controls as well as in terms of what I earlier called "intermediate" or "topological" level controls [9]. Next, there is the aspect of skill learning, the skill being, in the case that concerns us here, reaching. These two issues will now be addressed.

6.1 Active Vision and Task-Specific Models

There is little doubt that this work is only a preliminary study of a vast and complex topic. The thesis defended here is that, just as vision must be studied in the context of a task, the needs and the performance of the perceptual module must be taken into account in the generation of the controls that accomplish that task. If the robots are to escape from the laboratories and deal with the real world, then it no longer suffices to assume that their sensors will faithfully deliver measurements, plus or minus some *a priori* uncertainty estimate. Somehow, we must find ways to determine what constitutes a good action of the agent in terms of its visual module, and how to combine this with the more classical, task-specific action selection (control) process.

In a previous paper [10], we proposed a quantitative criterion that estimates the effect of observer displacements on the performance of (reconstruction) visual computations. The study presented here differs from it in two important respects. First, because the criterion by which actions of the observer are estimated is qualitative: their effect on the topology of the PCS. But also because this criterion is completely task-specific, since it is exclusively concerned with the hand/eye coordination problem. On the other hand, these approaches are similar in the sense that they are based on a particular representative model: linear features and a decomposition of the depth map as a sum of functions in the case of [10], the pair PKM-PCS in the case of the work presented here. The validity of both studies seems therefore dependent on the validity of their respective models.

This is where, in my mind, the deepest difference between the two approaches lies. Whereas the "linear features" and depth map are little more than convenient, artificial elements of the mathematical model in [10], I believe that the PCS, in one way or another, captures some essential information about the hand/eye coordination process. A case could be made against the choice of a camera space generated by the coordinates of image point features, *a fortiori* of a single image point, but this concern is—to some extent—addressed in [3], where a different, more robust type of visual feedback is used by the controller, with similar results. There may be a better camera space to work from, but the methodology of this approach and, most likely, its results would remain valid.

6.2 Active Vision and Skill Learning

The issue of skill learning *per se* has not been addressed in this first part of the report. The task that we have undertaken here, and will complete in Part II, is to establish a complete chart of the topological structure of the PCS: since a mathematical model of the object we want to "learn" is available to us, we begin first by determining what it can look like. At the end of Part I, we now have, for any possible geometry of a 2-dof manipulator, a list of organizing centers. This tells us what the singularities of the PKM can be expected to look like. In Part II of this report, we will give, for each of these organizing centers, and whenever it is at all possible, a universal unfolding expressed in terms of the camera pose parameters, as well as the equations of its transition set. In other words, Parts I and II together give us a complete description and list of all possible effects of observer displacements on the topology of the PCS.

Part III of this report is intended to be a "User Manual," rather than a technical discussion of the behavior of the PCS. There, I will, for each type of 2-dof manipulator

geometry, give the "family portrait" of all possible types of bifurcation diagrams (i.e., the diagram of singularities in the joint space) and resulting PCS. Finally, we will see how this information can be exploited, together with information collected by the low-level controller, to learn the shape of the PCS.

Acknowledgements

APPENDIX A: Bifurcations

A.1 Definition

Let us consider a smooth function $g : \mathbb{R}^2 \longrightarrow \mathbb{R}^2$ and the equation

$$g(x, \lambda) = 0. \tag{A.1}$$

The locus of solutions of (A.1) is called the bifurcation diagram of the equation, while x and λ are its *variable* and *bifurcation parameter*. For each λ_0, $n(\lambda_0)$ is defined as the number of x's such that $g(x, \lambda_0) = 0$. A solution (x_0, λ_0) of (A.1) is called a *bifurcation point* if $n(\lambda)$ varies in the neighborhood of λ_0. For example, there are three bifurcation points in the bifurcation diagram shown in Figure A.1.
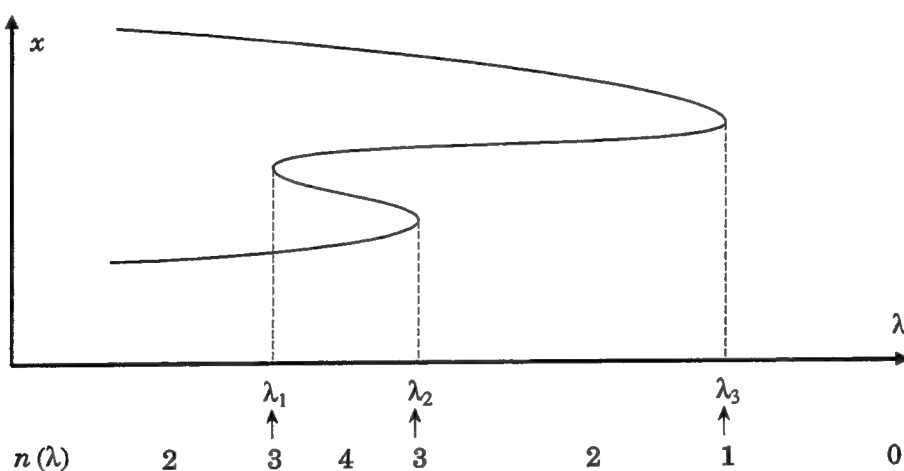

Figure A.1 — An example of bifurcation diagram

A necessary condition for the existence of a bifurcation can be expressed mathematically as follows:

$$g(x, \lambda) = g_x(x, \lambda) = 0.$$

The motivation for studying the bifurcations of problems such as (A.1) is that it is about such points that interesting changes in the shape of the bifurcation diagram can and will occur when the system is perturbed under the action of some parameters such as, in the case that interests us here, the pose of the camera relative to the manipulator.

A.2 Unperturbed vs. perturbed bifurcations

In the neighborhood of a bifurcation point, the initial function can be replaced by its Taylor expansion and then identified with one of the elementary bifurcations. For example, $g(x, \lambda)$ could be locally equivalent to the *simple bifurcation* defined about $(x_0, \lambda_0) = (0, 0)$ by the equation $x^2 - \lambda^2 = 0$. This equation admits as solutions the lines having equations $x = \lambda$ and $x = -\lambda$.

This is, however, only the solution of the *unperturbed* bifurcation (its normal form) that we are describing here. In practice, this solution cannot be observed since—hopefully,

53

small—error terms originating either in the system, the measuring apparatus, or even the model itself are inevitably added to the state equation. It is immediately verified that, if we add an arbitrarily small constant term to the equation of the simple bifurcation problem, important changes in the topology of the bifurcation diagram will occur. Figure A.2 shows the *persistent* bifurcation diagram of the *simple bifurcation* $(x^2 - \lambda^2 + \alpha = 0)$ and of another bifurcation that we will encounter later in this paper: the *isola* $(x^2 + \lambda^2 + \alpha = 0)$.
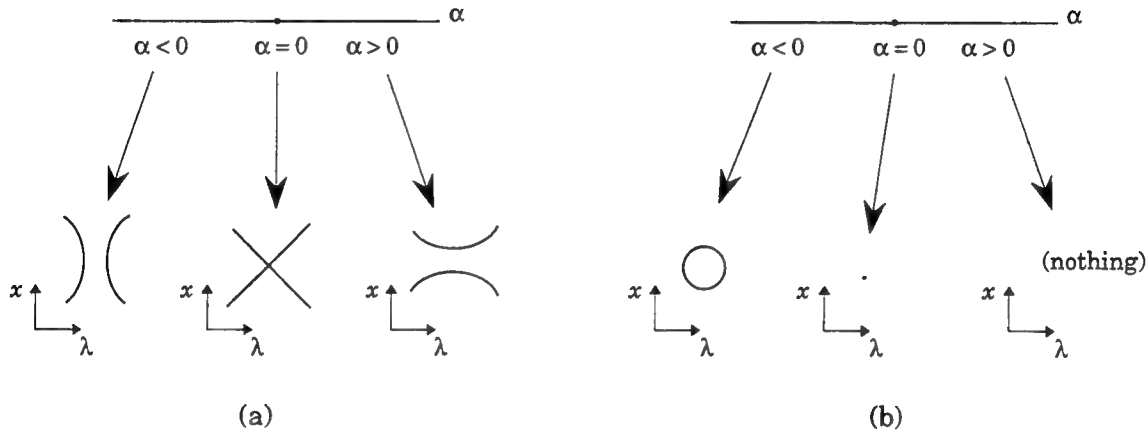

Figure A.2 — Persistent bifurcation diagrams of two elementary bifurcations (from [7]):
(a) The simple bifurcation: $x^2 - \lambda^2 + \alpha = 0$
(b) The isola: $x^2 + \lambda^2 + \alpha = 0$

Although the perturbed bifurcation diagrams look different from the unperturbed diagram, there is little doubt that the latter is the key to understanding how the system passes from a perturbed diagram form to another. The central idea of the approach presented in [7], and which we follow here in this study, is that for a large number of bifurcation problems it is possible to recognize that *organizing center* and use that knowledge to predict the possible perturbed bifurcation diagrams that can be measured for the real system.

For some highly degenerate bifurcation problems, very complex topological changes can occur as an effect of arbitrarily small perturbations. No matter how complex these changes, they will be combinations of the four basic phenomena shown in Figure A.3. We see for example that the *simple bifurcation* and the *isola* bifurcation are each composed of a single basic phenomenon. Other bifurcations that we shall encounter in this study, however, are significantly more complex.

A.3 Universal unfoldings

Figure A.2 showed the effect of adding a small constant perturbation term to the equation of the *simple bifurcation*. A natural question to ask is if other types of perturbations would result in different bifurcation diagrams. What if we were to study the solution of $x^2 - \lambda^2 + \alpha + \beta x = 0$ or $x^2 - \lambda^2 + \gamma \cdot \sin x = 0$ for small values of β or γ? It turns out that, in this particular case, the persistent bifurcation diagram would—qualitatively—be
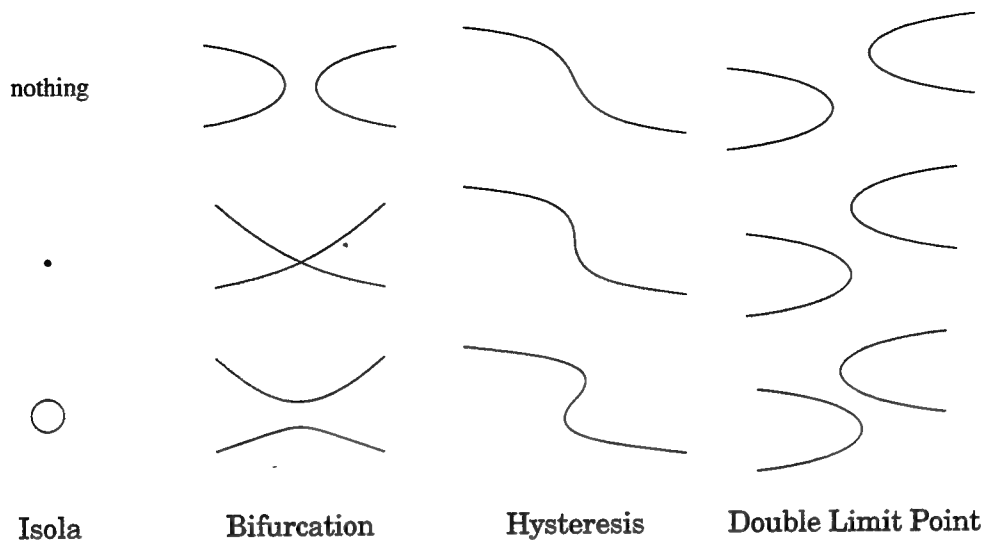
Figure A.3 — The four basic non persistent phenomena

the same since we are already dealing with a universal unfolding of the normal form in the first place. [7] defines a *k-parameter unfolding* of $g(x, \lambda)$ as a germ

$$G : \mathbb{R}^2 \times \mathbb{R}^k \longrightarrow \mathbb{R}$$
$$(x, \lambda; \alpha) \longmapsto G(x, \lambda; \alpha),$$

such that

$$G(x, \lambda; 0) = g(x, \lambda).$$

In other words, an unfolding $G(x, \lambda; \alpha)$ of $g(x, \lambda)$ is a perturbation of $g(x, \lambda)$, with $\alpha = (\alpha_1, \dots \alpha_1)$ as the vector of perturbation parameters. An universal unfolding of g is defined as an unfolding G of g such that every other unfolding of g factors through G and no other unfolding of g has fewer perturbation parameters than G. The number of parameters of G is then a characteristic of the bifurcation problem, and is called the *codimension* of g. Note that a germ g may have more than one universal unfolding, in which case [7] chooses the one with the lowest order (which may not necessarily be the one in which the perturbation parameters have the most physical meaning).

A.4 The Transition Set

Once a universal unfolding $G(x, \lambda; \alpha)$ of $g(x, \lambda)$ is defined the space $W \subset \mathbb{R}^k$ of perturbation parameters $\alpha = (\alpha_1, \dots \alpha_k)$ can be decomposed into regions for which *qualitatively different* bifurcation diagrams can be observed. Figure A.2 gave examples of this in the case of 1-parameter unfoldings.

For any bifurcation problem for which a universal unfolding $G(x, \lambda; \alpha)$ is known, the space of perturbation parameters, W, is partitioned by the *transition set* of the bifurcation, Σ, which [7] defines as follows:

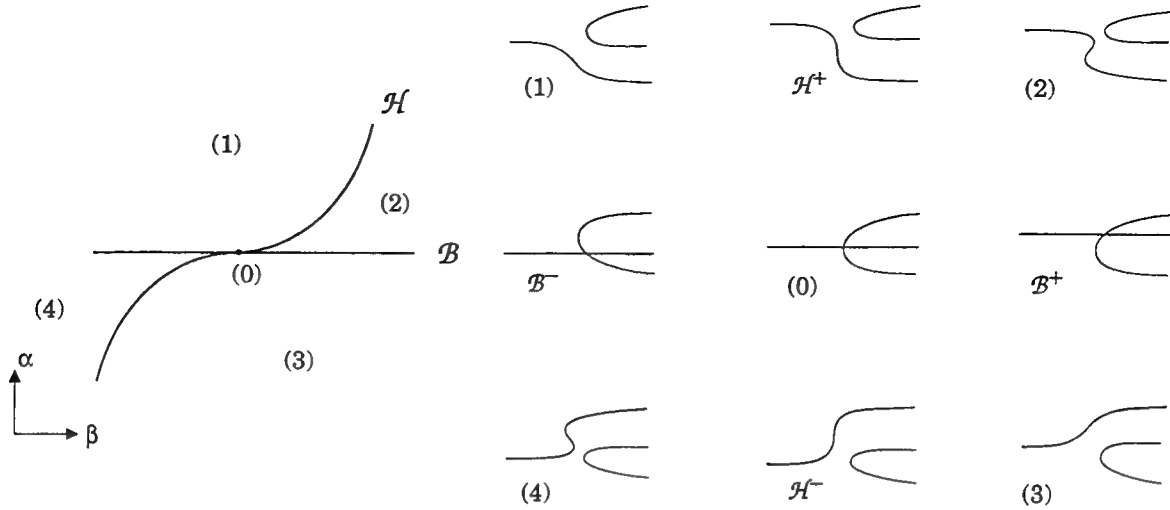$$\Sigma = \mathcal{B} \cup \mathcal{H} \cup \mathcal{D},$$

Figure A.4 — Persistent perturbations of the pitchfork bifurcation $x^3 - \lambda x + \alpha + \beta x^2 = 0$.

where $\mathcal{B}, \mathcal{H}$, and $\mathcal{D}$ are the subsets of W that contain those values of the perturbation terms for which the bifurcation (grouped together with the isola), hysteresis and double point limit phenomena, respectively can be observed. In other terms,

$$\mathcal{B} = \left\{\alpha \in \mathbb{R}^k : \exists(x, \lambda) \in \mathbb{R}^2 \text{ such that } G = G_x = G_\lambda = 0 \text{ at } (x, \lambda; \alpha)\right\}.$$

$$\mathcal{H} = \left\{\alpha \in \mathbb{R}^k : \exists(x, \lambda) \in \mathbb{R}^2 \text{ such that } G = G_x = G_{xx} = 0 \text{ at } (x, \lambda; \alpha)\right\}.$$

$$\mathcal{D} = \left\{\alpha \in \mathbb{R}^k : \exists(x_1, x_2, \lambda) \in \mathbb{R}^3, \ x_1 \neq x_2 \text{ such that }\right.$$
$$\left. G = G_x = 0 \text{ at } (x_i, \lambda; \alpha), \ i = 1, 2\right\}.$$

We can now enunciate the rather remarkable main theorem of this singularity-based approach to the study of bifurcations:

Main geometric theorem:

Let $G : U \times L \times W \longrightarrow \mathbb{R}$ be a family of bifurcation problems satisfying

$$G(x, \lambda, \alpha) \neq 0 \quad \forall(x, \lambda, \alpha) \in \partial U \times L \times W.$$

Let α and β be in the same connected component of $W \sim \Sigma$. Then $G(\cdot, \cdot; \alpha)$ and $G(\cdot, \cdot; \beta)$ are globally equivalent on $U \times L$.

A.4.1 Some Elementary Perturbed Bifurcations

A.4.1.1 The pitchfork bifurcation

The pitchfork is a bifurcation of codimension 2, which exhibits three different basic phenomena: two hysteresis points and one simple bifurcation. Figure A.4 shows the transition set for this bifurcation, as well as the types of persistent bifurcation diagrams that can be expected from experimental measurements. For completeness' sake, bifurcation diagrams theoretically observed along branches of the transition set are given as well.

56

A.4.1.2 The "swallowtail" bifurcation

Although the name "swallowtail" is in fact not used in [7], we will use it here, since the transition set of this bifurcation center is the surface representative of the classical catastrophe of the same name (Figure A.5). The swallowtail is a bifurcation of codimension 3, which exhibits two simple bifurcation phenomena.
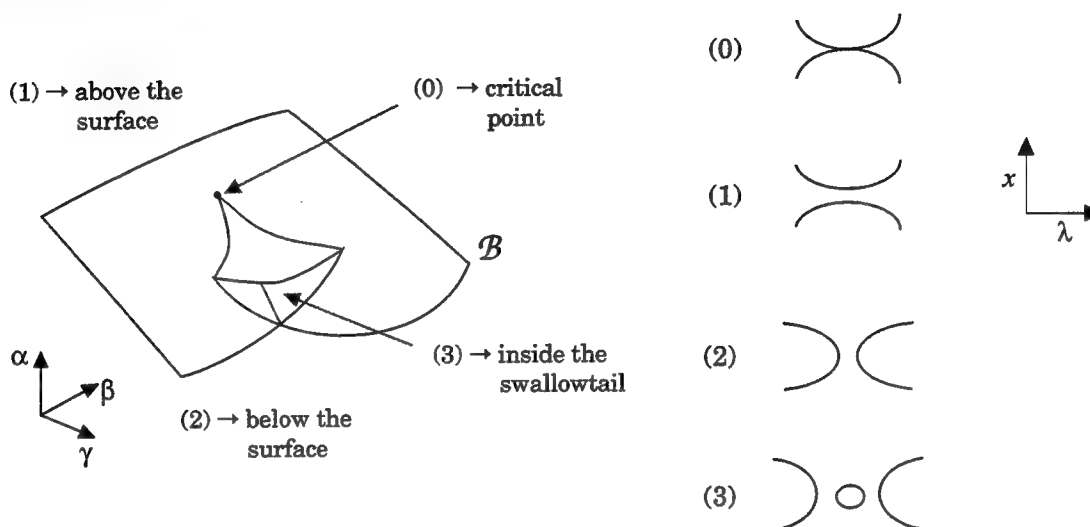

Figure A.5 — Persistent perturbations of the "swallowtail" bifurcation $x^3 - \lambda x + \alpha + \beta x = 0$.

A.4.1.3 The quartic fold bifurcation

The quartic fold is a bifurcation of codimension 3 that exhibits two kinds of basic phenomena: double limit point and hysteresis. Figure A.6 shows the transition set for this bifurcation, as well as the types of persistent bifurcation diagrams that can be expected from experimental measurements.
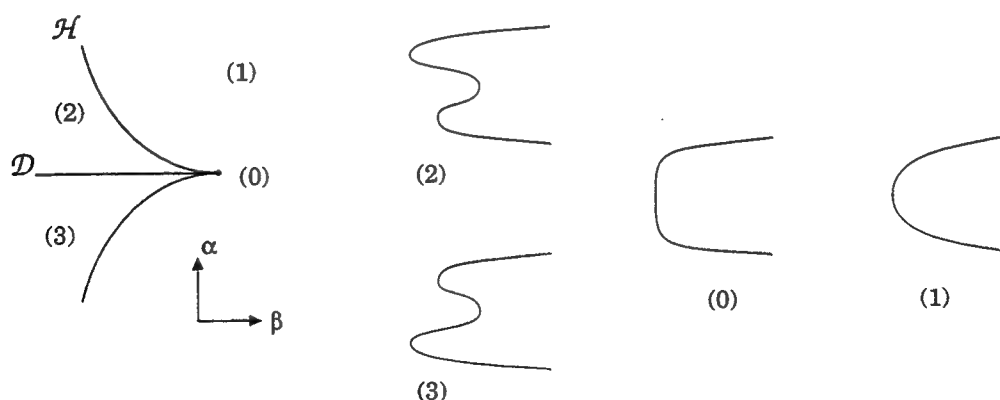

Figure A.6 — Persistent perturbations of the quartic fold bifurcation $x^4 - \lambda + \alpha x + \beta x^2 = 0$.

APPENDIX B: Various Derivations

B.1 Choosing the Right State Variable

We have seen in Subsection 4.2 that the condition for the existence of a singularity for a given joint configuration q_1, q_2) could be expressed in the following form:

$$
\begin{aligned}
g(q_1, q_2) = {}& \left[a_1 a_2 + \left(a_1^2 + a_2^2 + d_2^2 \right) C_2 + a_1 Z_c S_2 + a_1 a_2 C_2^2 + a_2 Z_c C_2 S_2 \right] + \\
& \left[(-a_1 X_c - d_2 Y_c) C_2 - a_2 X_c C_2^2 \right] \cdot C_1 + \\
& \left[(-a_1 Y_c + d_2 X_c) C_2 - a_2 Y_c C_2^2 \right] \cdot S_1 = 0,
\end{aligned}
$$

or

$$
g(q_1, q_2) = \beta_0 + \beta_1 \cdot C_1 + \beta_2 \cdot S_1 = 0,
$$

where the β_i are functions of the second joint variable, parameterized by the camera pose parameters.

If we treat q_1 as the state variable and q_2 as the bifurcation parameter of a bifurcation problem, then a necessary and sufficient condition for a joint configuration (q_1, q_2) to correspond to a bifurcation point is that

$$
g(q_1, q_2) = \beta_0 + \beta_1 \cdot C_1 + \beta_2 \cdot S_1 = 0
$$

$$
\frac{\partial g}{\partial q_1}(q_1, q_2) = \beta_2 \cdot C_1 - \beta_1 \cdot S_1 = 0.
$$

It is then trivial to verify that a necessary condition for these equations to hold is that $\beta_0^2 = \beta_1^2 + \beta_2^2$. The second partial derivative of g with respect to q_1 is then

$$
g_{xx}(q_1, q_2) = -\beta_1 \cdot C_1 - \beta_2 \cdot S_1 = \beta_0 - g(q_1, q_2),
$$

so g and its first two partial derivatives with respect to the state variable are zero if and only if $\beta_0 = \beta_1 = \beta_2 = 0$. In other words, if, for a particular pose of the camera and value of second joint angle, $q_2 = q_2^*$, $g(q_1, q_2^*) = g_x(q_1, q_2^*) = g_{xx}(q_1, q_2^*) = 0$, then this means that $g(\,\cdot\,, q_2^*)$ is the null function, which is not a very interesting function to talk about.

B.2 Case Study of h and Its Bifurcations

B.2.1 Introduction

Note that the decomposition into cases is different here from the one presented in Section 5, as the question we are trying to answer can be approximated as follows: "How can we pick all the parameters and variables so as to set as many derivatives of h as possible to zero." Section 5 not only summarizes the results obtained here, but also sorts out configuration parameters and variables in order to base the presentation on the type of the manipulator (i.e. on the relative value of its DH parameters).

We mentioned in Section 5 that S_2 and Z_c appear in the expression of h only when multiplied by each other so that $H(q_2, q_1; Z_c, R_c) = H(-q_2, q_1; -Z_c, R_c)$. As a consequence, we can restrict our study of the perturbed bifurcations of $h(q_2, q_1)$ to the case $Z_c \geq 0$, knowing that the topology for the other half can be built by simple symmetry.

Finally, since $\forall (K_1, K_2) \in \mathbb{R}^{*2}$, $\exists! (R_c, q_1) \in \mathbb{R} \times [0, 2\pi]$ such that $k_1(q_1) = K_1$ and $k_2(q_1) = K_2$, we will be able treat $k_1(q_1)$ and $k_2(q_1)$ as the unknowns of the system of linear equations defined by the conditions defining the existence of a bifurcation, $h = 0$ and $h_x = 0$:

$$(d_2 C_2) \cdot K_1 - (a_1 + a_2 C_2) C_2 \cdot K_2 = -(a_1 + a_2 C_2) \cdot k_3(q_2) \tag{B.1}$$
$$-(d_2 S_2) \cdot K_1 + (a_1 + 2a_2 C_2) S_2 \cdot K_2 = a_2 S_2 \cdot k_3(q_2) - (a_1 + a_2 C_2) \cdot k_3'(q_2) \tag{B.2}$$

The determinant of this linear system is

$$\begin{aligned} D_2 &= d_2 C_2 S_2 \cdot (a_1 + 2a_2 C_2) - d_2 C_2 S_2 \cdot (a_1 + a_2 C_2) \\ &= a_2 d_2 C_2^2 S_2. \end{aligned}$$

Our study can therefore be decomposed into 4 cases that will be addressed in Sections B.3 through B.6:

1. $d_2 = 0$,
2. $d_2 \neq 0$ and $C_2 = 0$,
3. $d_2 \neq 0$ and $S_2 = 0$,
4. $d_2 \neq 0$, $C_2 \neq 0$, and $S_2 \neq 0$.

But first we need to obtain a general expression for the partial derivatives of arbitrary order of h with respect to q_2.

B.2.2 Derivatives of h with respect to q_2

Since, as we shall see later, cases $a_1 = 0$ and $C_2 = 0$ play an important role in our study, we rewrite $h(q_1, q_2)$ as:

$$h(q_1, q_2) = a_1 \cdot (k_3(q_2) - C_2 \cdot K_2) + C_2 \cdot (a_2 \cdot k_3(q_2) - a_2 C_2 \cdot K_2 + d_2 \cdot K_1)$$

In order to compute the nth partial derivative of $h(q_1, q_2)$ with respect to q_2, we must proceed separately with cases where n is even and cases where n is odd.

- If $n = 2p$, with $p > 0$

$$\frac{\partial^{2p} h}{\partial q_2^{2p}} = a_1 \cdot \frac{\partial^{2p}}{\partial q_2^{2p}} \left(k_3\left(q_2\right) - C_2 \cdot K_2\right) +$$

$$\frac{\partial^{2p}}{\partial q_2^{2p}} \left(C_2 \cdot \left(a_2 \cdot k_3\left(q_2\right) - a_2 C_2 \cdot K_2 + d_2 \cdot K_1\right)\right)$$

$$= a_1 \cdot \left((-1)^{p-1} \cdot \left(a_2 - k_3\left(q_2\right)\right) + (-1)^{p-1} \cdot C_2 \cdot K_2\right) +$$

$$\sum_{i=0}^{2p} \binom{2p}{i} \cdot \frac{\partial^i}{\partial q_2^i} \left(C_2\right) \cdot \frac{\partial^{2p-i}}{\partial q_2^{2p-i}} \left(a_2 \cdot k_3\left(q_2\right) - a_2 C_2 \cdot K_2 + d_2 \cdot K_1\right)$$

$$= (-1)^{p-1} a_1 \cdot \left(a_2 - k_3\left(q_2\right) + C_2 \cdot K_2\right) +$$

$$\sum_{j=0}^{p} (-1)^j \cdot \binom{2p}{2j} \cdot C_2 \cdot \frac{\partial^{2p-2j}}{\partial q_2^{2p-2j}} \left(a_2 \cdot k_3\left(q_2\right) - a_2 C_2 \cdot K_2 + d_2 \cdot K_1\right) +$$

$$\sum_{j=0}^{p-1} (-1)^{j+1} \cdot \binom{2p}{2j+1} \cdot S_2 \cdot \frac{\partial^{2p-2j-1}}{\partial q_2^{2p-2j-1}} \left(a_2 \cdot k_3\left(q_2\right) - a_2 C_2 \cdot K_2 + d_2 \cdot K_1\right)$$

$$= (-1)^{p+1} a_1 \cdot \left(a_2 - k_3\left(q_2\right) + C_2 \cdot K_2\right) +$$
$$\qquad (-1)^p C_2 \cdot \left(a_2 \cdot k_3\left(q_2\right) - a_2 C_2 \cdot K_2 + d_2 \cdot K_1\right) +$$
$$\qquad (-1)^{p+1} \cdot a_2 C_2 \cdot \left(a_2 - k_3\left(q_2\right) + C_2 \cdot K_2\right) \cdot \sum_{j=0}^{p-1} \binom{2p}{2j} + \qquad\qquad \text{(B.3)}$$
$$\qquad (-1)^p a_2 S_2 \cdot \left(k_3'\left(q_2\right) + S_2 \cdot K_2\right) \cdot \sum_{j=0}^{p-1} \binom{2p}{2j+1}$$

- If $n = 2p + 1$, with $p \geq 0$

$$\frac{\partial^{2p+1} h}{\partial q_2^{2p+1}} = a_1 \cdot \frac{\partial^{2p+1}}{\partial q_2^{2p+1}} \left(k_3\left(q_2\right) - C_2 \cdot K_2\right) +$$

$$\frac{\partial^{2p+1}}{\partial q_2^{2+1p}} \left(C_2 \cdot \left(a_2 \cdot k_3\left(q_2\right) - a_2 C_2 \cdot K_2 + d_2 \cdot K_1\right)\right)$$

$$= a_1 \cdot \left((-1)^p \cdot k_3'\left(q_2\right) + (-1)^p \cdot S_2 \cdot K_2\right) +$$
$$\sum_{i=0}^{2p+1} \binom{2p+1}{i} \cdot \frac{\partial^i}{\partial q_2^i} \left(C_2\right) \cdot \frac{\partial^{2p+1-i}}{\partial q_2^{2p+1-i}} \left(a_2 \cdot k_3\left(q_2\right) - a_2 C_2 \cdot K_2 + d_2 \cdot K_1\right).$$

We finally obtain

$$\frac{\partial^{2p+1}h}{\partial q_2^{2p+1}} = (-1)^p \cdot a_1 \cdot \left(k_3'(q_2) + S_2 \cdot K_2\right) +$$

$$\sum_{j=0}^{p} (-1)^j \cdot \binom{2p+1}{2j} \cdot C_2 \cdot \frac{\partial^{2p-2j+1}}{\partial q_2^{2p-2j+1}} \left(a_2 \cdot k_3(q_2) - a_2 C_2 \cdot K_2 + d_2 \cdot K_1\right) +$$

$$\sum_{j=0}^{p} (-1)^{j+1} \cdot \binom{2p+1}{2j+1} \cdot S_2 \cdot \frac{\partial^{2p-2j}}{\partial q_2^{2p-2j}} \left(a_2 \cdot k_3(q_2) - a_2 C_2 \cdot K_2 + d_2 \cdot K_1\right)$$

$$= (-1)^p \cdot a_1 \cdot \left(k_3'(q_2) + S_2 \cdot K_2\right) +$$

$$(-1)^{p+1} S_2 \cdot (a_2 \cdot k_3(q_2) - a_2 C_2 \cdot K_2 + d_2 \cdot K_1) +$$

$$(-1)^p a_2 C_2 \cdot \left(k_3'(q_2) + S_2 \cdot K_2\right) \cdot \sum_{j=0}^{p-1} \binom{2p}{2j} + \tag{B.4}$$

$$(-1)^p a_2 S_2 \cdot (a_2 - k_3(q_2) + C_2 \cdot K_2) \cdot \sum_{j=0}^{p-1} \binom{2p}{2j+1}.$$

B.3 Case 1: $d_2 = 0$

The linear system simplifies to

$$(a_1 + a_2 C_2) C_2 \cdot K_2 = (a_1 + a_2 C_2) \cdot k_3(q_2) \tag{B.5}$$
$$(a_1 + 2a_2 C_2) S_2 \cdot K_2 = a_2 S_2 \cdot k_3(q_2) - (a_1 + a_2 C_2) \cdot k_3'(q_2) \tag{B.6}$$

An obvious necessary condition for the existence of a solution to the redundant system of equations $\{A \cdot K_2 = B, \ C \cdot K_2 = D\}$ is that $A \cdot D = B \cdot C$:

$$(a_1 + a_2 C_2) \cdot C_2 \cdot [a_2 S_2 \cdot (a_2 + a_1 C_2 + Z_c S_2) - (a_1 + a_2 C_2) \cdot (-a_1 S_2 + Z_c S_2)] =$$
$$(a_1 + 2a_2 C_2) \cdot S_2 \cdot (a_1 + a_2 C_2) \cdot (a_2 + a_1 C_2 + Z_c S_2)$$

Developing this necessary condition gives

$$a_2 C_2 S_2 \cdot (a_1 + a_2 C_2) \cdot (a_2 + a_1 C_2 + Z_c S_2) - C_2 \cdot (a_1 + a_2 C_2)^2 \cdot (-a_1 S_2 + Z_c S_2) =$$
$$a_2 C_2 S_2 \cdot (a_1 + a_2 C_2) \cdot (a_2 + a_1 C_2 + Z_c S_2) + S_2 \cdot (a_1 + a_2 C_2)^2 \cdot (a_2 + a_1 C_2 + Z_c S_2)$$

$$\Rightarrow C_2 \cdot (a_1 + a_2 C_2)^2 \cdot (a_1 S_2 - Z_c S_2) = S_2 \cdot (a_1 + a_2 C_2)^2 \cdot (a_2 + a_1 C_2 + Z_c S_2),$$

or

$$(a_1 + a_2 C_2)^2 \cdot (Z_c + a_2 S_2) = 0,$$

which allows us to further divide the problem into subcases.

B.3.1 Case 1.1: $d_2{=}0$ and $a_1{+}a_2{\cdot}C_2{=}0$ (only possible if $|a_1| \leq a_2$)

From (B.6), we obtain $a_2 C_2 S_2 \cdot K_2 = a_2 S_2 \cdot (a_2 + a_1 C_2 + Z_c S_2)$, so that we have again to distinguish subcases.

- **Case 1.1.1:** $d_2 = 0$, $a_1 + a_2 C_2 = 0$, and $C_2 = 0$ (and therefore $a_1 = 0$).
  Then $q_2^* = \varepsilon \pi/2$ and $S_2 = \varepsilon = \pm 1$. From (B.6) we get $Z_c = -a_2 S_2$, so that $\varepsilon = -1$, $q_2^* = -\pi/2$, and $Z_c = a_2$. A Taylor expansion of $h(q_2, q_1)$ in the neighborhood of $q_2^* = \varepsilon \pi/2, q_2 = q_2^* + dq_2$ gives

$$h(q_2^* + dq_2) = a_2 \cdot K_2 \cdot dq_2{}^2 - \frac{1}{2} a_2^2 \cdot dq_2{}^3 + o(dq_2{}^3).$$

If we choose $K_2 = 0$, then we can get the second derivative of h with respect to q_2 to be null as well, but the third derivative cannot be equal to zero.

- **Case 1.1.2:** $d_2 = 0$, $a_1 + a_2 C_2 = 0$, and $S_2 = 0$ (and therefore $a_1 = \pm a_2$)
  Then $q_2^* = 0$ or $q_2^* = \pi$ and $C_2 = \varepsilon = -\text{Sgn } a_1 = \pm 1$. A Taylor expansion of $h(q_2, q_1)$ in the neighborhood of q_2^* gives:

$$h(q_2^* + dq_2) = a_2 K_2 \cdot dq_2{}^2 - \frac{1}{2} a_2 Z_c \cdot dq_2{}^3 - \frac{1}{24} \cdot \left(6\varepsilon a_2^2 + 7 a_2 Z_c \right) dq_2{}^4 + o(dq_2{}^4).$$

If we choose $K_2 = 0$ and $Z_c = 0$, we can get the second and third derivatives of h with respect to q_2 to be null as well, but the fourth derivative then cannot be set equal to zero.

- **Case 1.1.3:** $d_2 = 0$, $a_1 + a_2 C_2 = 0$, $C_2 \neq 0$, and $S_2 \neq 0$ (and therefore $0 < |a_1| < a_2$).
  Then $C_2^* = -a_1/a_2$ and $S_2^* = \varepsilon(a_2^2 - a_1^2)^{1/2}/a_2$, so that, substituting in (B.6), we obtain for K_2:

$$K_2^* = \frac{-a_2}{a_1} \cdot \left(a_2^2 S_2^2 + Z_c \cdot S_2 \right)$$

$$= \frac{a_1^2 - a_2^2}{a_1} - \varepsilon \cdot Z_c \cdot \frac{\sqrt{a_2^2 - a_1^2}}{a_1}.$$

We use the expressions of C_2^*, S_2^2, and K_2^* to compute the value of the second derivative of h with respect to q_2:

$$\frac{\partial^2 h}{\partial q_2^2} = 3 a_1 a_2 - 2 a_2 K_2^* + \frac{1}{a_2^2} \cdot \left(-3a_1^2 + 3a_1^2 K_2^* + 3 a_1 \sqrt{a_2^2 - a_1^2} \cdot Z_c \right)$$

$$= -2 a_1 a_2 + \frac{2 a_2^3 + 2\varepsilon a_2 \sqrt{a_2^2 - a_1^2} \cdot Z_c}{a_1}.$$

In order to set this derivative to zero, one must have $Z_c = -\varepsilon\sqrt{a_2^2 - a_1^2}$, which means that $\varepsilon = -1$ and $K_2 = 0$), but the third derivative of h with respect to q_2 is then

$$\frac{\partial^3 h}{\partial q_2^3} = -3\varepsilon a_2\sqrt{a_2^2 - a_1^2} = 3a_2\sqrt{a_2^2 - a_1^2},$$

which cannot be null.

B.3.2 Case 1.2: $d_2=0$, $a_1+a_2\cdot C_2=0$, and $Z_c+a_2\cdot S_2=0$

We can divide by $a_1 + a_2 \cdot C_2$ on both sides of (B.5) to get $C_2 K_2 = k_3(q_2)$, which leads to another decomposition into two subcases:

- If $C_2 \neq 0$, then $C_2 \cdot K_2 = k_3(q_2) = a_2 + a_1 C_2 + Z_c S_2 \Rightarrow K_2 = a_1 + a_2 C_2$.

- If $C_2 = 0$ (that is, if $Z_c = a_2$), then $S_2 = -1$ and $k_3(q_2) = 0$, so that Equation (B.6) simplifies into $K_2 = a_1$

So we get in fact the same solution for K_2 in both cases, but the expression for the second derivative of h with respect to q_2 is then equal to $a_2 \cdot (a_1 + a_2 C_2)$, which cannot be zero.

B.4 Case 2: $d_2\neq0$ and $C_2=0$

Since $C_2 = 0$, we must have $q_2 = \varepsilon \cdot \pi/2$ ($\varepsilon = \pm 1$) and $S_2 = \varepsilon$. Then $k_3(q_2^*) = a_2 + \varepsilon Z_c$, $k_3'(q_2^*) = -\varepsilon a_1$, and the linear system takes the following form:

$$0 \cdot K_1 + 0 \cdot K_2 = -a_1 \cdot (a_2 + \varepsilon \cdot Z_c) \tag{B.7}$$
$$-\varepsilon \cdot d_2 \cdot K_1 + \varepsilon \cdot a_1 \cdot K_2 = \varepsilon \cdot (a_1^2 + a_2^2) + a_2 Z_c \tag{B.8}$$

We see from (B.7) that we must distinguish two subcases: $a_1 = 0$ and $a_1 \neq 0, a_2+\varepsilon\cdot Z_c = 0$.

B.4.1 Case 2.1: $d_2\neq0$, $C_2=0$, and $a_1=0$

The general expressions for derivatives of arbitrary order of h with respect to q_2 then simplify to

$$\frac{\partial^{2p} h}{\partial q_2^{2p}} = (-1)^p \varepsilon\, a_2 \cdot \left(\sum_{j=0}^{p-1} \binom{2p}{2j+1}\right) \cdot K_2,$$

$$\frac{\partial^{2p+1} h}{\partial q_2^{2p+1}} = (-1)^{p+1} \varepsilon \cdot (a_2(a_2 + \varepsilon Z_c) + d_2 \cdot K_1) + $$

$$(-1)^p \varepsilon \cdot (a_2 Z_c + \varepsilon a_2 \cdot K_2) \cdot \sum_{j=0}^{p-1} \binom{2p}{2j+1}.$$

It is then obvious that if $Z_c = 0$, $K_2 = 0$, and $K_1 = -a_2^2/d_2$, then all derivatives of arbitrarily high order of h with respect to q_2 are null (we shall see with Case 4.1 that this is fact just just a particular case of a very degenerate configuration).

B.4.2 Case 2.2: $d_2 \neq 0$, $C_2 = 0$, and $a_2 + \varepsilon \cdot Z_c = 0$

Then $Z_c = a_2$, $\varepsilon = -1$, and (B.8) simplifies to

$$d_2 \cdot K_1 - a_1 \cdot K_2 = -a_1^2. \tag{B.9}$$

In this case, $\partial h^2 / \partial q_2^2 = 3a_1 \cdot a_2 - 2a_2 \cdot K_2$, so we can get the first three terms of the Taylor expansion of h to be zero if and only if we have $K_1^* = a_1^2/2d_2$ and $K_2^* = 3a_1/2$. However, the third derivative of h with respect to q_2 is then $3a_2^2$, which cannot be equal to zero.

We must mention here an interesting peculiarity of $h(q_2, q_1)$, in the neighborhood of this organizing center, that results in a more complex bifurcation diagrams, and that had to be taken into account in Section 5. For *the same values of* Z_c^*, R_c^*, and q_2, another, less complex, bifurcation can be observed. Indeed, there is another value of q_1 for which $k_1(q_1)$ and $k_2(q_1)$ are solutions of (B.9):

$$d_2 K_1 - a_1 K_2 = -a_1^2.$$

Once expressed in terms of q_1, this equation becomes

$$d_2^2 + d_2 R_c^* S_1 - a_1 R_c^* C_1 = -a_1^2,$$

or

$$a_1 C_1 - d_2 S_1 = \frac{a_1^2 + d_2^2}{R_c^*} = L. \tag{B.10}$$

The angles q_1^* and q_1^{**} that are solutions of (B.10) correspond to the intersection of the circle of center $(0,0)$ and radius L with the circle whose diameter is defined by the points $(0,0)$ and $(a_1, -d_2)$ (and in turns defines angle ρ), as shown in Figure B.1.
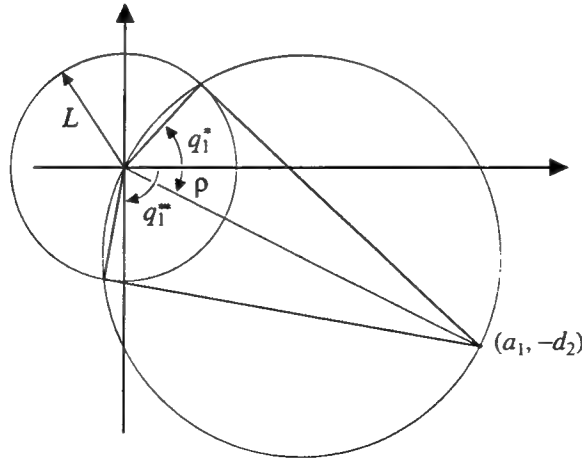

Figure B.1 — The two solutions of (B.9)

There is an obvious symmetry with respect to the direction of angle ρ: $q_1^* - \rho = \rho - q_1^{**}$. Using the values computed earlier for K_1^* and K_2^*, it is then easy to verify that

$$\cos q_1^{**} = \frac{a_1}{2R_c^*} \quad \text{and} \quad \sin q_1^{**} = -\frac{a_1^2 + 2d_2^2}{2d_2 R_c^*},$$

that is, $K_1^{**} = -a_1^2/2d_2$ and $K_2^{**} = a_1/2$.

B.5 Case 3: $d_2 \neq 0$ and $S_2 = 0$

Since $S_2 = 0$, we must have $q_2^* = (1 - \varepsilon) \cdot \pi/2$ ($\varepsilon = \pm 1$) and, therefore, $C_2 = \varepsilon$, $k_3(q_2^*) = a_2 + \varepsilon a_1$, and $k_3'(q_2^*) = \varepsilon Z_c$. The linear system then takes the following form:

$$\varepsilon \cdot d_2 \cdot K_1 - \varepsilon(a_1 + \varepsilon a_2) \cdot K_2 = -(a_1 + \varepsilon a_2) \cdot (a_2 + \varepsilon a_1) \tag{B.11}$$
$$0 \cdot K_1 + 0 \cdot K_2 = -\varepsilon(a_1 + \varepsilon a_2) \cdot Z_c \tag{B.12}$$

From Equation (B.12) we see that we must must decompose Case 3 into two subcases: $a_1 + \varepsilon a_2 = 0$ and $a_1 + \varepsilon a_2 \neq 0$, $Z_c = 0$.

B.5.1 Case 3.1: $d_2 \neq 0$, $S_2 = 0$, and $a_1 + \varepsilon \cdot a_2 = 0$

From the first equation we deduce that $K_1 = 0$ (since $d_2 \neq 0$). If we set K_1 to zero, then the Taylor expansion of h in the neighborhood of q_2^* becomes

$$h(q_2^* + dq_2) = \frac{1}{2} K_2 \cdot dq_2^2 - \frac{1}{2} a_2 Z_c \cdot dq_2^3 - \frac{1}{24} \varepsilon a_2 \cdot (6\varepsilon a_2 - 7K_2) \cdot dq_2^4 + o(dq_2^4).$$

If $Z_c = 0$ and $K_2 = 0$, then the second and third derivatives are null as well, but the coefficient of the fourth order term is then $-\varepsilon a_2^2/4$, which cannot be zero.

B.5.2 Case 3.2: $d_2 \neq 0$, $S_2 = 0$, $|a_1| \neq a_2$, and $Z_c = 0$

Since $q_2 = (1 - \varepsilon)\pi/2$, we have $k_3(q_2) = a_2 + \varepsilon a_1$ and $k_3'(q_2) = \varepsilon Z_c = 0$. The general expressions for derivatives of arbitrary order of h with respect to q_2 then simplify to

$$\frac{\partial^{2p+1} h}{\partial q_2^{2p+1}} = 0 \quad \forall p > 0,$$

$$\frac{\partial^{2p} h}{\partial q_2^{2p}} = (-1)^p \varepsilon a_1 \cdot (a_1 - K_2) + (-1)^p \cdot \left(a_2^2 + d_2 K_1\right) +$$

$$(-1)^p a_2 \cdot (a_1 - K_2) + (-1)^p \varepsilon a_2 \cdot (a_1 - K_2) \cdot \sum_{j=0}^{p-1} \binom{2p}{2j}.$$

- **Case 3.2.1: $a_1 = 0$**
  It is then obvious that, for $K_2 = 0$ and $K_1 = -a_2^2/d_2$, h and its partial derivatives of arbitrarily high order with respect to q_2 are equal to 0 (we shall see with Case 4.1 that this is fact just just a particular case of a very degenerate configuration).

- **Case 3.2.2:** $a_1 \neq 0$

In this case,

$$h(q_2, q_1) = \varepsilon \left((a_1 + \varepsilon a_2)^2 + d_2 \cdot K_1 - (a_1 + \varepsilon a_2) \cdot K_2 \right)$$

$$\frac{\partial^2 h}{\partial q_2^2} = -\frac{\varepsilon}{2} \left((a_1 + \varepsilon a_2)^2 + d_2 \cdot K_1 - (a_1 + 2\varepsilon a_2) \cdot K_2 \right)$$

$$= -\frac{\varepsilon}{2} h(q_2, q_1) + \frac{a_2}{2} \cdot K_2.$$

So, in order for the second derivative to be zero, one must have $K_2 = 0$ and then the condition $h = 0$ implies that $K_1 = -(a_1 + \varepsilon a_2)^2 / d_2$. However, the fourth partial derivative of h with respect to q_2 is then equal to $6a_1 a_2 \neq 0$.

Function h exhibits here the same type of "peculiar" behavior that we had reported in Case 2.2: For the same values of $x = q_2^*$, Z_c^*, and R_c^* that we just calculated, there is another value of $\lambda = q_1$, for which another, less complex, independent bifurcation can be observed. In this case, it is Equation (B.11), expressing the condition $h = 0$, that admits another solution (K_1^{**}, K_2^{**}) with the same value for R_c, $R_c^{**} = R_c^*$, as that of the "main" solution, (K_1^*, K_2^*).

$$\varepsilon d_2 K_1 - \varepsilon \cdot (a_1 + \varepsilon a_2) \cdot K_2 + (a_1 + \varepsilon a_2) \cdot (a_2 + \varepsilon a_1) = 0.$$

Once expressed in terms of q_1, this equation becomes, after dividing on both sides by ε,

$$(a_1 + \varepsilon a_2) \cdot R_c^* C_1 - d_2 R_c^* S_1 = (a_1 + \varepsilon a_2)^2 + d_2^2,$$

or

$$(a_1 + \varepsilon a_2) \cdot C_1 - d_2 S_1 = \frac{(a_1 + \varepsilon a_2)^2 + d_2^2}{R_c^*} = |d_2|, \qquad (\text{B.13})$$

The construction that gives us angles q_1^* and q_1^{**}, the solutions of (B.13), is similar to the one we gave in Case 2.2. Angles q_1^* and q_1^{**} correspond to the intersection of the circle of center $(0, 0)$ and radius $|d_2|$ with the circle whose diameter is defined by the points $(0, 0)$ and $(a_1 + \varepsilon a_2, -d_2)$ (and in turns defines angle ρ_ε'). There is an obvious symmetry with respect to the direction of angle ρ_ε': $q_1^* - \rho_\varepsilon' = \rho_\varepsilon' - q_1^{**}$. Using the values computed earlier for K_1^* and K_2^*, it is then easy to verify that

$$\cos q_1^{**} = \frac{2|d_2| \cdot (a_1 + \varepsilon a_2)}{(a_1 + \varepsilon a_2)^2 + d_2^2} \quad \text{and} \quad \sin q_1^{**} = \frac{\text{Sgn}\,(d_2) \cdot \left((a_1 + \varepsilon a_2)^2 - d_2^2 \right)}{(a_1 + \varepsilon a_2)^2 + d_2^2},$$

that is,

$$K_1^{**} = \frac{(a_1 + \varepsilon a_2)^2 - d_2^2}{d_2} \quad \text{and} \quad K_2^{**} = 2(a_1 + \varepsilon a_2).$$

B.6 Case 4: $d_2 \neq 0$, $C_2 \neq 0$, and $S_2 \neq 0$

B.6.1 Solution of the linear system

The determinant of the 2×2 linear system $D_2 = d_2 C_2^2 S_2$ is not equal to zero. We can easily compute the solution for $K_1 = k_1(q_1)$ and $K_2 = k_2(q_1)$ expressed as functions of q_2 and Z_c:

$$K_1 = \frac{-(a_1 + a_2 C_2)^2 \cdot (Z_c + a_2 S_2)}{a_2 d_2 C_2^2 S_2} \tag{B.14}$$

$$K_2 = -\frac{a_1 Z_c + a_2 Z_c C_2^3 + a_1 a_2 S_2^3}{a_2 C_2^2 S_2} \tag{B.15}$$

There are obviously an infinity of combinations of values for Z_c, R_c, q_1 and q_2 such that (B.14) and (B.15) are verified. Since we are looking for an organizing center, we have to look for the combination that leads to the most singular topology for h. We therefore substitute the values given by (B.14) and (B.15) in the expression for the second derivative of h relative to q_2. The equation $h_{xx} = \partial^2 h / \partial q_2^2 = 0$ gives us a condition allowing us to compute Z_c as a function of q_2:

$$\left[\frac{2a_1 - 3a_1 C_2^2 - a_2 C_2^3}{S_2 \, C_2^2} \right] \cdot Z_c + \frac{2a_1 a_2 S_2^2}{C_2^2} = 0.$$

We notice that since, in the case we are treating here, $S_2 \neq 0$ and $C_2 \neq 0$, the equation has no real solution for Z_c when $2a_1 - 3a_1 C_2^2 - a_2 C_2^3 = 0$. Reporting the solution of this linear equation in (B.14) and (B.15) gives new expressions for K_2 and K_1 as well:

$$Z_c = \frac{2a_1 a_2 S_2^3}{-2a_1 + 3a_1 C_2^2 + a_2 C_2^3}$$

$$K_1 = \frac{(a_1 + a_2 C_2)^3}{d_2 \left(2a_1 - 3a_1 C_2^2 - a_2 C_2^3 \right)} \tag{B.16}$$

$$K_2 = \frac{3a_1 (a_1 + a_2 C_2) S_2^2}{2a_1 - 3a_1 C_2^2 - a_2 C_2^3}$$

We substitute these values in the expression for $\partial^3 h / \partial q_2^3$ to get a new condition, which this time only depends on q_2:

$$\frac{\partial^3 h}{\partial q_2^3} = \frac{6 \, a_1 a_2 (a_2 + a_1 C_2) S_2}{-8a_1 + 12a_1 C_2^2 + 4a_2 C_2^3} = 0.$$

Since $S_2 \neq 0$, there are only be three cases that can give $\partial^3 h / \partial q_2^3$ (courage, we are almost there!): $a_1 = 0$, $a_2 + a_1 C_2 = 0$, and $a_1 \cdot (a_2 + a_1 C_2) \neq 0$.

B.6.2 Case 4.1: $d_2{\neq}0$, $C_2{=}0$, $S_2{=}0$, and $a_1{=}0$

In this case, $2a_1 - 3a_1C_2^2 - a_2C_2^3 = -a_2C_2^3$, which cannot be equal to zero. This implies that the expressions for Zc, K_1,, and K_2 given in (B.16) are defined, so that $Z_c = 0$, $K_2 = 0$, and $K_1 = -a_2^2/d_2$, from which we deduce that $R_c = (a_2^2 + d_2^2)/|d_2|$ and $q_1^* = -\mathrm{Sgn}\, d_2 \cdot \pi/2$. Then, for this pose of the observer and value of the first joint angle, $h(\,\cdot\,, q_1^*)$ is the null function.

B.6.3 Case 4.2: $d_2{\neq}0$, $C_2{=}0$, $S_2{=}0$, and $a_1{=}0$, and $a_1 + a_2 \cdot C_2{=}0$

Then $C_2 = -a_2/a_1$ and $S_2 = \varepsilon\sqrt{a_1^2 - a_2^2}/a_1$, with $\varepsilon = \pm 1$. Obviously S_2 and C_2 are defined if and only if $|a_1| \geq a_2$ and, since $S_2 \neq 0$, we cannot have $|a_1| = a_2$. We are therefore dealing with the case $|a_1| > a_2$, and then $2a_1 - 3a_1C_2^2 - a_2C_2^3 = (2a_1^2 - a_2^2) \cdot (a_1^2 - a_2^2)/a_1^3$, which cannot be equal to zero. The expressions for Zc, K_1, and K_2 given in (B.16) are therefore defined and simplify to

$$K_1 = \frac{\left(a_1^2 - a_2^2\right)^2}{d_2\left(2a_1^2 - a_2^2\right)}, \qquad K_2 = \frac{3a_1\left(a_1^2 - a_2^2\right)}{2a_1^2 - a_2^2}, \quad \text{and}$$

$$Z_c = \frac{-2\varepsilon a_1 a_2 \sqrt{a_1^2 - a_2^2}}{2a_1^2 - a_2^2}$$

Since Z_c must be positive, we have $\varepsilon = -\mathrm{Sgn}\, a_1$, so that $\sin q_2^* = -\sqrt{a_1^2 - a_2^2}/|a_1|$. These parameters were chosen so that h and its first three partial derivatives with respect to q_2 are zero, but the fourth order derivative is then equal to $6a_1^3 a_2/(2a_1^2 - a_2^2)$, which cannot be null.

B.6.4 Case 4.3: $d_2{\neq}0$, $C_2{=}0$, $S_2{=}0$, and $a_1{=}0$, and $a_1 + a_2 \cdot C_2{\neq}0$

This case is encountered when $|a_1| < a_2$. Then, $h_{xxx} = \partial^3 h/\partial q_2{}^3 \neq 0$, but there are still an infinity of configurations $Z_c(q_2), R_c(q_2), q_1(q_2), q_2$, such that $h = h_x = h_{xx} = 0$. What we observe then are singular branches of an organizing center that is not accessible to us.

References

[1] Y. Aloimonos, I. Weiss, and A. Bandopadhay, "Active vision," *International Journal of Computer Vision*, **2**(4): 333–356, 1988.

[2] R. Bajcsy, "Passive perception vs. active perception," in *Proceedings IEEE Workshop on Computer Vision*, Ann Arbor, MI, 1986.

[3] P. Cucka, Technical Report in preparation.

[4] J. Denavit and R.S. Hartenberg, "A kinematic notation for lower-pair mechanisms based on matrices," *ASME Journal of Applied Mechanics*, **2**: 215–221, 1955.

[5] J.T. Feddema and O.R. Mitchell, "Vision-guided servoing with feature-based trajectory generation," *IEEE Transactions on Robotics and Automation*, **2**(5): 691–700, 1989.

[6] J.J. Gibson, *The Perception of the Visual World*, Riverside Press, Cambridge, MA, 1950.

[7] M. Golubitsky and D.G. Schaeffer, *Singularities and Groups in Bifurcation Theory*, Vol. I, Springer-Verlag, New York, 1985.

[8] M. Golubitsky and V. Guillemin, *Stable Mappings and their Singularities* , Springer-Verlag, New York, 1973.

[9] J-Y. Hervé, "Navigational Vision," Ph.D. Thesis, Computer Science Department, University of Maryland, College Park, MD, 1993.

[10] J-Y. Hervé and Y. Aloimonos, "Exploratory active vision: Theory," in *Proceedings IEEE Conference on Computer Vision and Pattern Recognition*, pp. 10–15, Urbana Champain, IL, 1992.

[11] J-Y. Hervé, R. Sharma, and P. Cucka, "The geometry of visual coordination," in *Proceedings AAAI National Conference on Artificial Intelligence*, pp. 732–737, Anaheim, CA, 1991.

[12] J-Y. Hervé, R. Sharma, and P. Cucka, "Toward robust vision-based control: Hand/eye coordination without calibration," in *Proceedings IEEE International Symposium on Intelligent Control*, pp. 457–462, Arlington, VA, 1991.

[13] J.M. Hollerbach, "A survey of kinematic calibration," in *The Robotics Review* 1, O. Khatib, J.J. Craig, and T. Lozano-Pérez, editors, M.I.T. Press, Cambridge, MA, 1989.

[14] B.K.P. Horn, "Image intensity understanding," *Artificial Intelligence*, **2**(2): 201–231, 1977.

[15] M. Jeannerod, "Intersegmental coordination during reaching at natural visible objects," in *Attention and Performance IX*, J. Long and A. Baddeley, editors, Lawrence Erlbaum, Hillsdale, NJ, 1981.

[16] E. Krotkov, "Focusing," *International Journal of Computer Vision*, **2**: 223–237, 1987.

[17] K.N. Kutukalos and C.R. Dyer, "Recovering shape by purposive viewpoint adjustment," in *Proceedings IEEE Conference on Computer Vision and Pattern Recognition*, pp. 16–21, New York, NY, 1993.

[18] D. Manchester, "Prehensile development: A contrast of mature and immature patterns," in *Advances in Motor Development Research, vol. 2*, J.E. Clark and J.H. Humphrey, editors, AMS Press, Inc., New York, 1988.

[19] D. Marr, *Vision*, Freeman, San Francisco, CA, 1982.

[20] R.G. Marteniuk, "The role of eye and head positions in slow movement execution," in *Information Processing in Motor Control and Learning*, G.E. Stelmach, editor, Academic Press, New York, 1978.

[21] J. Maver and R. Bajcsy, "Occlusions and the Next View Planning," in *Proceedings IEEE International Conference on Robotics and Automation*, pp. 1806–1811, Nice, France, 1992.

[22] B.W. Mel, *Connectionist Robot Motion Planning*, Academic Press, San Diego, CA, 1990.

[23] W.T. Miller, R.P. Heewes, F.H. Glanz, and L.G. Kraft, "Real-time dynamic control of an industrial manipulator using a neural-network-based learning controller," *IEEE Transactions on Robotics and Automation*, $2(1)$: 1–9, 1990.

[24] D.W. Miller, F.H. Glanz, and L.G. Kraft, "Application of a general learning algorithm to the control of a robotic manipulator," *International Journal of Robotics Research*, $2(2)$: 84–98, 1987.

[25] A.C. Sanderson and L.E. Weiss, "Adaptive visual servo control of robots," in *Robot Vision*, A. Pugh, editor, Springer-Verlag, New York, 1983.

[26] S.B. Skaar, W.H. Brockman, and R. Hanson, "Three-dimensional camera-space manipulation", *International Journal of Robotics Research*, $2(4)$: 22–39, 1990.

[27] R.Y. Tsai and R.K. Lenz, "A new technique for fully autonomous and efficient 3D robotics hand/eye calibration," *IEEE Transactions on Robotics and Automation*, $2(3)$: 345–358, 1989.

[28] M.A. Vince, "Rapid response sequences and the psychological refractory period," *British Journal of Psychology*, **2**: 23–40, 1949.

[29] L.E. Weiss, A.C. Sanderson, and C.P. Neuman, "Dynamic sensor-based control of robots with visual feedback," *IEEE Journal of Robotics and Automation*, $2(5)$: 404–417, 1987.

[30] L.E. Weiss, "Dynamic Visual Servo Control of Robots: An Adaptive Image-based Approach," Ph.D. Thesis, Dept. of Electrical and Computer Engineering, Carnegie-Mellon University, Pittsburgh, PA, 1984.

[31] A.T. Welford, *Fundamentals of Skill*, Methuen, London, UK, 1968.

REPORT DOCUMENTATION PAGE

1. AGENCY USE ONLY (Leave blank)	2. REPORT DATE July 1994	3. REPORT TYPE AND DATES COVERED Technical Report

4. TITLE AND SUBTITLE	5. FUNDING NUMBERS
Learning Hand/Eye Coordination By an Active Observer Part I: Organizing Centers	DACA76-92-C-0009 N00014-93-1-0257 IRI-9057934

6. AUTHOR(S)

Jean-Yves Hervé

7. PERFORMING ORGANIZATION NAME(S) AND ADDRESS(ES)	8. PERFORMING ORGANIZATION REPORT NUMBER
Computer Vision Laboratory Center for Automation Research University of Maryland College Park, MD 20742-3275	CAR-TR-725 CS-TR-3319

9. SPONSORING/MONITORING AGENCY NAME(S) AND ADDRESS(ES)	10. SPONSORING/MONITORING AGENCY REPORT NUMBER
Advanced Research Projects Agency, 3701 N. Fairfax Dr., Arlington, VA 22203-1714 — U.S. Army Topographic Engineering Center, 7701 Telegraph Road, Bldg. #2592, Alexandria, VA 22310-3864 — Office of Naval Research, 800 North Quincy Street, Arlington, VA 22217-5000	

11. SUPPLEMENTARY NOTES

The content of the information in this report does not necessarily reflect the position or the policy of the Government, and no official endorsement should be inferred.

12a. DISTRIBUTION/AVAILABILITY STATEMENT	12b. DISTRIBUTION CODE
Approved for public release. Distribution unlimited.	

13. ABSTRACT (Maximum 200 words)

This report, the first of a three-part series, presents preliminary results in a study on the role of the active observer in the hand/eye coordination problem.

It has been shown that the hand/eye coordination problem can be represented, for a given pose of the observer, by the singularities of a surface, the PCS. Small changes in the pose of the observer generally produce smooth deformations of the PCS. There are configurations, however, from which arbitrarily small modifications of the point of view result in profound changes in the topological nature of the PCS. This paper studies these bifurcation configurations and, furthermore, investigates the possibility of determining *a priori* displacements of the observer that can achieve a desired effect on the PCS such as simplifying its topology or reducing the number of singularities separating the current configuration from a goal to be reached.

The result of this analysis takes the form of the "family portrait" of all possible aspects of the PCS, indexed by the geometry of the manipulator and the pose of the observer relative to it. A hand/eye system is then completely coordinated—has "learned its PCS"—when a "portrait" has been matched with the experimental data gathered by the low-level controller.

14. SUBJECT TERMS		15. NUMBER OF PAGES 74
Control surface, hand-eye coordination, singularities		**16. PRICE CODE**

17. SECURITY CLASSIFICATION OF REPORT	18. SECURITY CLASSIFICATION OF THIS PAGE	19. SECURITY CLASSIFICATION OF ABSTRACT	20. LIMITATION OF ABSTRACT
UNCLASSIFIED	UNCLASSIFIED	UNCLASSIFIED	UL

GENERAL INSTRUCTIONS FOR COMPLETING SF 298

The Report Documentation Page (RDP) is used in announcing and cataloging reports. It is important that this information be consistent with the rest of the report, particularly the cover and title page. Instructions for filling in each block of the form follow. It is important to *stay within the lines* to meet *optical scanning requirements*.

Block 1. Agency Use Only *(Leave blank)*.

Block 2. Report Date. Full publication date including day, month, and year, if available (e.g. 1 Jan 88). Must cite at least the year.

Block 3. Type of Report and Dates Covered. State whether report is interim, final, etc. If applicable, enter inclusive report dates (e.g. 10 Jun 87 - 30 Jun 88).

Block 4. Title and Subtitle. A title is taken from the part of the report that provides the most meaningful and complete information. When a report is prepared in more than one volume, repeat the primary title, add volume number, and include subtitle for the specific volume. On classified documents enter the title classification in parentheses.

Block 5. Funding Numbers. To include contract and grant numbers; may include program element number(s), project number(s), task number(s), and work unit number(s). Use the following labels:

C	- Contract	PR	- Project
G	- Grant	TA	- Task
PE	- Program Element	WU	- Work Unit Accession No.

Block 6. Author(s). Name(s) of person(s) responsible for writing the report, performing the research, or credited with the content of the report. If editor or compiler, this should follow the name(s).

Block 7. Performing Organization Name(s) and Address(es). Self-explanatory.

Block 8. Performing Organization Report Number. Enter the unique alphanumeric report number(s) assigned by the organization performing the report.

Block 9. Sponsoring/Monitoring Agency Name(s) and Address(es). Self-explanatory.

Block 10. Sponsoring/Monitoring Agency Report Number. *(If known)*

Block 11. Supplementary Notes. Enter information not included elsewhere such as: Prepared in cooperation with...; Trans. of...; To be published in.... When a report is revised, include a statement whether the new report supersedes or supplements the older report.

Block 12a. Distribution/Availability Statement. Denotes public availability or limitations. Cite any availability to the public. Enter additional limitations or special markings in all capitals (e.g. NOFORN, REL, ITAR).

DOD - See DoDD 5230.24, "Distribution Statements on Technical Documents."
DOE - See authorities.
NASA - See Handbook NHB 2200.2.
NTIS - Leave blank.

Block 12b. Distribution Code.

DOD - Leave blank.
DOE - Enter DOE distribution categories from the Standard Distribution for Unclassified Scientific and Technical Reports.
NASA - Leave blank.
NTIS - Leave blank.

Block 13. Abstract. Include a brief *(Maximum 200 words)* factual summary of the most significant information contained in the report.

Block 14. Subject Terms. Keywords or phrases identifying major subjects in the report.

Block 15. Number of Pages. Enter the total number of pages.

Block 16. Price Code. Enter appropriate price code *(NTIS only)*.

Blocks 17. - 19. Security Classifications. Self-explanatory. Enter U.S. Security Classification in accordance with U.S. Security Regulations (i.e., UNCLASSIFIED). If form contains classified information, stamp classification on the top and bottom of the page.

Block 20. Limitation of Abstract. This block must be completed to assign a limitation to the abstract. Enter either UL (unlimited) or SAR (same as report). An entry in this block is necessary if the abstract is to be limited. If blank, the abstract is assumed to be unlimited.